Jorge Miguel Martins Santos

Bachelor of Science in Chemical and Biochemical Engineering

Understanding the Microbial Ecology and Ecophysiology of Enhanced Biological Phosphorus Removal Processes through Metabolic Modelling and Experimental Studies

Dissertation to obtain the degree of Master in Chemical and Biochemical Engineering

Supervisor: Adrian M. Oehmen, PhD, FCT/UNL

Jury:

President: Prof. Dr. Maria da Ascensão Carvalho Fernandes Miranda Reis
Examiner: Dr. Gilda de Sousa Carvalho Oehmen

FACULDADE DE CIÊNCIAS E TECNOLOGIA
UNIVERSIDADE NOVA DE LISBOA

September, 2013

Jorge Miguel Martins Santos

Bachelor of Science in Chemical and Biochemical Engineering

Understanding the Microbial Ecology and Ecophysiology of Enhanced Biological Phosphorus Removal Processes through Metabolic Modelling and Experimental Studies

Dissertation to obtain the degree of Master in Chemical and Biochemical Engineering

Supervisor: Adrian M. Oehmen, PhD, FCT/UNL

Jury:

President: Prof. Dr. Maria da Ascensão Carvalho Fernandes Miranda Reis
Examiner: Dr. Gilda de Sousa Carvalho Oehmen

September, 2013

Understanding the microbial ecology and ecophysiology of enhanced biological phosphorus removal processes through metabolic modelling and experimental studies

Acknowledgements

I would like to express my deep gratitude to my supervisor Dr. Adrian Oehmen for his guidance, patient and useful advices.

I would also like to thank Dr. Gilda Oehmen, Ricardo Marques, Mónica Carvalheira, and Margarida Carvalho for their support in the laboratory.

In addition, I would like to thank Mr. Oliver Schraa and Dr. Spencer Snowling, President and Vice-President of Business and Product Development of Hydromantis Environmental Software Solutions, Inc, respectively, for their collaborations in the implementation of the model developed into GPSX-6.2 program.

Por fim, gostaria de dedicar esta tese às pessoas que me apoiaram nestes últimos anos:

- Mário Dessa e Cristina Barata
-Mauro, Tânia e Joana
-Hélder Pereira e Isabel Pereira
-Pais e irmãos, em especial ao meu irmão Daniel Santos

A todos,

Muito Obrigado!

Abstract

The enhanced biological phosphorus removal (EBPR) process in activated sludge systems has become a widely applied wastewater treatment technology to control eutrophication. The success of this process relies on the sludge enrichment with polyphosphate accumulating organisms (PAOs), while one of the main causes for its failure is due to microbial competition between PAOs and another group of organisms known as the glycogen accumulating organisms (GAOs). The microbial ecology and ecophysiology of these two groups have been investigated through metabolic modelling and experimental studies in order to provide a better understanding of EBPR systems.

This thesis focuses on researching the P removal efficiency and metabolic behaviour of an enriched culture containing two PAOs: *Tetrasphaera*-related organisms and *Accumulibacter*, which were acclimatized with casamino acids as sole carbon source in a sequencing batch reactor (SBR). Both organisms were identified through fluorescence *in situ* hybridization (FISH), and this culture demonstrated anaerobic P release, glycogen hydrolysis, a very low poly-β-hydroxyalkanoates (PHA) synthesis and high casamino acids uptake; followed by aerobic P uptake, glycogen formation and a very low PHA oxidation. Different carbon sources (glucose, acetate, propionate, glutamate, aspartate, glycine and casamino acids) were studied through batch tests inoculated with sludge from the main SBR. Through experimental data, it was suggested that *Accumulibacter* were responsible for the uptake of volatile fatty acids (VFAs), and *Tetrasphaera*-related organisms were likely responsible for both glucose and amino acids uptake.

This thesis also focuses on the development of a model that combines a PAO-GAO metabolic model with activated sludge model no. 2d (ASM2d) in collaboration with Hydromantis Environmental Software Solutions, Inc.. The combined model was implemented in the GPS-X software and will provide a new and advanced platform for wastewater treatment modelling, which will be available to practitioners.

Keywords: Enhanced biological phosphorus removal (EBPR), "*Candidatus Accumulibacter phosphatis*", *Tetrasphaera*-related organisms, metabolic model, activated sludge model (ASM), GPS-X.

Resumo

O processo de remoção biológica de fósforo (EBPR) em sistemas de lamas activadas tem vindo a ser cada vez mais utilizado no tratamento de águas residuais a fim de controlar a eutrofização. O sucesso deste processo depende do enriquecimento das lamas com organismos acumuladores de polifosfatos (PAOs). Por outro lado, uma das principais causas responsáveis pelo seu insucesso é devido à competição entre os PAOs e outro grupo de organismos conhecidos como organismos acumuladores de glicogénio (GAOs). A ecologia e a eco fisiologia destes dois grupos têm vindo a ser investigadas através de estudos experimentais e de modelação metabólica, a fim de se obter uma melhor compreensão dos sistemas (EBPR).

Esta tese foca-se no estudo da eficiência da remoção de fósforo (P) e do comportamento metabólico de uma cultura enriquecida com dois grupos PAOs: *Tetrasphaera*-related organisms e *Accumulibacter*, que foram aclimatizados apenas com casamino ácidos num reactor descontínuo sequencial (SBR). Ambos os organismos foram identificados através de fluorescence *in situ* hybridization (FISH), e a cultura em estudo durante a fase anaeróbia demonstrou as seguintes transformações: libertação de P, hidrólise do glicogénio, baixa produção de poli-β-hidroxialcanoatos (PHA) e consumo de casamino ácidos. Na fase aeróbia houve consumo de P, produção de glicogénio e uma baixa oxidação do PHA. Além disso, foram realizados testes descontínuos inoculados com lamas provenientes do SBR principal, e alimentados com diferentes fontes de carbono (glucose, acetato, propionato, glutamato, aspartato, glicina e casamino ácidos). Com base nos resultados experimentais, foi sugerido que os *Accumulibacter* foram os responsáveis pelo consumo dos ácidos gordos voláteis (VFAs), e os *Tetrasphaera*-related organisms foram provavelmente responsáveis pelo consumo da glucose e dos aminoácidos.

Nesta tese também foi desenvolvido um modelo que combina os modelos metabólicos PAO-GAO com o modelo de lamas activas nº 2d (ASM2d) em colaboração com a Hydromantis Environmental Software Solutions, Inc.. O modelo combinado foi implementado no programa GPS-X e em breve irá fazer parte da biblioteca de modelos deste programa.

Palavras-chave: Remoção biológica de fósforo (EBPR), "*Candidatus Accumulibacter phosphatis*", *Tetrasphaera*-related organisms, modelo metabólico, modelo de lamas activadas (ASM), GPS-X.

Contents

List of figures

List of tables

List of abbreviations

ASM	Activated sludge model
ATU	Allyl-N thiourea
BNR	Biological nutrient removal
COD	Chemical oxygen demand
COD/P ratio	Ratio of organic carbon to P
DDEF	Denitrifying *Defluviicoccus*
DEF	Non-denitrifying *Defluviicoccus*
DGB	Denitrifying *Competibacter*
DGGE	Denaturing gradient gel electrophoresis
DPAOs	Denitrifying PAOs
EBPR	Enhanced biological phosphorus removal
ED	The Entner-Doudoroff
EDTA	Ethylene-diaminetetraacetic
EMP	Embden-Meyerhof-Parnas
fddef	DDEF fraction
FISH	Fluorescence *in-situ* hybridization
fpaoI	PAO I fraction
GAOs	Glycogen accumulating organisms
GB	Non-denitrifying C*ompetibacter*
GB	*Competibacter*
HPLC	High-performance liquid chromatography
HRT	Hydraulic retention time
i_{ci}	Conversion factor
IWA	International Water Association
MAR-FISH	Microautoradiography combined with FISH
MD	Model developer
N	Nitrogen
ν_{ji}	Stoichiometric coefficient
P	Phosphorus
PAOs	Polyphosphate accumulating organisms
PH2MB	Poly-β-hydroxy-2-methylbutyrate
PH2MV	Poly-β-hydroxy-2-methylvalerate
PHA	Poly-β-hydroxyalkanoates
PHB	Poly-β-hydroxybutyrate
PHV	Poly-β-hydroxyvalerate
pmf	Proton motive force
poly-P	Polyphosphate
ppk1	Poly-P kinase 1 gene
qh_ac	Fermentation maximum rate on acetate
qh_prop	Fermentation maximum rate on propionate
qPCR	Quantitative real-time polymerase chain reaction
RAS	Return activated sludge

ratio_prop_ac	Propionate to acetate ratio
Sac	Acetate
Salk	Alkalinity
SBR	Sequencing batch reactor
Sf	Fermentable readily biodegradable substrate
Si	Soluble inert organic material
Sn2	Di-nitrogen
Snh	Free and ionized ammonia
Sno2	Nitrite
Sno3	Nitrate
Spo4	Soluble ortho-phosphate
Sprop	Propionate
SRT	Sludge retention time
TCA	Tricarboxylic acid
TOC	Total organic carbon
TSS	Total suspended solids
VFAs	Volatile fatty acids
VSS	Volatile suspended solids
WAS	Waste activated sludge
WWTPs	Wastewater treatment plants
Xdef	Active *Defluviicoccus* biomass (DEF), a glycogen accumulating organism
Xdef_gly	Cell-internal storage of glycogen in DEF
Xdef_pha	Cell-internal storage of PHA in DEF
Xgb	Active *Competibacter* biomass (GB), a glycogen accumulating organism
Xgb_gly	Cell-internal storage of glycogen in GB
Xgb_pha	Cell-internal storage of PHA in GB
Xh	Active heterotrophic biomass
Xi	Particulate inert organic material
Xmeoh	Metal-hydroxides
Xmep	Metal-phosphates
Xnh	Active autotrophic ammonia oxidisers
Xno2	Active autotrophic nitrite oxidisers
Xpao	Active *Accumulibacter* biomass, a poly-P accumulating organism (PAO)
Xpao_gly	Cell-internal storage of glycogen in PAOs
Xpao_pha	Cell-internal storage of polyhydroxyalkanoates (PHA) in PAOs
Xpp	Stored polyphosphate
Xs	Slowly biodegradable substrate

1 INTRODUCTION

Phosphorus (P) removal from sewage and industrial wastewater is the key factor in preventing eutrophication of surface and coastal waters, since P stimulates the growth of algae and other photosynthetic microorganisms, such as toxic cyanobacteria (blue-green algae) (Oehmen et al., 2007a). These organisms are responsible for the depletion of dissolved oxygen, causing the death of fish, and some blue-green algae produce compounds that have been implicated in the poisoning of fish (Yeoman et al., 1988). The major sources of P in raw wastewater are derived from agricultural land, excreta from livestock, municipal and industrial effluents (for example effluents rich in detergents and cleaning compounds) (Yeoman et al., 1988).

Chemical precipitation has long been used for P removal by the addition of calcium, aluminium and iron salts. However, this method produces large quantities of sludge, which causes handling problems and disposal costs, besides, some chemicals are expensive (Yeoman et al., 1988). These disadvantages are attenuated by the enhanced biological phosphorus removal (EBPR) process, when operated successfully, it can be an inexpensive and environmentally sustainable option to reach relatively high P removal efficiency (effluent P concentrations less than 1 mg/L) (Oehmen et al., 2007a).

1.1 Enhanced biological phosphorus removal principles

The EBPR process consists in the enrichment of polyphosphate accumulating organisms (PAO) by recirculating the activated sludge through anaerobic and aerobic conditions or anaerobic and anoxic conditions (Oehmen et al., 2007a). The last configuration is possible due to the ability of some PAOs to use nitrate or nitrite instead of oxygen as electron acceptors (see section 1.2.1). Hence, they perform nitrogen (N) and P removal simultaneously. The term biological nutrient removal (BNR) is employed to describe these cases. In practice, EBPR can be carried out in a sequencing batch reactor (SBR) operated with anaerobic and aerobic (or anoxic) phases, or in a continuous activated sludge process shown in Figure 1.1 (Oehmen, 2004).

Anaerobically, PAOs in the sludge have a selective advantage for volatile fatty acids (VFAs) uptake, while most ordinary heterotrophic organisms are unable to take up VFAs. Consequently, PAOs store the carbon source intracellularly as carbon polymers designated by poly-β-hydroxyalkanoates (PHAs). This conversion requires energy mainly generated by the cleavage of polyphosphate (poly-P) and release of P from the cell and by the reducing power produced through the glycolysis of internally stored glycogen (Mino et al., 1987), the tricarboxylic acid (TCA) cycle (Comeau et al., 1986, Louie et al., 2000) or both (Pereira et al., 1996, Wexler et al., 2009, Zhou et al., 2009). Aerobically or anoxically, PAOs degrade PHA as the energy source for P uptake and poly-P production, glycogen regeneration, biomass growth and cell maintenance. At the end of these phases, net P removal from the wastewater is achieved through the removal of waste activated sludge (WAS) containing a high poly-P content. The process is cyclic because the P rich sludge is separated from

the effluent with low P concentration through sedimentation in the clarifier, and it is recycled back to the anaerobic zone. The concentrated sludge mixture recycled is known as return activated sludge (RAS) (Oehmen et al., 2007a, Oehmen, 2004).

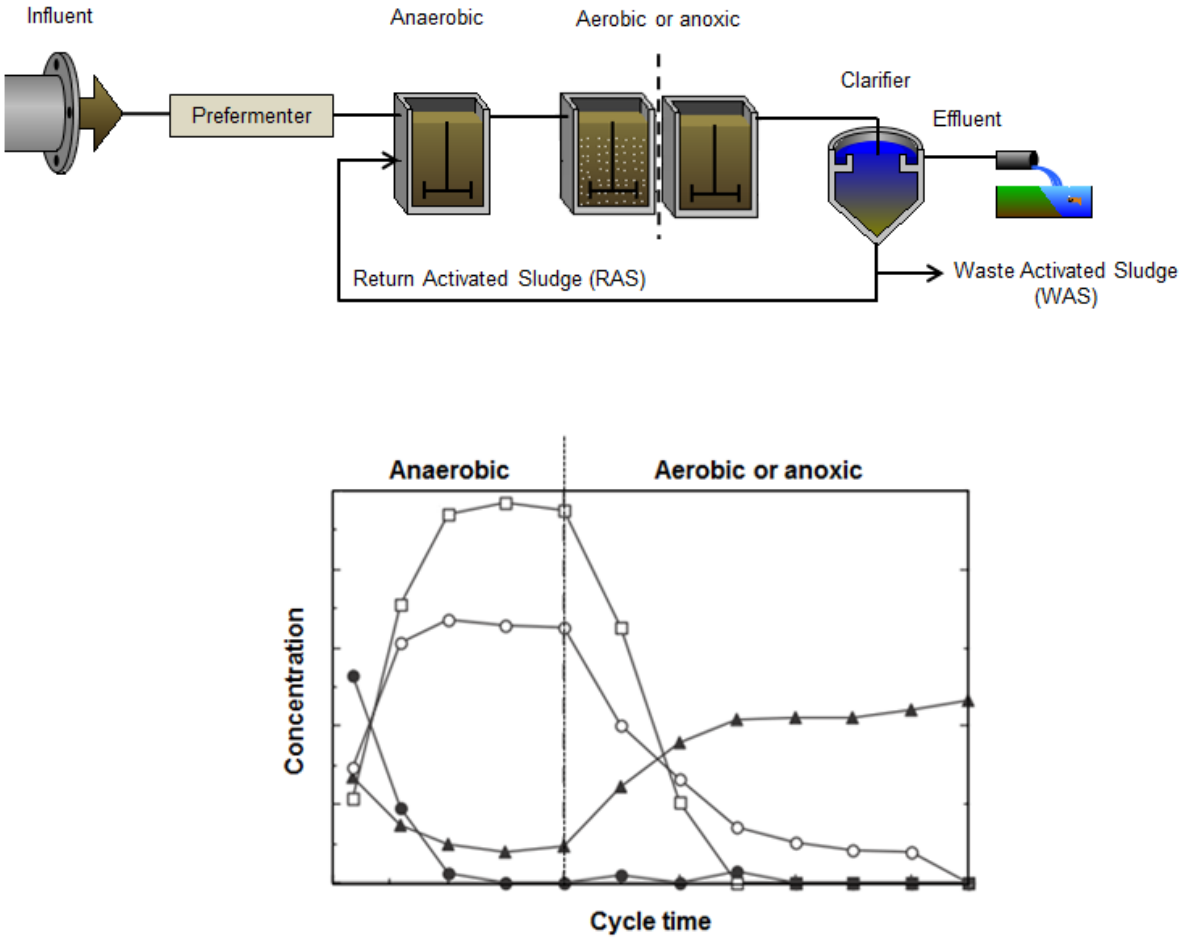

Figure 1.1- Schematic representation of the EBPR process. The graph show the typical profiles of extracellular phosphate-P (□), VFAs (●), PHA (○), and glycogen (▲) from a SBR cycle study of an enriched PAO culture. The graph was adapted from (Oehmen, 2004).

The main disadvantages of the EBPR process are related to its stability and reliability, since it is known that EBPR plants may experience process upsets, deterioration in performance and even failure, causing violations to discharge regulations. High rainfall, excessive nitrate loading to the anaerobic reactor or nutrient limitations are possible causes of process upsets (Oehmen et al., 2007a). For example, in some full-scale EBPR plants, prefermenters or additional supply of carbon sources are required because VFAs are often limiting in wastewaters (Oehmen, 2004). Consequently, it increases operational expenses. However, in recent times, it has been found that one of the causes for EBPR failure is due to microbial competition between PAOs and glycogen accumulating organisms (GAOs) (Oehmen et al., 2007a). These organisms are also able to proliferate under alternating anaerobic and aerobic or anoxic conditions. Anaerobically, they compete with PAOs for VFAs uptake, and they also convert them to PHA intracellularly. The energy required for theses biotransformations comes only from the glycolysis of glycogen. At the aerobic or anoxic phases, GAOs use PHA as

energy source for biomass growth, glycogen replenishment and cell maintenance. As shown in Figure 1.2, GAOs are unable to perform anaerobic P release and aerobic P uptake. Since GAOs compete with PAOs by VFAs uptake and they not contribute to P removal from EBPR systems, minimizing their growth have been a priority by researchers in the last years (Oehmen et al., 2007a).

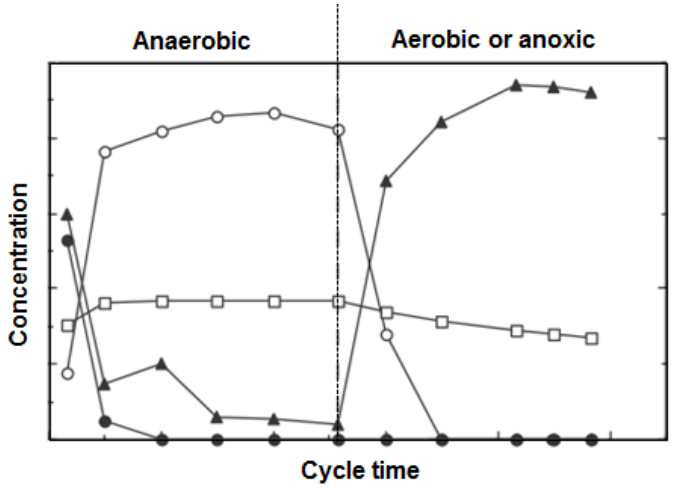

Figure 1.2- Typical profiles of extracellular phosphate-P (□), VFAs (●), PHA (○), and glycogen (▲) from a SBR cycle study of an enriched GAO culture. Adapted from (Oehmen, 2004).

1.2 Microbiology

In recent years, the detection, quantification and metabolic properties of different PAO and GAO groups/subgroups have been possible thanks to the application of the following molecular techniques: fluorescence *in situ* hybridisation (FISH), 16S rRNA-based clone libraries, denaturing gradient gel electrophoresis (DGGE), quantitative real-time polymerase chain reaction (qPCR), chemical staining of stored polymers and microautoradiography combined with FISH (MAR-FISH) (Oehmen et al., 2010b, Oehmen et al., 2007a). More recently, high-throughput sequencing techniques (e.g. pyrosequencing) and the -omics methods (e.g. metagenomics, metaproteomics and metatranscriptomics) have also been applied for this purpose.

1.2.1 Microbial identification of PAOs

The most well-known PAO group is "*Candidatus Accumulibacter phosphatis*" (referred to as *Accumulibacter* hereafter), which is a bacterium closely related to *Rhodocyclus* in the *Betaproteobacteria* group (Oehmen et al., 2010b). Hesselmann et al., (1999) and Crocetti et al., (2000) demonstrated that *Accumulibacter* corresponds to the characteristic PAO phenotype described in the section 1.1. Several studies have shown that *Accumulibacter* was present in relative abundance in many lab-scale systems (Crocetti et al., 2000, Hesselmann et al., 1999, Liu et al., 2001) and in full-scale EBPR systems (4-22% of all bacteria) (Zilles et al., 2002, Saunders et al., 2003, Kong et al., 2004).

Through qPCR using poly-P kinase 1 gene (*ppk*1) primers, it was found that the *Accumulibacter* cluster is comprised of two types (I and II), each divided into several clades (IA-E and IIA-G) (Peterson

et al., 2008, He et al., 2007). This fact is also evidenced by some distinct metabolic features, which have been observed from different *Accumulibacter* types, such as denitrification capacity and anaerobic utilization of the TCA cycle (Oehmen et al., 2010b).

As mentioned in the previous section, P uptake also occurs in anoxic conditions. This configuration allows the removal of N and P simultaneously, reduces process operational costs due to savings in aeration as well as in the amount of carbon sources needed for denitrification and minimizes sludge disposal (Carvalho et al., 2007, Oehmen et al., 2007a). Thanks to the studies of Carvalho et al., (2007) and Oehmen, Carvalho, Freitas & Reis (2010a), it was possible to clarify the presence of two different phylogenetic types of *Accumulibacter*, each displaying different affinities for nitrate: the denitrifying PAOs (or DPAOs) and non-DPAOs (or simply, PAOs). According to these studies, DPAOs are able to use nitrate, nitrite (i.e. denitrify from nitrate onwards) and oxygen as electron acceptors. Moreover, they correlate well with type I *Accumulibacter*. While PAOs are unable to reduce nitrate but able to use oxygen, and denitrify from nitrite onwards. Furthermore, they have been correlated with type II *Accumulibacter*. These findings are in agreement with the metagenomic study of two *Accumulibacter* enrichments performed by Martin et al., (2006). They revealed that their *Accumulibacter* dominant strain (clade IIA) lacked the gene *nar* that encodes for the nitrate reductase enzyme, although the genes that encode for the rest of the denitrification pathway were detected (Carvalho et al., 2007). In order to avoid confusion with the terms DPAOs and PAOs, since both organisms are able to denitrify from nitrite onwards, and they correlate strongly with type I *Accumulibacter* and type II *Accumulibacter*, respectively, it is used in this thesis the same terminology adopted by Oehmen, Lopez-Vazquez et al., (2010c): PAO I and PAO II to designate DPAOs and PAO, respectively. In this way, the term PAOs continues to be used to describe all organisms that contribute to EBPR in activated sludge systems. Figure 1.3 shows the conclusions achieved by Carvalho et al., (2007), where the rod morphotype was proposed to be characteristic of PAO I, and the coccus morphotype characteristic of PAO II.

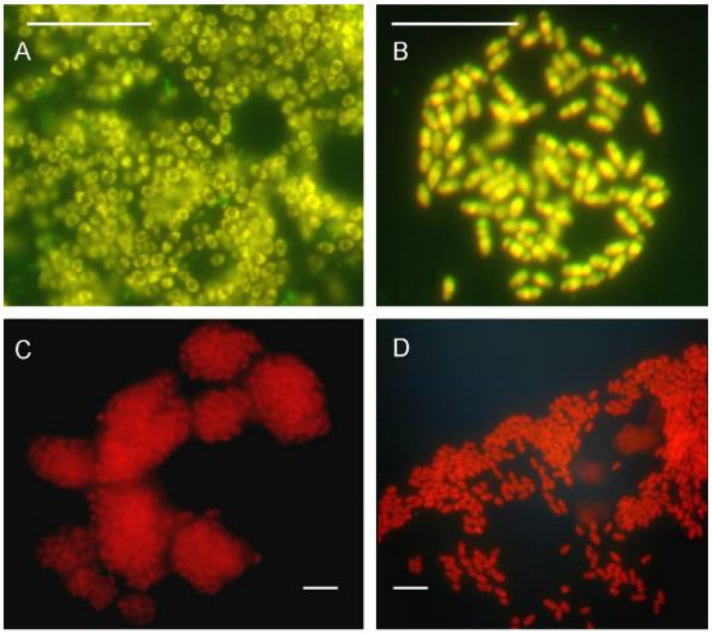

Figure 1.3- Epifluorescence micrographs of sludge hybridised with Cy3-labelled PAOMIX probes and FITC-labelled BET42a probe. *Accumulibacter* are shown in yellow in A) and B), while any other β-*Proteobacteria* are shown in green. *Accumulibacter* are shown in red in C) and D). The figures A and C display the cocci morphology proposed as characteristic of PAO II. The figures B and D display the rod morphology proposed as characteristic of PAO I. Scale bar of 10 μm for all images (Carvalho et al., 2007).

Dechloromonas-related PAOs are another group of *Betaproteobacteria* found in low numbers (≤3%) in EBPR plants. They may be similar to *Accumulibacter* in terms of metabolism, and they are also potentially involved in nitrate and nitrite reduction. However there is little information available about their anaerobic/aerobic or anoxic cycle and it requires further investigation in order to be confirmed their metabolism (Oehmen et al., 2010b).

Besides *Accumulibacter* and *Dechloromonas*-related organisms, Gram-positive *Tetrasphaera*-related organisms within the *Actinobacteria* are also putative PAOs that are abundant in domestic wastewaters (3-16%), and even more so in industrial wastewater plants (17-35%) (Oehmen et al., 2010b). However, they do not share all typical PAO characteristics known from *Accumulibacter*. Y.H. kong et al., (2005) showed that they are able to take up phosphate and form poly-P under aerobic conditions, only after taking up some amino acids, anaerobically. According to these authors, they cannot take VFAs, and do not store PHAs in that phase. Y. kong et al., (2008) showed that they also seem capable of fermenting glucose, and according to Xia et al., (2008) they express extracellular surface-associated amylases for degradation of starch (Hien et al., 2011). A few isolated species of the genus *Tetrasphaera* were found. These include *Tetrasphaera* (*T.*) *australiensis*, *T. japonica*, *T. elongata* (strain LP2), *T. elongata* (strain ASP12), and the filamentous *T. jenkinsii*, *T. vanveenii* and *T.veronensis*. Recent studies of Hien et al, (2011) and Kristiansen et al, (2013) have helped to increase the knowledge about the phylogeny and ecophysiology of *Tetrasphaera*-related organisms.

Hien et al., (2011) found that the genus *Tetrasphaera* (belonged to the family *Intrasporangiaceae* in the *Actinobacteria*) forms three clades. Clade 1 includes clones related to sequences of *T. elongata* and *T. duodecadis*, and clade 2 contains four isolated species: *T. jenkinsii*, *T. australiensis*,

T.veronensis and the filamentous "*Candidatus Nostocoida limicola*", while clade 3 contains only sequences from uncultured clones. The Figure 1.4 shows some of the six different morphotypes (short rods, branched rods, small cocci, cocci in tetrads, filaments, and thin filaments) detected by the authors in the *Tetrasphaera* clades 1-3. Hien et al., (2011) also showed that active uptake of P and formation of poly-P took place in most of the probe-defined *Tetrasphaera* populations (only in bacteria targeted by probe Tet3-19 in clade 3 and most filamentous morphotypes this did not occur). However aerobic uptake of P only took place after uptake of certain carbon sources under anaerobic conditions: amino acids and glucose (for all clades), and acetate (only observed in clade 2 and 3). It is noteworthy that despite all *Tetrasphaera* were able to consume glucose anaerobically, not all take up P in the following aerobic phase. Moreover, the filamentous "*Candidatus Nostocoida limicola*" in clade 2 did not actively take up P aerobically and may not be active PAOs despite the presence of intracellular P. (Hien et al., 2011) also performed staining with Nile Blue or Sudan Black in order to detect the presence of PHAs. However, the identity of any intracellular compound was not found and is still unknown.

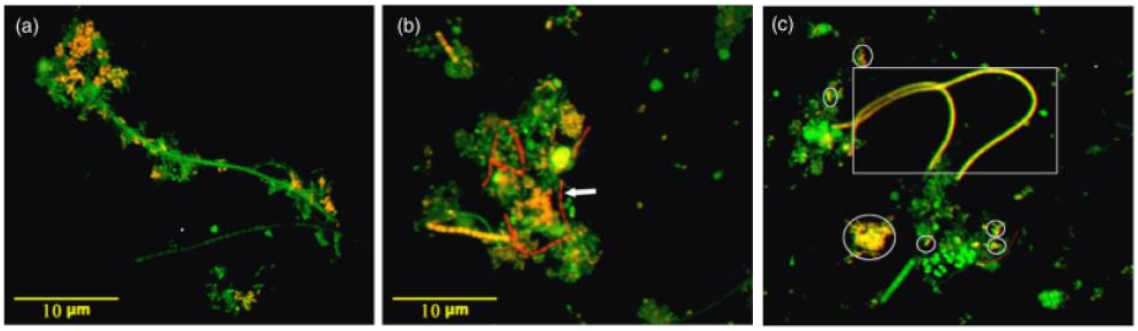

Figure 1.4: Epifluorescence micrographs of *Tetrasphaera*-PAO in activated sludge hybridised with probes Tet3-654 (a), Tet2-892 (b) and Tet2-174 (c) (Cy3-labelled). All samples were also hybridised with FITC-labelled EUBMIX. *Tetrasphaera* are shown in yellow and other *Bacteria* are shown in green. The arrow, the circles and the square indicate thin filaments, branched rods, and filaments, respectively. Scale bar of 10 µm for all images. Adapted from (Hien et al., 2011).

Recently, Kristiansen et al., (2013) proposed a metabolic model for members of the genus *Tetrasphaera* involved in EBPR systems. They suggested that under anaerobic conditions the *Tetrasphaera*-related PAOs take up glucose and ferment this to succinate and other components. Furthermore, glycogen is produced as a storage polymer and the energy required for these anabolic reactions is obtained from fermentation and poly-P degradation. Aerobically, the stored glycogen is degraded to provide carbon and energy for growth, P uptake and poly-P formation (see Figure 1.5). Kristiansen et al., (2013) observed that *Tetrasphaera*-related PAOs are also able to denitrify like *Accumulibacter* clade IA members.

As shown in this section, the physiology of *Tetrasphaera*-PAOs is more complex and in several aspects very different from *Accumulibacter*. By this reason further research is required to elucidate their metabolic pathways and the conditions that select for their growth in EBPR systems.

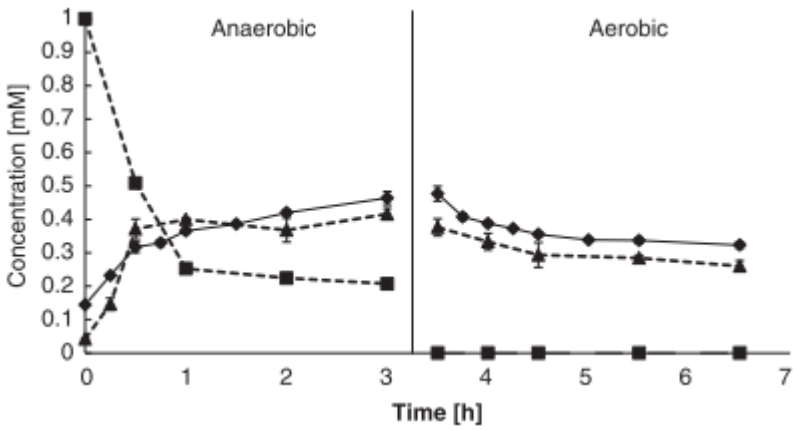

Figure 1.5: Profiles of glucose (■), extracellular phosphate-P (◆) and glycogen (▲) from a SBR cycle study of an enriched *T. elongata* culture (Kristiansen et al., 2013).

1.2.2 Microbial identification of GAOs

Phylogenetic diversity has also been observed among the GAOs. It was Crocetti et al., (2002) who identified organisms displaying the GAO phenotype (described in the section 1.1), and named them as "*Candidatus Competibacter phosphatis*" (henceforth referred to as *Competibacter*) belonging to the *Gammaproteobacteria* phylum (Oehmen, 2004). Later, Y. H. Kong et al., (2002) observed that *Competibacter* (also known as GB lineage) are composed of at least seven different sub-groups (GB 1-7), and these bacteria exhibited cocci and rod morphologies, as shown in Figure 1.6 (Oehmen et al., 2007a). Through MAR-FISH analysis, Y. H. Kong et al., (2006) hypothesized that the different subgroups of *Competibacter* display varying denitrification capacities. This work suggested that GB 6 was capable of nitrate and nitrite reduction, while GB 1, 4 and 5 were able to reduce nitrate only, and GB 3 and 7 were unable to denitrify (Oehmen et al., 2010b, Oehmen et al., 2010c). The *Competibacter* percentage found in full-scale EBPR plants is about ≤12% of all bacteria (Oehmen et al., 2010b).

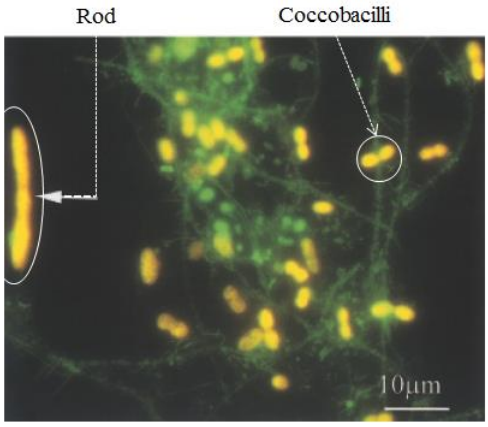

Figure 1.6: Epifluorescence micrographs of sludge hybridised with Cy3-labelled GB probe and FITC-labelled Eub338 probe. *Competibacter* are shown in yellow, while any other bacteria are shown in green. Scale bar of 10 μm. Adapted from (Kong et al., 2002).

Another group of organisms related to *Defluviicoccus vanus* has been observed to display the GAO phenotype in anaerobic-aerobic activated sludge systems, without the detection of *Competibacter*.

These organisms have been identified to belong to the *Alphaproteobacteria* phylum, and seem to display tetrad morphology, see Figure 1.7 (Oehmen et al., 2007a). *Defluviicoccus* vanus were observed be present (about 9% of all bacteria) in full-scale EBPR plants (Oehmen et al., 2010b).

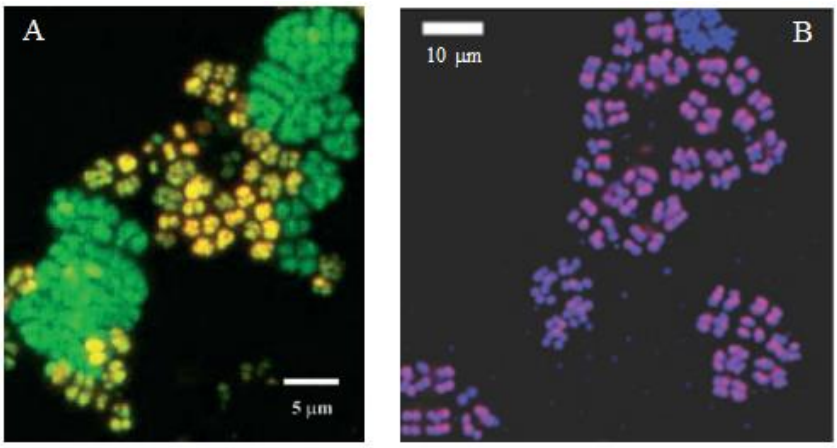

Figure 1.7: Meta confocal laser scanning microscope (CLSM) micrographs of FISH showing two clusters of *Defluviicoccus vanus*: I (A) and II (B). A) Sludge hybridized with probes TFO_DF618 (Cy5-labelled, red) and TFO_DF218 (Cy3-labelled, green). In this figure there are two FISH-positive signals: one fluoresced with both probes (yellow) and the other fluoresced only with probe TFO_DF218 (green). Scale bar of 5 μm (Wong et al., 2004). B) Sludge hybridized with probes DF988 and DF1020, DF2MIX (Cy3-labelled, red) and EUBMIX (Cy5-labelled, blue). In this figure cluster II *D.vanus* cells are magenta and other Bacteria are blue. In both figures the cells had a tetrad morphology. Scale bar of 10 μm. Adapted from (Meyer et al., 2006).

Similarly to *Competibacter*, *Defluviicoccus* GAOs are composed of at least four different clusters, where different sub-groups of each organism have varying denitrification capabilities. Wang et al., (2008) showed that an enrichment of *Defluviicoccus* Cluster I was able to reduce nitrate, but not nitrite, and Burow et al., (2007) suggested that *Defluviicoccus* Cluster II was unable to denitrify (Oehmen et al., 2010c).

1.3 Factors affecting the competition between PAOs and GAOs

The well-known factors that affect the competition between PAOs and GAOs are the ratio of organic carbon to P (COD/P ratio), the type of carbon source present in the influent, pH and temperature.

Relatively to COD/P ratio, high values (e.g. >50 mg COD/mg P) in the wastewater feed tends to favour the growth of GAOs, while low values (e.g. 10-20 mg COD/mg P) should be more favourable to the growth of PAOs (Oehmen et al., 2007a).

Different carbon sources, VFAs (such as acetate, propionate, butyrate, valerate, lactate and isovalerate) and non-VFAs substrates (such as amino acids and glucose) have been shown to have an impact on the PAO-GAO competition. However, it has only practical interest the study of the most abundant carbon sources in the influents of the EBPR plants, which is the case of acetate and in plants where prefermentation is employed, propionate is often present in substantial quantities (25-45 wt%) (Oehmen et al., 2007a). The non-VFAs substrates such as glucose and amino acids are also

present, although the latter may be particularly abundant in industrial wastewater systems. Therefore, in this section only are described the effects caused by the acetate, propionate, glucose and amino acids on the PAO-GAO competition.

According to Oehmen, Saunders, et al., (2006a); Oehmen, Yuan, et al., (2005b) and Oehmen, Zeng, et al., (2006b), *Accumulibacter* are able to take up acetate and propionate with the same efficiency and at a similar kinetic rate, while *Competibacter* can store acetate at a similar rate but take up propionate at negligible rates. However, the *Defluviicoccus* GAOs can take up propionate at a similar rate as *Accumulibacter* but take up acetate at about 50% of their rate. Thus, the type of carbon source has a direct effect on the anaerobic metabolism of PAOs and GAOs. Nonetheless, it also has an indirect effect on the aerobic metabolism, since the uptake of either acetate or propionate leads to different total anaerobic PHA productions per C mol of carbon source, and also to the storage of different PHA fractions: poly-β-hydroxybutyrate (PHB), poly- β-hydroxyvalerate (PHV) and poly- β-hydroxy-2-methylvalerate (PH2MV), which will affect their aerobic yields (Lopez-Vazquez et al., 2009).

The effect of amino acids has already been discussed in section 1.2.1, as favouring the growth of *Tetrasphaera*-related PAOs. However, it is currently unclear which preferred amino acids are taken up by this group.

In relation to glucose, there are studies proving the success of EBPR plants when this carbon source is fed, and also studies showing its deterioration. Y. H. Kong et al., (2006) suggested a possible explanation for that, wherein *Competibacter* and *Accumulibacter* are unable to assimilate glucose directly, and so they rely on the consumption of fermentation products, such as acetate and propionate (competition explained above). However, glucose has been observed to be directly taken up by *Defluviicoccus*-related organisms. On the other hand, other possible explanation that supports the proliferation of GAOs organisms is that external glucose can replace internally stored glycogen and serve as the energy source and reducing power for PHA accumulation, reducing the dependency on poly-P (Mino et al., 1998). Nevertheless, *Tetrasphaera* PAOs also consume glucose. Consequently, its effect on the PAO-GAO competition remains unclear.

Several studies have demonstrated that pH affects the anaerobic and aerobic metabolisms of PAOs and GAOs, wherein high pH values (>7.25) improves P removal performance by selecting PAOs over GAOs, while low pH values (<7.25) promote the proliferation of GAOs (Filipe et al., 2001b). Smolders et al., (1994a) observed that the ratio of anaerobic P release to acetate uptake varied from 0.25 to 0.75 P-mol/C-mol in a pH range of 5.5 to 8.5. They explained this fact as follows: under the assumption that the internal pH and the overall proton motive force (pmf) of a cell is kept constant, at a high external pH than the internal, the pH gradient increases as well as the electrical potential difference ($\Delta\Psi$) across the cell membrane in order to maintain a constant pmf. Consequently, for the uptake of acetate (a negatively charged ion) more work must be done to overcome $\Delta\Psi$. This increased work is generated through an increase in poly-P degradation (Oehmen et al., 2007a).

Experimental evidences obtained thus far suggest that at higher temperatures, GAOs tend to become stronger competitors with PAOs, and in some cases, lower temperatures have been found to improve EBPR performance (Oehmen et al., 2007a).

The metabolic model developed by Lopez-Vazquez et al., (2009) achieved important conclusions about the effects caused by the combination of the factors mentioned above on PAO-GAO competition, as shown in Figure 1.8. According to this study, the growth of PAOs is favoured over GAOs at lower temperatures (10ºC), independently of pH and carbon source; at moderate temperature (20ºC) and acetate to propionate ratios of 75-25% and 50-50%, regardless of the applied pH. On the other hand, if propionate and acetate are used as sole carbon source at 20ºC, PAOs are only dominant at pH equals to 7.5.

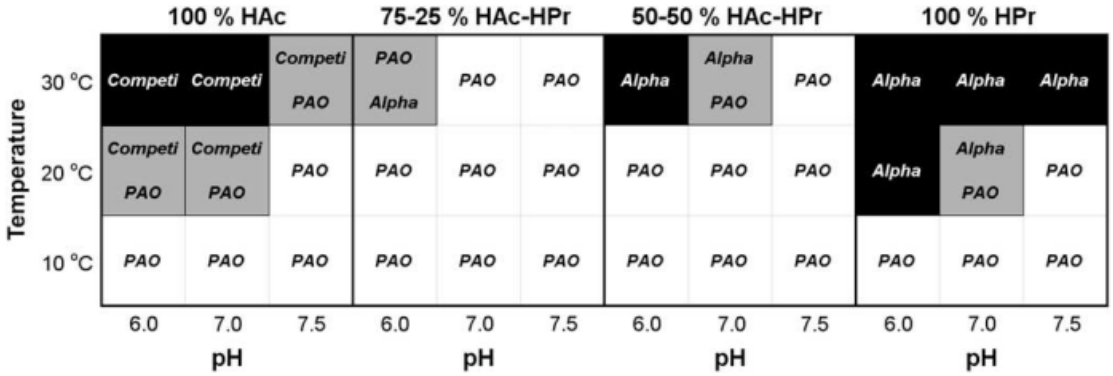

Figure 1.8: Summary of the bacterial population distributions showing the dominant or coexisting microorganisms as a function of the carbon source, pH and temperature. *Accumulibacter* (PAO) is signalled by white cells while *Competibacter* (*Competi*) or *Defluviicoccus*-related organisms (*Alpha*) are in black cells. Light grey tones indicate the coexistence of two microorganisms (Lopez-Vazquez et al., 2009).

1.4 Process modelling

Nowadays, mathematical modelling has become an integral part of biological wastewater treatment, often for optimization and prediction of process performance, and as a supporting tool for design (Lopez-Vazquez et al., 2009). Two different types of models have been used to describe EBPR processes: activated sludge models (ASM) and metabolic models. EBPR metabolic models can be combined with ASM models in order to simulate the behaviour of full-scale EBPR pants.

ASM models use a “black-box” approach to describe the bulk biochemical transformations without providing the details of how these transformations occur (Oehmen, 2004). While metabolic models rely on known (or postulated) metabolic pathways involved in the biochemical transformations that take place within the cells, providing a better definition of the biological processes (Oehmen et al., 2010b). A key difference between these two types of models is the way the yield coefficients are determined. In the ASM models they are determined experimentally while in metabolic models most of them are calculated theoretically through substrate, energy and reducing power balances, and only a few are determined experimentally (Oehmen et al., 2007a). The last method not only increases the consistency and reliability of the model but also facilitates the calibration process by reducing the number of parameters to calibrate (Oehmen et al., 2010b).

1.4.1 Metabolic models

In this section, the anaerobic and aerobic/anoxic stoichiometry of the metabolic model developed by Oehmen, Lopez-Vazquez, et al., (2010c) will be described, since this model describes the biochemical activity of six microbial groups of PAOs and GAOs: PAOI and PAOII; denitrifying (DGB) and non-denitrifying *Competibacter* (GB); denitrifying (DDEF) and non-denitrifying *Defluviicoccus* (DEF). In addition, this model also incorporates the carbon source (acetate and propionate), temperature and pH dependencies of these microorganisms obtained through several lab-scale studies.

Anaerobic stoichiometry

According to Oehmen, Lopez-Vazquez, et al., (2010c), the anaerobic stoichiometry is identical for all subgroups of PAOs (PAOI and PAOI) and subgroups of GAOs (DGB, GB, DDEF and DEF).

Smolders et al., (1994a) based on theory of Mino et al. (1987) developed the anaerobic metabolism of PAOs fed with acetate as the sole carbon source (see Figure 1.9). As depicted, PAOs transport acetate across the cell membrane and convert it to acetyl-coa. The energy required for these two steps comes mainly from the cleavage of poly-P and release of phosphate from the cell. The parameter α represents the ATP necessary to transport 1 C-mmol acetate through cell membrane and according to Smolders et al., (1994a) and Filipe et al., (2001c), this parameter is linearly dependent on pH. The origin of reducing power (i.e. NADH) required for the synthesis of PHA has been a topic of discussion by many authors, wherein Mino et al. (1987) supported that come from glycolysis of internally stored glycogen, (Comeau et al., 1986, Louie et al., 2000) from TCA cycle and (Pereira et al., 1996, Wexler et al., 2009, Zhou et al., 2009) from both. Even those that support glycogen degradation as origin of reducing power, there are controversial studies about which pathways PAOs employ for glycolysis: the Entner-Doudoroff (ED) (Maurer et al., 1997, Hesselmann et al., 2000) pathway or the Embden-Meyerhof-Parnas (EMP) pathway (Martin et al., 2006, Wexler et al., 2009, Mino et al., 1987). In the metabolic model developed by Oehmen, Lopez-Vazquez, et al., (2010c), the reducing power is generated through the EMP pathway as theorised by Mino et al. (1987) and confirmed by Martin et al., (2006). Thus, NADH is consumed when two acetyl-CoA molecules are combined together to yield the formation of PHB (Oehmen, 2004).

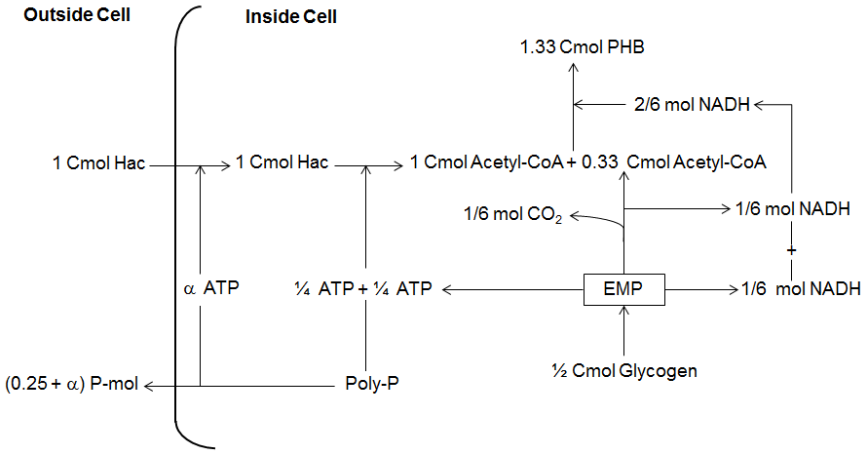

Figure 1.9: Schematic diagram of the anaerobic metabolism of PAOs fed with acetate (Hac) as the sole carbon source (Filipe et al., 2001c).

Figure 1.10 shows the anaerobic metabolism of PAOs fed with propionate as the sole carbon source. Propionate is taken up by PAOs cells and converted to propionyl-CoA, using both poly-P and glycogen hydrolysis as energy sources. Similarly to acetate metabolism, it is unclear the potential contribution of the right branch of the TCA in the production of NADH, while the involvement of glycogen was clearly demonstrated (Oehmen et al., 2007a). The preferred glycolysis pathway is also unclear (Oehmen et al., 2010b). However, Oehmen, Zeng, et al., (2005c) proposed that glycogen is glycolysised to acetyl-CoA, CO_2 and $NADH_2$ through ED pathway. Nevertheless, Oehmen, Lopez-Vazquez, et al., (2010c) later showed that the model is relatively insensitive towards the EMP vs ED pathways for PAOs. Consequently, acetyl-CoA and propionyl-CoA are reduced and condensed to form PHA. As such, four fractions of PHA may be produced, which depends on the molecules that bind together during condensation: PHB, PHV, poly- β-hydroxy-2-methylbutyrate (PH2MB) and PH2MV. Note that PHV and PH2MB are isomers of each other, and by this reason they are grouped together and referred to simply as PHV, which indicates the sum of these two polymers (Oehmen et al., 2005c).

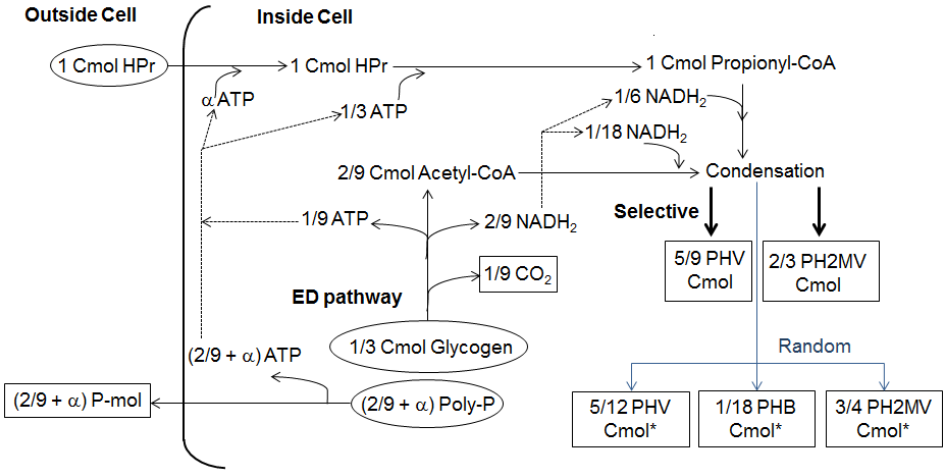

Figure 1.10: Schematic diagram of the anaerobic metabolism of PAOs fed with propionate (HPr) as the sole carbon source (Oehmen et al., 2005c).

The following reaction describes the cell maintenance in anaerobic conditions (Smolders et al., 1995):

$$-HPO_3\ (polyP) - H_2O + H_3PO_4\ (phosphate) = 0$$

The anaerobic processes of GAOs and DGAOs are similar to PAOs, except that poly-P hydrolysis and release as phosphate does not occur (Oehmen et al., 2010c). As shown in Figure 1.11, the main differences, besides those already mentioned, in anaerobic metabolism of GAOs fed with acetate as the sole carbon source in relation to the PAOs are that glycogen hydrolysis to pyruvate provides all the required ATP in the overall process and some of the $NADH_2$. A part of pyruvate is decarboxylated to form acetyl-CoA and CO_2 (providing the additional $NADH_2$), and the rest is converted to propionyl-CoA via the succinate-propionate pathway, which consumes $NADH_2$. Consequently, the acetyl-CoA and propionyl-CoA produced condense randomly to form PHB, PHV and PH2MV (Zeng et al., 2003a).

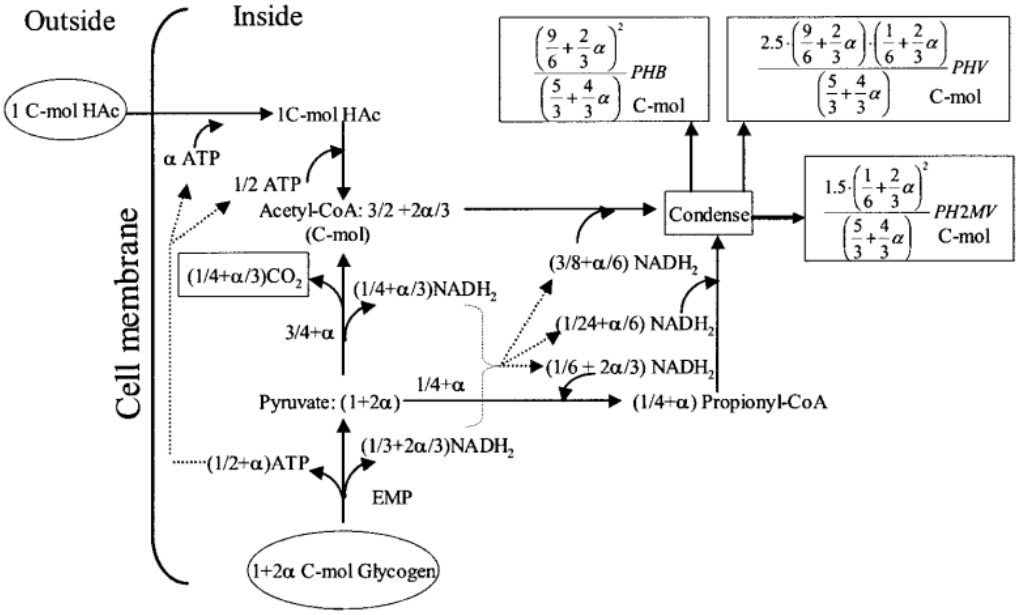

Figure 1.11: Schematic diagram of the anaerobic metabolism of GAOs fed with acetate (Hac) as the sole carbon source (Zeng et al., 2003a)**.**

The Figure 1.12 illustrates the anaerobic metabolism of GAOs fed with propionate, which is very similar to acetate. Note that similarly to PAOs, there are also controversial studies on which pathways: ED (Lemos et al., 2007) or EMP (Filipe et al., 2001a, Zeng et al., 2003a, Oehmen et al., 2006b) GAOs employ for glycolysis. This controversy could be explained by both pathways being active in different subgroups of GAOs.

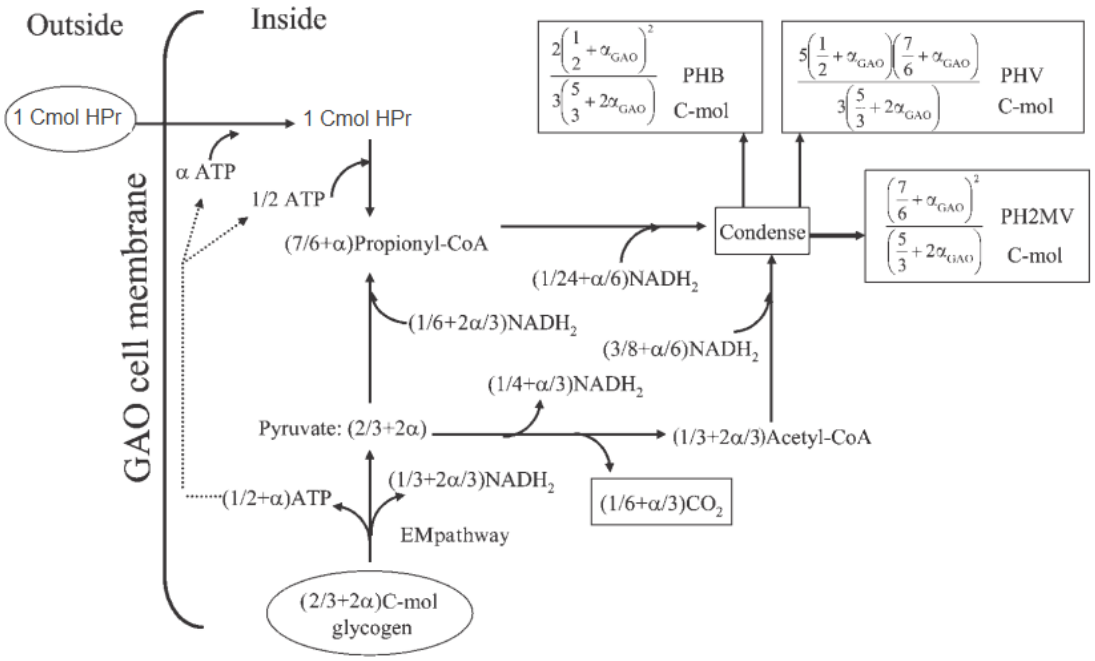

Figure 1.12: Schematic diagram of the anaerobic metabolism of GAOs fed with propionate (HPr) as the sole carbon source (Oehmen et al., 2006b).

Filipe et al., (2001a) proposed that the sole energy source for anaerobic maintenance in GAOs is obtained through glycogen hydrolysis, and Zeng et al., (2003a) showed that glycogen was directly converted to PHA, according to the following reaction:

$$-Glycogen + \frac{1}{6}PHB + \frac{5}{12}PHV + \frac{1}{4}PH2MV + \frac{1}{6}CO_2 + \frac{1}{2}ATP = 0$$

Aerobic and anoxic stoichiometry

The aerobic and anoxic stoichiometry is identical for both conditions, with the sole difference being the electron acceptor (nitrate, nitrite or oxygen) utilised for ATP production (Oehmen et al., 2010c). As already mentioned, PAOs degrade the different fractions of PHA produced in the anaerobic phase, and consequently, they produce acetyl-CoA and propionyl-CoA, which proceed to the TCA cycle by the respective pathways to generate NADH and subsequently ATP through oxidative phosphorylation of NADH (Oehmen et al., 2010c, Oehmen et al., 2007a). As such, this energy is used for P uptake and poly-P production, glycogen production and biomass growth. The GAOs metabolism is similar, except that do not perform P uptake and poly-P production (see Figure 1.13 and Figure 1.14).

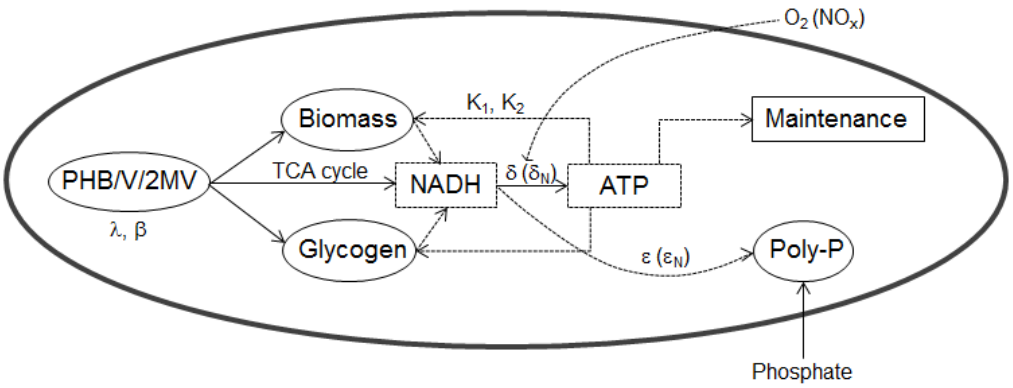

Figure 1.13: Schematic diagram of the aerobic/anoxic metabolism for PAOs. Adapted from (Smolders et al., 1995).

The aerobic and anoxic PHA-based yield coefficients are a function of the P/O ratio (δ and δ_N, also known as Y_{NADH_ATP}. Note that the subscript N is used to refer anoxic conditions), which represents the ATP produced per NADH oxidised during oxidative phosphorylation; the phosphate transport energy (ε and ε_N); the ATP necessary for biomass synthesis (K_1 and K_2) and the percentage of acetyl-CoA* (λ) and propionyl-CoA* (β) in the PHA polymer. The NO_x and oxygen-based yield coefficients were calculated by the PHA-based yield coefficients and the degree of reduction of the PHA polymer, as performed by Zeng et al., (2003a). The biomass degree of reduction was also incorporated in the oxygen and NOx consumed per biomass growth yield coefficient, as performed by Lopez-Vazquez et al., (2009) and A. Oehmen, Lopez-Vazquez, et al., (2010c).

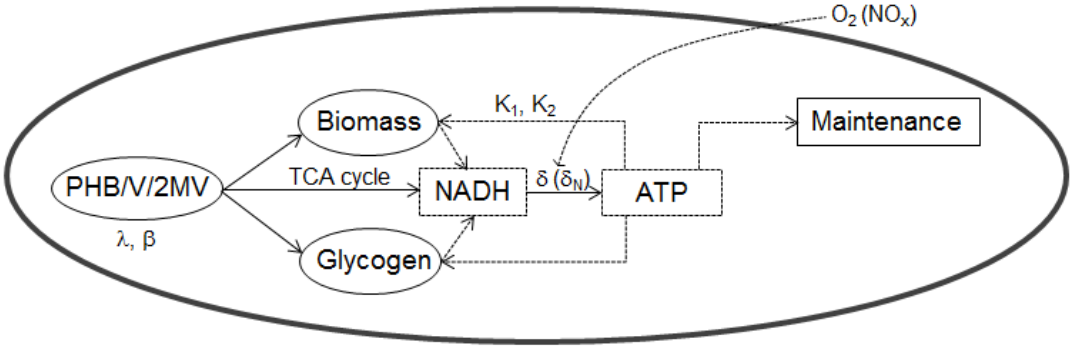

Figure 1.14: Schematic diagram of the aerobic/anoxic metabolism for GAOs. Adapted from (Oehmen, 2004).

1.4.2 ASM models

The International Association on Water Pollution Research and Control (since 2000 the International Water Association, IWA) introduced the ASM1 model for chemical oxygen demand (COD) and N removal in activated sludge systems in 1987 (Meijer, 2004). The ASM3 model comes later, correcting a number of defects that have appeared during the usage of ASM1 model (Gernaey et al., 2004). One of them is that ASM3 model recognises the importance of storage polymers in the heterotrophic activated sludge conversions (Gernaey et al., 2004). The incorporation of the EBPR and

chemical P removal via precipitation comes with ASM2 model and later with ASM2d model. The latter is an extension of the first, which includes two additional processes to account for the fact that PAOs can use cell internal organic storage products for denitrification, i.e. PAOs are able to proliferate not only in aerobic conditions (as proposed by ASM2) but also in anoxic conditions (Henze et al., 1999). The Figure 1.15 illustrates the EBPR approach in ASM2d model, wherein under anaerobic conditions acetate is stored intracellularly as PHB polymer, and the energy source for this conversion comes from the cleavage of poly-P and release of P from the cell. It is noteworthy that all organic storage products are lumped into one model component (X_{PHA}), excluding glycogen in order to reduce model complexity (Gernaey et al., 2004, Henze et al., 1999). Under aerobic or anoxic conditions, PHB is used as energy source for P uptake and biomass growth. Rieger et al., (2001) have incorporated the EBPR process in the ASM3 model, creating the ASM3-BioP model. The ASM2d and ASM3-BioP models have been used in the modelling of full-scale EBPR systems (Wichern et al., 2001, Ingildsen et al., 2006, Lee et al., 2006, Carrette et al., 2001).

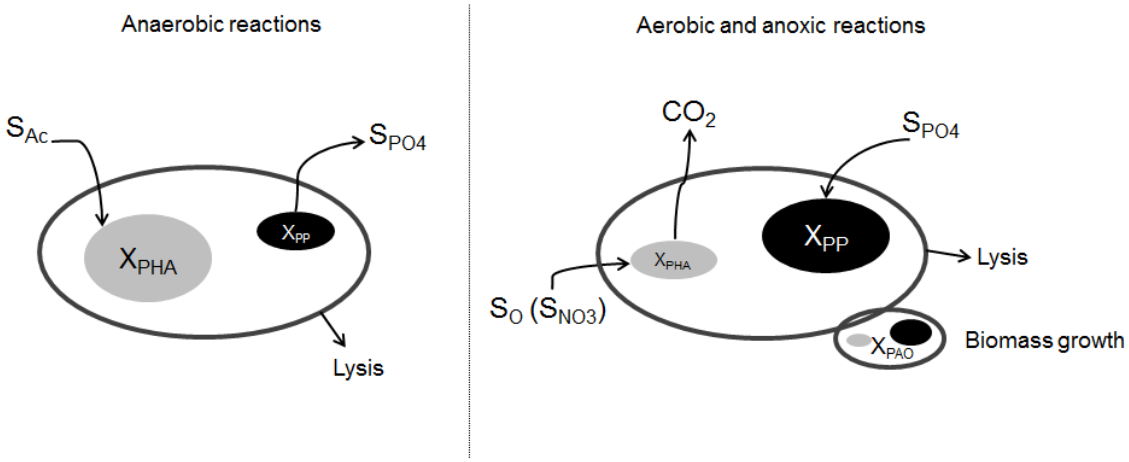

Figure 1.15: EBPR approach of ASM2d model. S_{ac}: acetate; S_{PO4}: soluble otho-phosphate; X_{PHA}: cell-internal storage of PHAs; X_{PP}: stored poly-P; X_{PAO}: active PAO biomass; S_o: dissolved oxygen; S_{NO3}: nitrate plus nitrite nitrogen. Adapted from (Meijer, 2004).

1.4.3 Combined metabolic and ASM models

The most common example of this combination is the TUDP model developed by Technical University of Delft, which combines the metabolic models for denitrifying and non-denitrifying EBPR of Murnleitner et al., (1997) with the ASM2d model (Gernaey et al., 2004). This model has been successfully applied to domestic wastewater treatment plants (WWTPs) with numerous configurations such as University of Cape Town (UCT), modified UCT and A_2N (Oehmen et al., 2007a). Contrary to ASM2d, the TUDP model considers the importance of glycogen as an intermediate product in the P release and P uptake activity of the metabolism of PAOs (Gernaey et al., 2004). However, there are cases of full-scale EBPR plants in the literature where the predicted P release/VFA uptake ratio by this model was substantially higher than that observed experimentally (Brdjanovic et al., 2000, Ky et al., 2001). The main causes for this difference are likely due to the activity of GAOs as well as the effects caused by the uptake of propionate on the metabolism of PAOs and GAOs (Oehmen et al., 2007a).

Therefore, the combination of metabolic model developed by Oehmen, Lopez-Vazquez, et al., (2010c) with ASM2d is very interesting, since this model, as already mentioned, incorporates the varied denitrification tendencies of the different groups and subgroups of PAOs and GAOs as well as their different dependencies on the following factors: carbon source (acetate and/or propionate), temperature and pH.

A summary of the properties of the most important ASM models is given in Table 1.1.

Table 1.1: Overview of activated sludge models. Adapted from (Gernaey et al., 2004).

	ASM1	ASM3	ASM2	ASM2d	ASM3-bio-P	TUDP [1]
Nitrification	X	X	X	X	X	X
Denitrification	X	X	X	X	X	X
Heterotrophic/autotrophic decay	DR, Cst	ER, EA	DR, Cst	DR, Cst	ER, EA	DR, Cst
Hydrolysis	EA	Cst	EA	EA	Cst	EA
EBPR			X	X	X	X
Denitrifying.PAOs				X	X	X
Lysis of PAO/PHA			Cst	Cst	EA	EA
Fermentation			X	X		X
Chemical P removal			X	X		
Reactions	8	12	19	21	23	21
State variables	13	13	19	19	17	17

DR: death regeneration concept; EA: electron acceptor depending; ER: endogeneous respiration concept; Cst: not electron acceptor depending;
[1] TUDP model is a combination of ASM2d model with metabolic models.

1.5 Thesis objectives

The overall objectives of this thesis are:

(1) Understand the behaviour of *Accumulibacter* - *Tetrasphaera* mixed cultures, which are representative of the microbial community of many full-scale EBPR plants.

(2) Combine PAO-GAO metabolic models with ASM models in order to describe better the performance of full-scale EBPR plants.

(3) Through this work, better understand the metabolism of the relevant microbial communities in EBPR systems.

2 ENRICHMENT OF A MIXED CULTURE OF *ACCUMULIBACTER* AND *TETRASPHAERA*-RELATED PAOs

2.1 Objectives

The lack of biochemical knowledge about the metabolism of *Tetrasphaera*-related organisms has been a limiting factor to understand the behaviour of full-scale EBPR systems. Therefore, the aim of this study was to investigate the P removal efficiency and metabolic behaviour of an enriched culture of *Tetrasphaera*-related organisms and *Accumulibacter*, which were acclimatized with casamino acids as sole carbon source. As such, the substrate uptake profile of this mixed culture was investigated by performing batch tests with individual feeding of the following carbon sources: glucose, acetate, propionate, glutamate, aspartate and glycine; and combined feeding of acetate, propionate and casamino acids in order to assess their relative preferences.

2.2 Methods and materials

2.2.1 SBR operation

A SBR with 500 ml of working volume was operated to obtain an enriched culture of *Tetrasphaera*-related organisms and *Accumulibacter* using casein hydrolysate (i.e. casamino acids) as sole carbon source. The SBR was inoculated with sludge from a WWTP in Setubal, Portugal. The cycle time of the SBR was 8 h: 4 h of anaerobic phase, 1 h of settle/decant phase and 3h of aerobic phase. The SBR was fed continuously during the first 3 h of the anaerobic phase with 150 ml of synthetic carbon medium containing casein hydrolysate as the sole carbon source, resulting in a casein concentration in the reactor of 154 mg/L. It was also fed during the first 3 minutes of the aerobic phase with 50 ml of mineral medium and 50 ml of phosphate medium (300 mg P/L). The hydraulic retention time (HRT) and sludge retention time (SRT) were 16 h and 19 days, respectively. Argon was bubbled into the reactor during the anaerobic phase to maintain strict anaerobic conditions. In the aerobic phase, air was bubbled into the reactor at a flow rate of approximately 4.5 L/min. The temperature was controlled at 20 $\pm$ 1ºC and the pH was controlled at 7.1 $\pm$ 0.1 by automatic addition of HCl 0.1 M when the pH was above the set point. The stirring rate was kept constant at 200-400 rpm during the anaerobic and aerobic phases.

The performance of the SBR was monitored through cyclic studies, whereby samples to analyse the carbon source, PHA, glycogen and orthophosphate were taken every hour throughout a cycle and analysed via chemical analytical methods (detailed below). These samples were centrifuged at 10 000 rpm for 5 min and the supernatant and pellet were stored separately at -20ºC, except for orthophosphate samples, wherein it was added 15 μl of H_2SO_4 4.0 M to the supernatant and stored at -4ºC. At the beginning of the anaerobic phase and at the end of the anaerobic and aerobic phases samples to measure total suspended solids (TSS) and volatile suspended solids (VSS) were taken. At

the end of anaerobic and aerobic phases samples for FISH analysis were also taken, and at the end of the aerobic phase a sample to measure total P concentration was taken, which was stored at -20ºC.

2.2.2 Batch tests

A series of batch tests was performed in order to investigate the preferred carbon sources (glucose, acetate, propionate, glutamate, aspartate and glycine) by the enriched culture from the SBR. As such, 3 types of experiments were planned: 1) study the individual uptake of each carbon source during anaerobic phase (4h); 2) same study, but this time for a full anaerobic/aerobic cycle (8h) and 3) study the effect of combined feeding of 3 carbon sources (acetate, propionate and casamino acids) for a full cycle.

For the first experiment, it was performed 7 batch tests: one for each carbon source (glucose, acetate, propionate, glutamate, aspartate and glycine) and another one was selected as blank without carbon source. The tests were conducted in flasks with a working volume of 50 ml. Each flask was inoculated with approximately 17 ml of sludge collected from the main SBR at the end of the cycle, and the sludge was diluted with 33 ml of mineral medium. To ensure anaerobic conditions, nitrogen gas was bubbled into the flasks for 15 minutes and then the flasks were capped and sealed. At the beginning of the experiment a feed pulse of each carbon source (5ml) was added to the respective flask, and samples to analyse carbon source, PHA, glycogen and orthophosphate were taken at various points throughout the anaerobic phase. At the end of the anaerobic phase, samples were taken to measure TSS and VSS. The stirring rate in all batch tests was 250 rpm, the room temperature was 21 $\pm$ 1ºC, the pH of culture media was set at 7.4 $\pm$ 0.1 and the pH of sludge before inoculation was 6.95.

For the second experiment, it was performed 8 batch tests: one for each carbon source (glucose, acetate, propionate, glutamate, aspartate and glycine) and another two were selected as blanks (without carbon source), one was under anaerobic conditions and the other under aerobic conditions. All tests were conducted in batch reactors with 500 ml of working volume, and with the exception of the test without carbon source operated under anaerobic conditions, the others were connected to a respirometer with a working volume of 45 ml, where an oxygen electrode was introduced.

For batch tests with only one carbon source, each reactor was inoculated with approximately 95 ml of sludge collected from the main SBR at the end of the cycle, and the sludge was diluted with 355 ml of effluent from the main SBR. The cycle began after a feed pulse of each carbon source (50 ml) added in the respective reactor. The anaerobic phase lasted 4 h and at the end of this phase the sludge was taken from the reactor and centrifuged (10 min, 6000 rpm). The supernatant was removed in order to prevent cases where the carbon source was not completely consumed. No sludge was wasted and this operation took about 1 h. The reactors were again inoculated with this biomass, diluted with 250 ml of effluent from the main SBR and 50 ml of mineral medium. At the beginning of the aerobic phase, a feed pulse of phosphate media (50 ml) was added to each reactor, and this phase lasted 3 h. This procedure ensured that, besides the carbon source added, the experimental conditions were similar to the main SBR.

In batch tests without carbon source, each reactor was also inoculated with approximately 95 ml of sludge collected from the main SBR at the end of the cycle. However, for reactor under anaerobic conditions the sludge was diluted with 355 ml of effluent from the main SBR and with 50 ml of distilled water. This reactor was operated for 7 h. While for the reactor under aerobic conditions, the sludge was diluted with 155 ml of effluent and 50 ml of mineral medium. The experiment began after a feed pulse of phosphate media (50 ml) and the operation lasted for 7 h.

The setup of the third experiment and the operation conditions were similar to the batch reactors with only one carbon source, except for the following changes. The sludge was diluted with 255 ml of effluent from the main SBR. The cycle began after a feed pulse (150 ml) of a synthetic medium containing acetate, propionate and casamino acids.

The anaerobic and aerobic conditions were maintained by bubbling continuously argon and air, respectively, into the batch reactors. The pH was controlled at 7.1 $\pm$ 0.1 by the addition of HCl 1M and NaOH 1M, and the room temperature was 22 $\pm$ 1 ºC. Samples were taken to analyse the carbon source, PHA, glycogen, orthophosphate, total P concentration, TSS and VSS, and were processed in the same way as that in the main SBR.

2.2.3 Culture media

The composition of the SBR culture media are described as follow: the synthetic carbon medium contained per litre 0.53 g casein hydrolysate (Fluka); the mineral medium contained per litre: 0.74 g NH_4Cl, 1.19 g $MgSO_4.7H_2O$ g, 0.55 g $CaCl_2.2H_2O$, 0.01 g allyl-N thiourea (ATU, a nitrification inhibitor), 0.04 g ethylene-diaminetetraacetic (EDTA) and 3.96 ml micronutrient solution. The micronutrient solution used was identical to that in (Smolders et al., 1994a) and consisted of per litre: 1.5 g $FeCl_3.6H_2O$, 0.15 g H_3BO_3, 0.03 g $CuSO_4.5H_2O$, 0.18 g KI, 0.12 g $MnCl_2.4H_2O$, 0.06 g $Na_2MoO_4.2H_2O$, 0.12 g $ZnSO_4.7H_2O$ and 0.15 g $CoCl_2.6H_2O$. The phosphate medium contained 0.95 g K_2HPO_4 and 0.58 g KH_2PO_4 per litre. The synthetic media of carbon and mineral as well as micronutrient solution were autoclaved at 121ºC and 1 bar during 20 min, but prior to this, the pH was set to 7.4 $\pm$ 0.1 by the addition of NaOH 1.0 M in the casein and the mineral media.

In the batch tests, the mineral and phosphate media had the same composition described for the SBR. For the batch tests with only one carbon source performed in flasks (1st experiment) and in reactors (2nd experiment), it was selected an initial concentration of 2mM for the carbon sources (glucose, acetate, propionate, glutamate, aspartate and glycin). For the 3rd experiment, it was selected an initial concentration in reactor of 2.90 C-mmol/L for each carbon source (acetate, propionate and casein hydrolysate), which was similar to the initial concentration in the main SBR. Therefore, the synthetic medium contained per litre: 0.66 g $CH_3COONa.3H_2O$, 0.24 g $C_3H_6O_2$ and 0.18 g casein hydrolysate. In all carbon source media, the pH was set to 7.4 $\pm$ 0.1 by the addition of NaOH 1.0 M.

2.2.4 Chemical analyses

Inorganic phosphate was determined by segmented flow analysis (Skalar 5100, Skalar Analytical, The Netherlands) by the colorimetric method based on the reduction of the phosphomolybdate complex with ascorbic acid, as described by Serafim et al., (2004).

Total P concentration was also determined by segmented flow analysis (Skalar 5100, Skalar Analytical, The Netherlands). Prior to injection, 0.5 ml cell suspension (stored at -20ºC) was mixed with 400 mg potassium persulphate and 5 ml H_2SO_4 0.3 M, and digested for 1 h at 100ºC.

VFAs and glucose were measured by high-performance liquid chromatography (HPLC) using a Metacarb 87 H (Varian) column and a refractive index detector (RI-71, Merck). The mobile phase was H_2SO_4 0.01 N solution at a flow rate of 0.6 ml/min and the column was operated at 50ºC. Prior to injection, 700 μl of supernatant (stored at -20ºC) was acidified with 50 μl of H_2SO_4 0.05N and filtered using a 0.2 μm membrane.

The casein hydrolysate uptake was assessed through the analysis of total organic carbon (TOC) by a Shimadzu analyser.

PHA was determined according to the methodology described by (Lanham et al.). Briefly, the pellet stored at -20ºC was lyophilized overnight and 4 mg of biomass was then mixed with 1 ml of acidic methanol (20% H_2SO_4 v/v) and 1 ml of chloroform solution, which contained 1 mg/ml heptadecane (Fluka) as internal standard. This mixture was digested for 5 h at 100ºC. After cooling, 0.5 ml of water was used for extraction, and the sample was then mixed for 1 minute in a vortex mixer. The chloroform phase was collected and molecular sieves (0.4 nm, Prolabo) were added for water adsorption. The organic phase was injected into a gas chromatograph (Bruker 430-GC) coupled to a flame ionization detector and equipped with BR-SWax column (60 m, 0.53 mm internal diameter, 1 μm film thickness, Bruker, USA). Helium was the carrier gas at a constant pressure (14.5 psi). The temperature of injection was 280ºC, the temperature of the detector was 230ºC and the temperature ramp started at 40ºC, then increased at a rate of 20ºC/min until 100ºC, further increased at a rate of 3ºC/min until 175ºC, and finally increased again at 20ºC/min until 220ºC, to ensure a cleaning step of the column after each injection. The calibration curve was obtained by injecting standards of HB, HV, H2MB (by a co-polymer of PHB-PHV, 88:12 wt, Aldrich) and H2MV (by a 2-hydroxy-caproic acid, Aldrich) with different dilutions.

Glycogen was determined using the method described by Lanham et al., (2012). Briefly, the pellet stored at -20ºC was lyophilized overnight and 2 mg biomass was then mixed with 2 ml of HCl 0.9 M and digested for 3h at 100ºC. The samples were cooled in an ice bath, the supernatant was extracted, filtered using a 0.2 μm membrane and glucose was analysed by HPLC. A CarboPac PA10 column (Dionex) and an amperometric detector were used and the analyses were operated at 30ºC and a flow rate of 0.8 ml/min, with sodium hydroxide (NaOH 18 mM) as eluent.

TSS and VSS were determined according to standard methods (APHA-American Public Health Association, 1995).

2.2.5 Microbial characterisation

Sludge samples for probing gram-positive and gram-negative *Bacteria* were fixed in 98% ethanol and 4% paraformaldehyde, respectively. FISH was performed according to Amann, (1995) to assess the evolution of the microbial population in the SBR. The following oligonucleotide probes were used: EUBMIX (equimolar concentrations of EUB338, EUB338II, and EUB338III, see (Amann et al., 1990,

Daims et al., 1999)) that target all *Bacteria*; PAOMIX (PAO651, PAO462 and PAO846, see (Crocetti et al., 2000)) that target most members of the *Accumulibacter* cluster; and Tet1-266, Tet2-892, Tet2-174 and Tet3-654 that target most *Tetrasphaera*-related organisms (Hien et al., 2011). Details on oligonucleotide probes employed for FISH as well as the percentage of formamide used to hybridize each probe are listed in Table 2.1. FISH samples were observed using an Olympus BX51 epifluorescence microscope.

Table 2.1: Oligonucleotide FISH probes employed in this study.

Probe	Sequence 5'-3'	Specifity	Formamide (%)	Reference
EUB338	GCTGCCTCCCGTAGGAGT	Most *Bacteria*	0-50	Amann et al., (1990)
EUB338-II	GCAGCCACCCGTAGGTGT	*Planctomycetales* and other *Bacteria* not detected by EUB338	0-50	Daims et al., (1999)
EUB338-III	GCTGCCACCCGTAGGTGT	*Verrucomicrobiales* and other *Bacteria* not detected by EUB338	0-50	Daims et al., (1999)
PAO462	CCGTCATCTACWCAGGGTATTAAC	Most *Accumulibacter*	35	Crocetti et al., (2000)
PAO651	CCCTCTGCCAAACTCCAG	Most *Accumulibacter*	35	Crocetti et al., (2000)
PAO 846	GTTAGCTACGGCACTAAAAGG	Most *Accumulibacter*	35	Crocetti et al., (2000)
Tet1-266	CCCGTCGTCGCCTGTAGC	Uncultured *T. elongata*	25	Hien et al., (2011)
Tet2-892	TAGTTAGCCTTGCGGCCG	Clone ASM47	5	Hien et al., (2011)
Tet2-174	GCTCCGTCTCGTATCCGG	*T. jenkinsii*, *T. australiensis*, *T. veronensis*, and *Candidatus N. limicola*	20	Hien et al., (2011)
Tet3-654	GGTCTCCCCTACCATACT	Uncultured *Tetrasphaera*	35	Hien et al., (2011)

2.3 Results and discussion

2.3.1 Main SBR performance

Cyclic studies were performed for the SBR to display typical reactor phenotypes and to ensure steady state operation before batch tests with different carbon sources. As shown in Figure 2.1, both PAOs groups in study (*Tetrasphaera*-related organisms and *Accumulibacter*) were identified by their respective hybridization probes. However, *Tetrasphaera*-related organisms were the most abundant PAO group in all cyclic studies performed before batch tests. The Table 2.2 show the different morphologies observed in each probes (note that not all morphologies are visible in Figure 2.1). It is noteworthy that the same diversity of morphotypes was observed by Hien et al. (2011) in *Tetrasphaera*-related organisms.

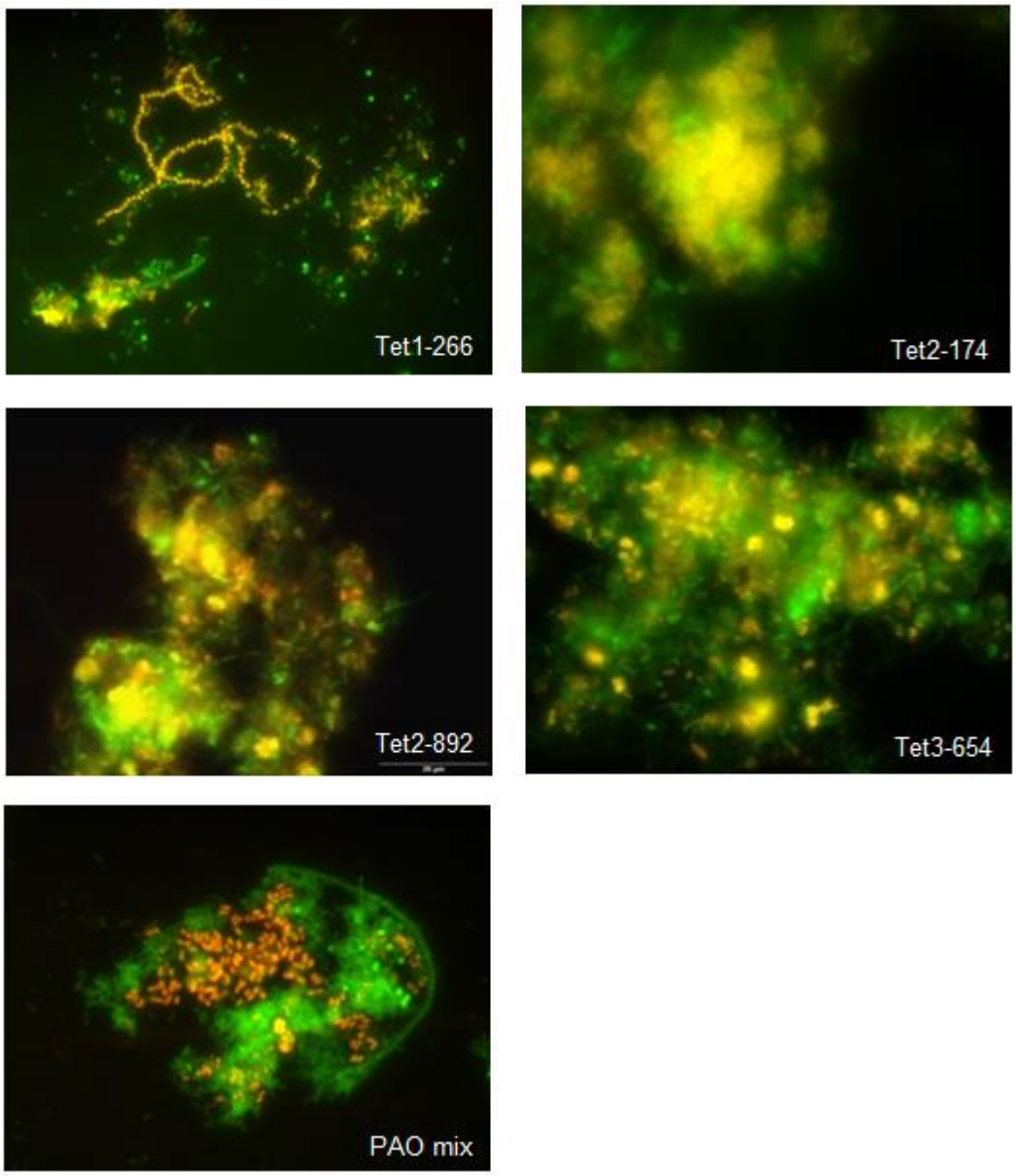

Figure 2.1: Epifluorescence micrographs of SBR sludge hybridised with probes Tet1-266, Tet-892, Tet2-174, Tet3-654, PAOMIX (Cy3-labelled). All samples were also hybridised with FITC-labelled EUBMIX. *Accumulibacter* and *Tetrasphaera* are shown in yellow and other *Bacteria* are shown in green.

Table 2.2: Different morphologies observed by FISH in the SBR sludge.

Probe	Morphology
Tet1-266	Branched rods, short rods in clumps, cluster of tetrads and irregular cocci
Tet2-892	Cluster of tetrads, filaments and short rods in clumps
Tet2-174	Small cocci and irregular cocci
Tet3-654	Branched rods, short rods in clumps and irregular cocci
PAOMIX	Rods and short rods in clumps

Figure 2.2 shows the metabolic transformations of the SBR, wherein the culture in study demonstrated anaerobic P release, glycogen hydrolysis, a very low PHA synthesis and high casamino acids uptake (about 77-83%); followed by aerobic P uptake (about 100%), glycogen formation and a very low PHA oxidation.

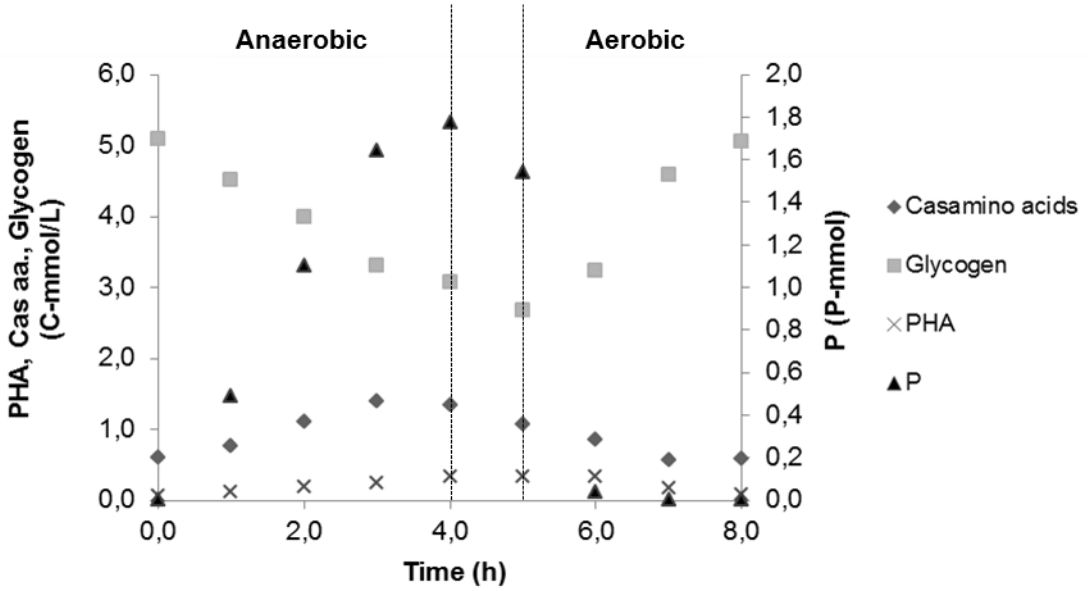

Figure 2.2: Cycle study showing carbon, glycogen, PHA and P transformations from a typical cycle in the SBR. Note that the amount of PHA is the sum of the values of PHB, PHV and PH2MV. However, PHV was the most significant fraction.

The chemical data summarized in Table 2.3 shows that the PHA to substrate uptake ratios of this mixed culture are negligible compared to *Accumulibacter* ratios. It agrees with several studies, which refer that most *Tetrasphaera*-related organisms are not able to produce and oxidize PHA, except in filamentous species and *Tetrasphaera japonica* (McKenzie et al., 2006, Kristiansen et al., 2013). Contrary to what Kristiansen et al., (2013) observed in their studies, in this study glycogen is degraded anaerobically and regenerated aerobically. Thus, it is still unknown which internal storage polymer is used as carbon source by this mixed culture, and consequently, energy source for their aerobic biochemical pathways. This contrast may be due to the fact that glucose, instead of casamino acids was fed in Kristiansen et al., (2013). The ratios of P release and glycogen hydrolysis per carbon mol of substrate uptake are very similar to *Accumulibacter* ratios. It suggests that the energy required for substrate uptake comes mainly from the cleavage of poly-P and release of phosphate from the cell, since if this energy came from glycogen hydrolysis, the glycogen to substrate ratio would be higher as it happens with GAOs. Note that this conclusion is possible because methylene blue staining was employed to confirm the cycling of stored poly-P (data not shown). Aerobically, this mixed culture was able to take up P and produce poly-P as shown by the data in Table 2.3, wherein the percentage of P in TSS was very similar to the *Accumulibacter*.

Table 2.3: Biochemical transformations from a typical cycle in the SBR: comparison with metabolic models of *Accumulibacter* fed with acetate or propionate as sole carbon source.

Anaerobic results			
	Accumulibacter+Tetrasphaera (this study)	*Accumulibacter*	
Carbon source	Casein hydrolysate	Acetate	Propionate
P release/substrate (P-mol/C-mol)	0.40	0.50 [a]	0.40 [b]
Glycogen/substrate (C-mol/C-mol)	0.45	0.50 [a]	0.33 [b]
PHB/substrate (C-mol/C-mol)	0.01	1.33 [a]	0.00 [b]
PHV/substrate (C-mol/C-mol)	0.04	0.00 [a]	0.56 [b]
PH2MV/substrate (C-mol/C-mol)	0.01	0.00 [a]	0.67 [b]
PHA/substrate (C-mol/C-mol)	0.06	1.33 [a]	1.23 [b]
Anaerobic pH	6.7±0.1	7	7
Aerobic results			
P uptake (Pmmol/L)	1.54	2.50 [c]	2.20 [c]
% P in TSS	8-19	7-17 [d]	7-17 [d]
Glycogen production (C-mmol)	2.38	3.62 [e]	3.78 [f]

[a] (Smolders et al., 1994a); [b] (Oehmen et al., 2005a); [c] (Oehmen et al., 2005b); [d] (Oehmen et al., 2007a); [e] (Smolders et al., 1994b) and [f] (Oehmen et al., 2007b).

2.3.2 Batch tests performance

Batch tests were performed with sludge from the main SBR to study the effects of a switch in carbon source from casein hydrolysate to one of the following carbon sources: glucose, acetate, propionate, glutamate, aspartate and glycine. The batch tests results are presented in Figure 2.3, Figure 2.4 and Figure 2.5. However, this discussion will be more focused on batch tests with individual feeding of acetate, propionate and glucose, and on the batch test with combined feeding of acetate, propionate and casamino acids, since it was not possible to have ready the results of amino acids uptake prior to the date of delivery of this thesis.

Comparing the profiles of acetate uptake obtained in the first two experiments (performed in flasks and in a batch reactor, respectively), it is possible to observe that both have a similar trend (see Figure 2.3-A and D). In both experiments acetate was completely consumed (about 4.0 C-mmol/L) and accompanied by anaerobic P release. A significant level of anaerobic propionate uptake was also observed in the 1st experiment and 2nd experiments (see Figure 2.3-A and D). Propionate was also completely consumed in the 1st experiment (about 6.0 C-mmol/L, after 2.25 h of operation) and almost consumed in the 2nd experiment (about 84%, 5.0 C-mmol/L). The profile of glucose uptake was significant in both experiments, although it was not completely consumed over time (only 3.5 C-mmol/L and 2.71 C-mmol/L in the 1st and 2nd experiments, respectively), and slightly lower as compared with propionate (5.0 C-mmol/L and 6.0 C-mmol/L, respectively) and acetate (4.0 C-mmol/L

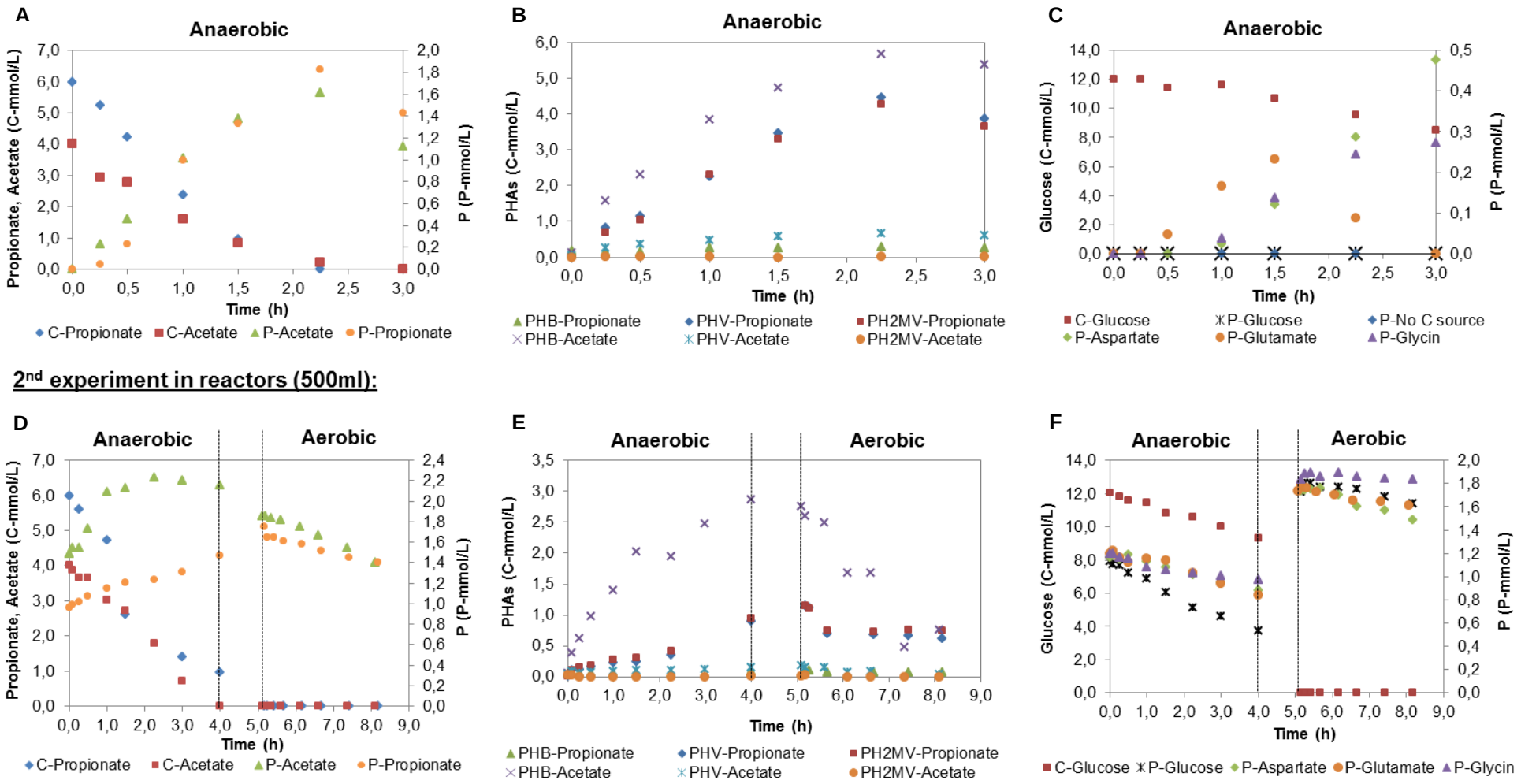

Figure 2.3: Comparison of carbon, P and PHAs profiles between batch experiments (1st and 2nd) performed with different carbon sources (acetate, propionate, glucose, glutamate, aspartate and glycine. Carbon profiles are only shown for tests with acetate (A and D), propionate (A and D) and glucose (C and F); P profile is shown for each test (A, C, D and F); PHAs profiles are only shown for tests with acetate and propionate (B and E).

3rd experiment in reactors (500 ml):

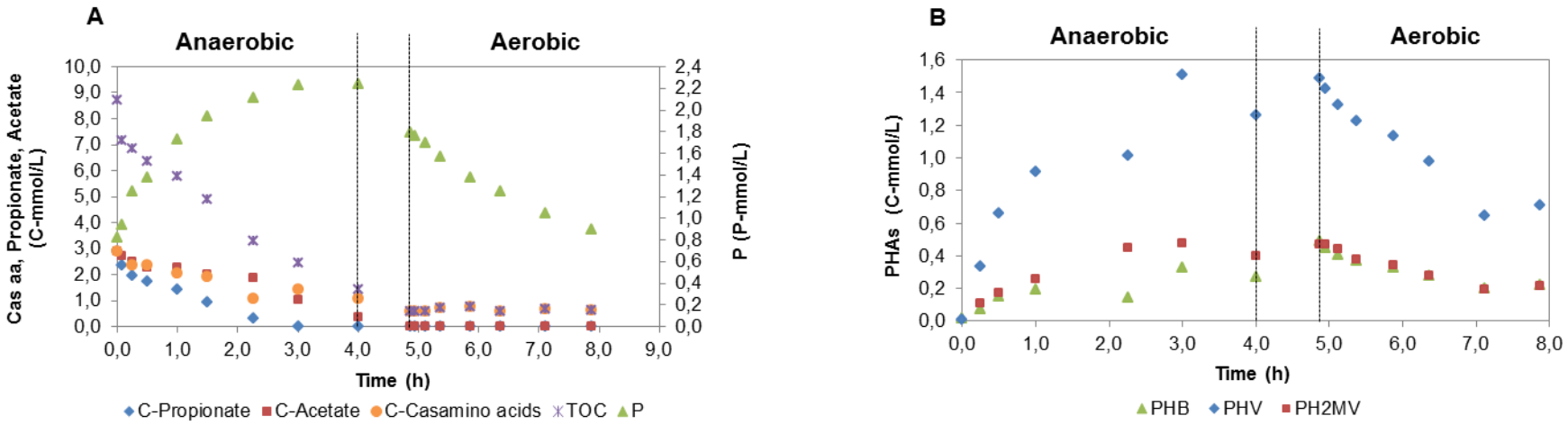

Figure 2.4: Results of batch experiment (3rd) performed with a combined feeding of acetate, propionate and casamino acids. A) Carbon and P profiles and B) PHAs profiles.

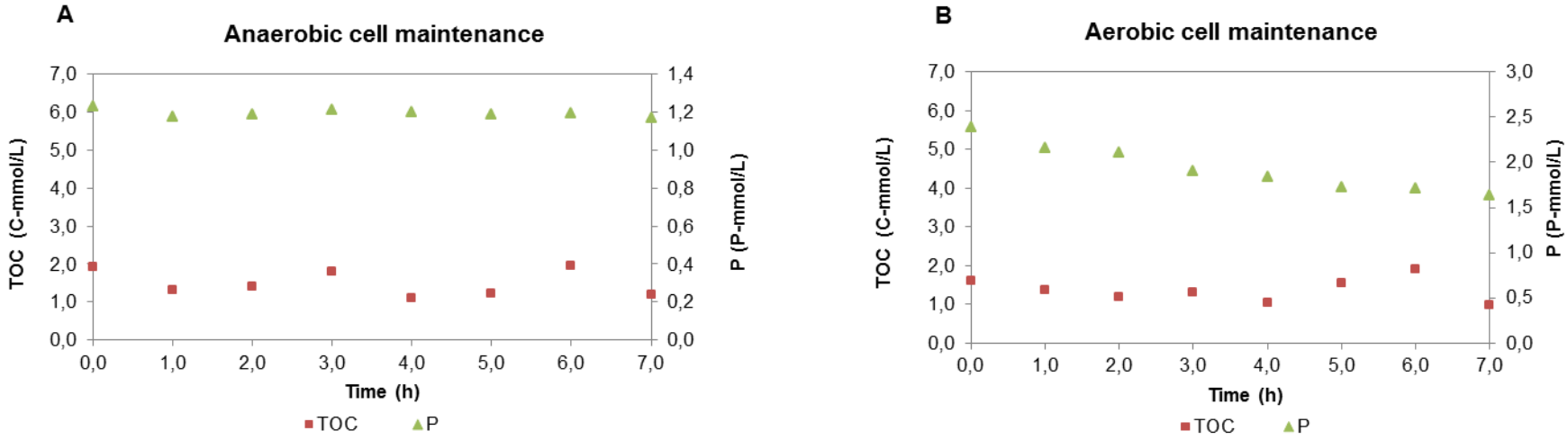

Figure 2.5: Comparison of TOC and P profiles between anaerobic (A) and aerobic (B) maintenance experiments.

in both experiments) (see Figure 2.3-C and F).

The comparison between the uptake rates of acetate and propionate in the 1st and 2nd experiments is not very appropriate because they were fed different concentrations in C-mmol/L of each carbon source (this was performed in order to be consistent on a molar basis). However, this comparison can be made in the 3rd experiment since it was fed 2.90 C-mmol/L of each of the following carbon sources: acetate, propionate and casamino acids. As shown in Figure 2.4-A, the propionate was completely taken up by the mixed culture, and its uptake rate was the highest. About 88% of the acetate was consumed (corresponding to 2.54 C-mmol/L) and about 64% of casamino acids (corresponding to 1.85 C-mmol/L) were consumed. Noteworthy in this test, is that the uptake rate of acetate increased after propionate depletion, showing that propionate was preferred over acetate by the culture.

Relatively to P profiles, in both experiments with individual feed of acetate and propionate, P release was observed during the anaerobic phase (see Figure 2.3-A and D), and the same happened in the 3rd experiment with combined feeding of 3 carbon sources (see Figure 2.4-A). Aerobic P uptake was observed in the 2nd and 3rd experiments (these values are listed in Table 2.4). It is noteworthy that the initial concentration of phosphorus in the 2nd and 3rd experiments was different from zero (about 25-46 mg P/L) because contrary to what was done in the 1st experiment, wherein the sludge was diluted only with mineral medium, in these experiments the sludge was also diluted with effluent from the main SBR. Nonetheless, this effluent contains P since the settle/decant phase occurs between the anaerobic and aerobic phase. However, the fact that the initial concentration of P was different from zero makes these results more interesting since it is closer to the operation of a WWTP.

For this reason, surprising results were achieved relatively to P profiles with individual feed of glucose, aspartate, glutamate and glycine in the 2nd experiment. As shown in Figure 2.3-F, P uptake was observed during anaerobic phase in all tests: 19 ppm with glucose and 7-11 ppm with the other carbon sources (see Table 2.4). Considering that a typical value of P uptake in WWTPs is about 10 ppm, the values obtained in these tests cannot be ignored. The same did not happen in the 1st experiment, because as already mentioned the initial concentrations of P in these tests were zero. Consequently, there was a slight release of P with these carbon sources, except in the glucose test (see Figure 2.3-C and Table 2.4).

An important observation must be evidenced based on the results obtained with glucose. It means that in the 1st experiment no P release happened during anaerobic phase, in the 2nd experiment instead of P release there was anaerobic P uptake (19 ppm) and the aerobic P uptake was insignificant (3 ppm). Therefore, this may suggest that anaerobically, this mixed culture is able to uptake P through fermentation of glucose that provides the required energy. On the other hand, the fact of P uptake in the aerobic phase was insignificant may suggest that the cells depleted all energy produced by fermentation of substrates in anaerobic P uptake. However, this observation can be confirmed only when no other source of energy is present in the anaerobic phase. No PHA production was found with glucose as carbon source, and relatively to glycogen it was not possible to have the results ready prior to the date of delivery of this thesis.

Table 2.4: Batch tests results of P release and uptake.

Carbon source	Anaerobic P release or uptake (mg P/L)	Aerobic P uptake (mg P/L)
-Acetate		
1st exp. in flasks	49.98	-
2nd exp. in reactor	20.71	14.13
-Propionate		
1st exp. in flasks	56.49	-
2nd exp. in reactor	15.60	10.84
-Glucose		
1st exp. in flasks	0.00	-
2nd exp. in reactor	-18.51	3.07
-Aspartate		
1st exp. in flasks	14.76	-
2nd exp. in reactor	-8.90	7.69
-Glutamate		
1st exp. in flasks	7.18	-
2nd exp. in reactor	-11.14	3.72
-Glycine		
1st exp. in flasks)	8.47	-
2nd exp. in reactor	-7.03	0.00
-Acetate + Propionate + Casein	43.93	27.70

Relatively to the results obtained with aspartate, glutamate and glycine, although there was a slight P release in the 1st experiment, when its values are compared with those of acetate and propionate, it is evident that these releases were insignificant. On the other hand, in all tests (2nd experiment) the anaerobic P uptake was higher than aerobic P uptake. Thus, the same explanation given for the glucose test may be applied here, since no PHA production was found in all tests.

Anaerobic PHA production and aerobic PHA oxidation were obtained with batch tests fed with acetate and propionate as sole carbon sources and with combined feed of 3 carbon sources (see Figure 2.3-B and E and Figure 2.4-B). Analysing the chemical data summarized in Table 2.5, it is possible to verify that the ratios of PHA production per substrate uptake obtained with acetate and propionate in the 1st experiment are very close to *Accumulibacter* ratios, as well as the ratios of P release to substrate uptake. PHB was the fraction most produced when acetate was fed as sole carbon source, and PHV and PH2MV were the most produced when propionate was fed as sole carbon source. This correlates very well with *Accumulibacter* activity, since the same happens when this culture is dominant. Therefore, it may be suggested that the percentage of *Accumulibacter* present in this culture was mainly responsible for acetate and propionate uptake. However, it must be confirmed by MAR-FISH analysis. On the other hand, comparing the ratios obtained in the 1st experiment with the 2nd, it is clear that although the same trend remains relative to the fractions with higher production by each carbon source, in the 2nd experiment the ratios are lower. It may be suggested that a possible change in microbial population existed between these two tests, wherein *Accumulibacter* activity seems to be more inhibited in the 2nd experiment. In the 3rd experiment with combined feed of acetate, propionate and casamino acids, the PHA production led mainly to PHV, although the ratios were quite low as was the case in the 2nd experiment. Relatively to the P release to substrate uptake ratio, they are also similar to the *Accumulibacter* ratios in the 1st experiment. This again suggests that *Accumulibacter* were the main organisms responsible for the activity with acetate

and propionate substrates. The P release to substrate uptake ratio was also lower in the 2nd experiment and of a similar level in the 3rd experiment. It should be noted that it could be that the presence of GAOs also had an influence on the activity of the culture. This can only be confirmed after further FISH analysis and comparison of the results with the glycogen utilisation ratios.

Table 2.5: Comparison of anaerobic biochemical transformations between batch experiments and metabolic models of *Accumulibacter*.

Carbon source	P release or uptake/subs.	PHB/subs.	PHV/subs.	PH2MV/subs.	PHA/subs.
- Acetate					
1st exp. in flasks (this study)	0.40	1.38	0.15	0.00	1.53
2nd exp. in reactor (this study)	0.17	0.70	0.03	0.00	0.72
Accumulibacter	0.50 [a]	1.33 [a]	0.00 [a]	0.00 [a]	1.33 [a]
-Propionate					
1st exp. in flasks (this study)	0.30	0.02	0.74	0.71	1.47
2nd exp. in reactor (this study)	0.10	0.00	0.18	0.18	0.36
Accumulibacter	0.40 [b]	0.00 [b]	0.56 [b]	0.67 [b]	1.23 [b]
-Glucose					
1st exp. in flasks (this study)	0.00	0.00	0.00	0.00	0.00
2nd exp. in reactor (this study)	-0.22	0.00	0.00	0.00	0.00
-Acetate + Propionate + Casein (this study)	0.19	0.04	0.17	0.05	0.26

Note: All data expressed in C-mol/Cmol, apart from P release or uptake/subs., which is expressed in P-mol/Cmol.
[a] (Smolders et al., 1994a); [b] (Oehmen et al., 2005a); [c] (Oehmen et al., 2005b); [d] (Oehmen et al., 2007a); [e] (Smolders et al., 1994b) and [f] (Oehmen et al., 2007b).

The results summarized in Table 2.6 show that comparing to *Accumulibacter*, less PHA was used by the culture in this study for P uptake in acetate and propionate tests. However, the fact that the PHA oxidised to P uptake ratio was higher for the experiments as compared to the metabolic model, may also suggest that GAOs were present in the tests, contributing to PHA oxidation. However, this observation must be confirmed by FISH analysis. In the combined feed test less PHA was used per P uptake. This may also reflect that storage compounds from casamino acids were also contributing towards aerobic P uptake in this test.

Table 2.6: Comparison of aerobic biochemical transformations between batch experiments and metabolic models of *Accumulibacter*.

Carbon source	PHA oxidation/P uptake (C-mol/P-mol)	PHA oxidation/PHA storage (%)
- Acetate		
2nd exp. in reactor (this study)	4.66	73.59
Accumulibacter	3.0 [a]	93.9 [a]
-Propionate		
2nd exp. in reactor (this study)	2.79	53.26
Accumulibacter	2.3 [a]	78.1 [a]
-Acetate + Propionate + Casein (this study)	1.46	68.59

[a] (Oehmen et al., 2005b).

The results of anaerobic and aerobic cell maintenance are represented in Figure 2.5-A and B, respectively. As shown in this Figure, the TOC profiles are constant over time, which makes sense since no carbon source was fed in these tests. No P release was found in anaerobic cell maintenance, while in the aerobic test, P uptake (23.57 mg P/L) was found. It suggests that in anaerobic maintenance, the cells use other type of energy source instead of P. On the other hand, in the test of aerobic maintenance, it is observable that the cells were able to use the energy provided by the remaining unidentified internal storage compound for P uptake. It means that the internal storage compound was not completely oxidized during the aerobic phase of the main SBR (note that the batch tests were inoculated with sludge from the main SBR at the end of the aerobic phase).

2.4 Conclusions and recommendations for future research

The metabolic behaviour of an enriched culture of *Tetrasphaera*-related organisms and *Accumulibacter* acclimatized with casamino acids as sole carbon source was identified. Anaerobically, this culture was able to perform: casamino acids uptake, P release, glycogen hydrolysis and very low PHA synthesis. On the other hand, in the aerobic phase this culture was able to perform: P uptake, glycogen formation and very low PHA oxidation. Future work is recommended in order to identify which polymer is produced in the anaerobic phase, and is used as carbon source, and consequently, energy source in the subsequent aerobic phase. It is noteworthy that both PAO groups were identified by their respective hybridization probes. However, *Tetrasphaera*-related organisms were the most abundant PAO group in all cyclic studies.

The substrate uptake profile of this culture and their relative preferences was found by performing batch tests with individual feeding of glucose, acetate, propionate, glutamate, aspartate and glycine; and combined feeding of acetate, propionate and casamino acids. Carbon uptake was found in the tests with acetate, propionate and glucose as sole carbon source and in the test with combined feeding of 3 carbon sources. Relatively to the amino acids uptake, it was not possible to have their results ready to be presented in this thesis.

By comparing the ratios of PHA produced per substrate uptake between *Accumulibacter* model and the tests performed with acetate and propionate as sole carbon source, it was found similar ratios and the same trend relatively to the fractions with higher production. Therefore, it is possible to conclude that the *Accumulibacter* population present in this culture was likely responsible for the uptake of acetate and propionate and production of PHAs. However, MAR-FISH analysis must be done in order to confirm this theory and the same tests should be repeated, because in the 2nd experiment the activity of *Accumulibacter* population seems to be inhibited, and due to this reason, the ratios of PHA produced per substrate uptake were smaller. Anaerobic P release and aerobic P uptake was clearly found in these tests as well as in the test fed with 3 carbon sources. However, in the last test the PHA production was not as high as in the previous tests.

Interesting results were obtained relative to the P profiles in the tests fed with aspartate, glutamate, glycine and glucose as sole carbon source. In these tests (2nd experiment) the sludge was diluted with effluent from the main SBR (rich in P). Consequently, it was found anaerobic P uptake in all tests and the aerobic P uptake was negligible in most of them, particularly in the tests fed with glucose, glutamate and glycine. Based on these results and also due to the fact of in the 1st experiment the P release was insignificant, it is possible to suggest that this mixed culture is able to perform anaerobic P uptake through fermentation of these substrates that provides the required energy. MAR-FISH analysis must be performed in order to detect which PAO group is responsible for the uptake of these carbon sources. However, since P profiles of these tests were different from the P profiles obtained when acetate and propionate were fed as sole carbon source, and considering that it was suggested that *Accumulibacter* were responsible for the uptake of VFAs, it is possible to conclude that *Tetrasphaera*-related organisms were likely responsible for both glucose and amino acids uptake.

As described, the goals of this thesis were achieved and some of the observations evidenced may contribute to a better understanding of the metabolism of *Tetrasphaera*-related organisms and also to clarify their behaviour in a mixed culture enriched with them and *Accumulibacter* organisms. However, these tests must be repeated in order to confirm these conclusions, and also should be compared with MAR-FISH results. It is noteworthy that some of these comments were made without knowledge of the glycogen activity and amino acids uptake, thus these results must be analysed further in order to confirm or not the observations suggested.

3 IMPLEMENTATION OF EBPR METABOLIC MODELS INTO GPS-X 6.2 PROGRAM

3.1 Objectives

The aim of this study is to combine the metabolic model developed by Oehmen, Lopez-Vazquez, et al., (2010c) with ASM2d in collaboration with Hydromantis Environmental Software Solutions, Inc.. This model will provide an improved prediction of full-scale EBPR performance with the advantage of requiring fewer parameters to be calibrated. As such, the model will be available to be used by practitioners in the GPS-X 6.2 software, which is a very powerful simulator for dynamic simulation of municipal and industrial WWTPs.

3.2 Methods and materials

3.2.1 Model development

The model was developed by incorporating, in an overall model, the metabolic model developed by Oehmen, Lopez-Vazquez, et al., (2010c) and the ASM2d developed by Henze et al., (1999). A brief introduction about these two models was made in the section 1.4-Process modelling.

The integrated metabolic/activated sludge model was implemented in the Model Developer (MD) tool, which is an application within GPS-X. The following sections of MD were filled and adapted according to the model developed: GPS-X libraries, stoichiometric matrix, model kinetics, model parameters and composite variables. The GPS-X libraries tab contains information on the existing set of state variables, composite variable stoichiometry parameters and composite variable calculations. Modifications were made in the cnpiplib library of MD in order to adapt their terminology according to the metabolic model of Oehmen, Lopez-Vazquez, et al., (2010c) (see Appendix I). The stoichiometric matrix tab shows all available models, including this model, and has information about stoichiometric matrix and conservation matrix of each model (see Appendix II). The saturation/inhibition functions, kinetic equations and any other additional rates of each model are listed in the model kinetics tab (see Appendix III). All parameters (state variables, stoichiometric parameters and kinetic parameters) are detailed in the model parameters tab (see Appendix IV). Composite variables are the last tab of MD, and here, the stoichiometry of each model is assigned to the fixed GPS-X composite variable stoichiometry (see Appendix V).

A criterion of the tool is that the concentration of all organic materials, including biomass, must be defined in COD units. This condition was suggested by International Water Association, IWA, since this measure provides a link between electron equivalents in the organic substrate, the biomass and the oxygen utilized. As such, one of the tasks of this work was to convert the C-mol units used in the metabolic model developed by Oehmen, Lopez-Vazquez, et al., (2010c) to COD units. In the calculation a value of 34.4 g COD/C-mol biomass was used (as performed by Van Veldhuizen et al.,

(1999)) for both PAOs and GAOs, since in the metabolic model of Oehmen, Lopez-Vazquez, et al., (2010c) the same biomass composition was assumed for both PAOs and GAOs.

3.3 Results and discussion

3.3.1 Model description

The first step in setting up the matrix is to identify the components (i) of relevance in the model. According to IWA nomenclature, insoluble or particulate components are indicated with the symbol X and the soluble components with S. The X components are assumed to be associated with the activated sludge, and they can be concentrated by sedimentation/thickening in clarifiers whereas S components will only be transported with the water phase (Henze et al., 1999).

The model accounts for biomass distribution among 17 particulate or insoluble components and for 11 soluble components. In the MD these components (i) are listed as state variables (see Table 3.1). The following simplifications were introduced in the both models: denitrification was modelled as a multi-step process from nitrate (Sno3) to nitrite (Sno2), and finally from Sno2 to di-nitrogen gas (Sn2). The different subgroups of *Accumulibacter* (PAO I and PAO II), *Competibacter* (GB and DGB) and *Defluviicoccus vanus* (DEF and DDEF) were combined in one particulate component for each group, and the same was made relatively to their storage compounds. However, stoichiometric parameters were defined (see section 3.3.2) in order to take into account the effects of each subgroup in the anaerobic and aerobic stoichiometry. The active autotrophic biomass was split in two particulate components, active ammonia oxidizers (Xnh) and active nitrite oxidizers (Xno2), since contrary to ASM2d where one-step nitrification/denitrification is modelled, in this model nitrification was modelled as a two-step process from free and ionized ammonia (Snh) to Sno2 and from Sno2 to Sno3.

Table 3.1: State variables.

Components (i)	Description	Units
So	Dissolved oxygen	g O_2/m^3
Sf	Fermentable readily biodegradable substrate	g COD/m^3
Sac	Acetate	g COD/m^3
Sprop	Propionate	g COD/m^3
Si	Soluble inert organic material	g COD/m^3
Snh	Free and ionized ammonia	g N/m^3
Sno3	Nitrate	g N/m^3
Sno2	Nitrite	g N/m^3
Sn2	Di-nitrogen	g N/m^3
Spo4	Soluble ortho-phosphate	g P/m^3
Salk	Alkalinity	mole/m^3
Xi	Particulate inert organic material	g COD/m^3
Xs	Slowly biodegradable substrate	g COD/m^3
Xh	Active heterotrophic biomass	g COD/m^3
Xpao	Active *Accumulibacter* biomass, a poly-P accumulating organism (PAO)	g COD/m^3
Xpp	Stored polyphosphate	g P/m^3
Xpao_pha	Cell-internal storage of poly-β-hydroxyalkanoates (PHA) in PAOs	g COD/m^3
Xpao_gly	Cell-internal storage of glycogen in PAOs	g COD/m^3

Table 3.1 (cont.)

Components (i)	Description	Units
Xgb	Active *Competibacter* biomass (GB), a glycogen accumulating organism	g COD/m^3
Xgb_pha	Cell-internal storage of poly-β-hydroxyalkanoates (PHA) in GB	g COD/m^3
Xgb_gly	Cell-internal storage of glycogen in GB	g COD/m^3
Xdef	Active *Defluviicoccus* biomass (DEF), a glycogen accumulating organism	g COD/m^3
Xdef_pha	Cell-internal storage of poly-β-hydroxyalkanoates (PHA) in DEF	g COD/m^3
Xdef_gly	Cell-internal storage of glycogen in DEF	g COD/m^3
Xnh	Active autotrophic ammonia oxidisers	g COD/m^3
Xno2	Active autotrophic nitrite oxidisers	g COD/m^3
Xmeoh	Metal-hydroxides	g /m^3
Xmep	Metal-phosphates	g /m^3

The model stoichiometric matrix is composed by 58 processes (j) and 28 (soluble and particulate) components (i: see Table II.1 in Appendix II). Some processes were added and others removed due to changes made in the state variables (see Table 3.2). Relatively to ASM2d, the following processes were added in order to take into account: denitrification (r8-r13) and nitrification as a multi-step process (r53 and r54); Sno2 may be an electron acceptor in anoxic hydrolysis (r3); acetate (Sac) and propionate (Sprop) are both fermentation products, and for this reason aerobic and anoxic growth of heterotrophs is also modelled with Sprop (r7, r10 and r13). Consequently, fermentation processes were split into two processes (r14 and r15), where readily biodegradable substrates (Sf) are transformed into Sac and Sprop, respectively. In the metabolic model developed by Oehmen, Lopez-Vazquez, et al., (2010c), the anaerobic, aerobic and anoxic processes performed by different subgroups of PAOs and GAOs (i.e. PAOI and PAOII, GB and DGB, and DEF and DDEF) were combined into only PAO, GB and DEF. This was performed for simplification purposes, although the different denitrification capabilities of each organisms are still included as explained below in section 3.3.2. Furthermore, nitrous oxide reduction processes were incorporated into the denitrification of nitrite as opposed to separately modelling their stoichiometry and kinetics.

Table 3.2: Description of the processes.

Process (j)	Description	Units
Hydrolysis:		
r1	Aerobic hydrolysis of Xs	g COD/m^3/d
r2	Anoxic hydrolysis of Xs (on NO_3)	g COD/m^3/d
r3	Anoxic hydrolysis of Xs (on NO_2)	g COD/m^3/d
r4	Anaerobic hydrolysis of Xs	g COD/m^3/d
Heterotrophic organisms:		
r5	Aerobic growth of Xh on Sf	g COD/m^3/d
r6	Aerobic growth of Xh on Sac	g COD/m^3/d
r7	Aerobic growth of Xh on Sprop	g COD/m^3/d
r8	Anoxic growth (on NO_3) of Xh on Sf	g COD/m^3/d
r9	Anoxic growth (on NO_3) of Xh on Sac	g COD/m^3/d
r10	Anoxic growth (on NO_3) of Xh on Sprop	g COD/m^3/d
r11	Anoxic growth (on NO_2) of Xh on Sf	g COD/m^3/d
r12	Anoxic growth (on NO_2)of Xh on Sac	g COD/m^3/d
r13	Anoxic growth (on NO_2) of Xh on Sprop	g COD/m^3/d
r14	Sac production from fermentation of Sf	g COD/m^3/d
r15	Sprop production from fermentation of Sf	g COD/m^3/d

Table 3.2 (cont.)

Process (j)	Description	Units
r16	Lysis of Xh	g COD/m^3/d
Polyphosphate accumulating organisms:		
r17	Anaerobic Sac uptake by PAOs	g COD/m^3/d
r18	Anaerobic Sprop uptake by PAOs	g COD/m^3/d
r19	Anaerobic maintenance by PAOs	g P/m^3/d
r20	Aerobic Xpao_pha degradation by PAOs	g COD/m^3/d
r21	Aerobic Xpao_gly production by PAOs	g COD/m^3/d
r22	Aerobic Xpp formation by PAOs	g P/m^3/d
r23	Aerobic maintenance by PAOs	g COD/m^3/d
r24	Anoxic Xpao_pha degradation by PAO I (on NO_3)	g COD/m^3/d
r25	Anoxic Xpao_gly production by PAO I (on NO_3)	g COD/m^3/d
r26	Anoxic Xpp formation by PAO I (on NO_3)	g P/m^3/d
r27	Anoxic maintenance by PAO I (on NO_3)	g COD/m^3/d
r28	Anoxic Xpao_pha degradation by PAOs (on NO_2)	g COD/m^3/d
r29	Anoxic Xpao_gly production by PAOs (on NO_2)	g COD/m^3/d
r30	Anoxic Xpp formation by PAOs (on NO_2)	g P/m^3/d
r31	Anoxic maintenance by PAOs (on NO_2)	g COD/m^3/d
Glycogen accumulating organisms:		
r32	Anaerobic Sac uptake by GB and DGB	g COD/m^3/d
r33	Anaerobic Sprop uptake by GB and DGB	g COD/m^3/d
r34	Anaerobic maintenance by GB and DGB	g COD/m^3/d
r35	Aerobic Xgb_pha degradation by GB and DGB	g COD/m^3/d
r36	Aerobic Xgb_gly production by GB and DGB	g COD/m^3/d
r37	Aerobic maintenance by GB and DGB	g COD/m^3/d
r38	Anoxic Xgb_pha degradation by DGB (on NO_3)	g COD/m^3/d
r39	Anoxic Xgb_gly production by DGB (on NO_3)	g COD/m^3/d
r40	Anoxic maintenance by DGB (on NO_3)	g COD/m^3/d
r41	Anoxic Xgb_pha degradation by DGB (on NO_2)	g COD/m^3/d
r42	Anoxic Xgb_gly production by DGB (on NO_2)	g COD/m^3/d
r43	Anoxic maintenance by DGB (on NO_2)	g COD/m^3/d
r44	Anaerobic Sac uptake by DEF and DDEF	g COD/m^3/d
r45	Anaerobic Sprop uptake by DEF and DDEF	g COD/m^3/d
r46	Anaerobic maintenance by DEF and DDEF	g COD/m^3/d
r47	Aerobic Xdef_pha degradation by DEF and DDEF	g COD/m^3/d
r48	Aerobic Xdef_gly production by DEF and DDEF	g COD/m^3/d
r49	Aerobic maintenance by DEF and DDEF	g COD/m^3/d
r50	Anoxic Xdef_pha degradation by DDEF (on NO_3)	g COD/m^3/d
r51	Anoxic Xdef_gly production by DDEF (on NO_3)	g COD/m^3/d
r52	Anoxic maintenance by DDEF (on NO_3)	g COD/m^3/d
Autotrophic organisms:		
r53	Aerobic growth of Xnh	g COD/m^3/d
r54	Aerobic growth of Xno2	g COD/m^3/d
r55	Lysis of Xnh	g COD/m^3/d
r56	Lysis of Xno2	g COD/m^3/d
Simultaneous precipitation of P with $Fe(OH)_3$:		
r57	Precipitation of phosphates with Xmeoh	g P/m^3/d
r58	Redissolution of Xmep	g P/m^3/d

The conservation matrix (see Table II.2 in Appendix II) contains information about conversion factors (i_{ci}) to be applied in the conservation Equation 3.1 in order to calculate unknown model stoichiometry via mass balance (for more information see section 3.3.2). The changes to $i_{COD,Sno3}$, $i_{COD,Sno2}$ and $i_{COD,Sn2}$ were based on Moussa et al., (2005), and the same logic in particulate components of PAOs were employed in the particulate components of GAOs.

$$\sum \nu_{ji} . i_{ci} = 0 \text{ over all components i}$$ **Equation 3.1**

Where,

ν_{ji} =stoichiometric coefficient for component i in process j;

i_{ci}=conversion factor to convert the units of component i to the units of the material c (COD, N, P and charge, CH), to which conservation is to be applied.

3.3.2 Stoichiometric parameters

The stoichiometric parameters are defined in Table IV. 1 (see APPENDIX IV). In addition to unit conversions from a C-mmol to g COD basis, the following changes were added to the metabolic model:

(1) Three stoichiometric parameters were defined in order to take into account the denitrification tendencies of the different subgroups of PAOs and GAOs. Since PAO I is the sole subgroup which performs nitrate reduction, all ν_{ji} in the nitrate reduction processes (r24-r27) were multiplied by PAO I fraction (fpaoI). The same logic were employed in GAOs, wherein all ν_{ji} in nitrate and nitrite reduction processes (r38-r43) were multiplied by the DGB fraction (fdgb) and all ν_{ji} in nitrate reduction processes (r50-r52) were multiplied by the DDEF fraction (fddef). This is due to the fact that some GB can denitrify from nitrate to N_2 gas and others cannot denitrify, while some DEF can denitrify from nitrate to nitrite, while others cannot denitrify at all.

(2) In the MD, the ν_{ji} in the model stoichiometric matrix that will be calculated from the conservation matrix is filled with the symbol @ c (c means COD, N, P or charge, CH). Therefore, the same logic was employed in order to predict the ν_{ji} for components Snh and Salk in all processes.

(3) One of the limitations found in the MD is that it is not possible to define stoichiometric parameters as a function of other parameters. As mentioned in the section 1.4.1, the aerobic and anoxic PHA-based yield coefficients are a function of δ or δ_N, ε or ε_N, K_1 and K_2, λ and β. On the other hand, the NO_x and oxygen-based yield coefficients are a function of these PHA-based yield coefficients and the degree of reduction of the PHA polymer. The oxygen and NOx consumed per biomass growth yield coefficient are also a function of biomass degree of reduction. Therefore, all these parameters mentioned above were directly substituted in the respective aerobic stoichiometric parameters through incorporating the constants defined previously in Oehmen, Lopez-Vazquez, et al., (2010c).

However, a limitation arose with λ and β parameters that depend on the yields for anaerobic formation of PHA from Sac and Sprop, and the latter depend on the acetate to propionate ratios in the influent. One of the advantages of the metabolic model developed by Oehmen, Lopez-Vazquez, et al., (2010c) is that it allows the practitioners to evaluate the effect of different acetate to propionate ratios on the PAOs-GAOs competition, it was developed the following logic in order to maintain the same freedom. The propionate to acetate ratio (ratio_prop_ac) was defined, and it allows the practitioners to define any percentage of propionate and acetate in the influent, except that the percentage of acetate can never be zero. This is because the division of a coefficient by

zero is undefined. However, if 99% and 1% of propionate and acetate, respectively, are defined the results obtained are approximately equal to those obtained with 100% of propionate, thus this does not present a practical limitation. Furthermore, acetate is generally more abundant in WWTP influents as compared to propionate, thus a situation of 100% propionate is unlikely. Therefore, different λ and β parameters were defined for PAOs (see Equation 3.2 and Equation 3.3) and GAOs (see Equation 3.4 and Equation 3.5), and these parameters are a function of ratio_prop_ac in PAOs, and also a function of pH in GAOs.

$$\lambda_{PAOs} = \frac{\frac{369.ratio\_prop\_ac}{400} + \frac{615}{112}}{\frac{45387.ratio\_prop\_ac}{8960} + \frac{615}{112}} \quad \textbf{Equation 3.2}$$

$$\beta_{PAOs} = \frac{ratio\_prop\_ac}{\frac{615.ratio\_prop\_ac}{503} + \frac{2000}{1509}} \quad \textbf{Equation 3.3}$$

$$\lambda_{GAOs} = \frac{\frac{35739.pH.ratio\_prop\_ac}{12500000} + \frac{20577.pH^2}{62500000} + \frac{50901.pH}{3125000} + \frac{57057.ratio\_prop\_ac}{1250000} + \frac{330239}{1875000}}{\frac{3249.pH.ratio\_prop\_ac}{250000} + \frac{20577.pH^2}{25000000} + \frac{5187.ratio\_prop\_ac}{25000} + \frac{29241.pH}{1250000} + \frac{122759}{750000}} \quad \textbf{Equation 3.4}$$

$$\beta_{GAOs} = \frac{\frac{42237.pH.ratio\_prop\_ac}{6250000} + \frac{20577.pH^2}{62500000} + \frac{14801.pH}{3125000} + \frac{67431.ratio\_prop\_ac}{625000} - \frac{5187}{625000}}{\frac{1083.pH.ratio\_prop\_ac}{125000} + \frac{6859.pH^2}{12500000} + \frac{1729.ratio\_prop\_ac}{12500} + \frac{9747.pH}{625000} + \frac{122759}{1125000}} \quad \textbf{Equation 3.5}$$

Where,

λ_x= Percentage of Acetyl-CoA in PHA for PAOs or GAOs (C-mol/Cmol);

β_x= Percentage of Propionyl-CoA in PHA for PAOs or GAOs (C-mol/Cmol).

Therefore, with this new model it is now possible to directly relate the factors affecting PAO and GAO stoichiometry (i.e. carbon source for PAOs and GAOs, and pH for GAOs) to the wastewater influent quality (C source) or an easily measureable operational parameter (pH).

3.3.3 Model kinetics

The kinetic expressions as well as their saturation/inhibition functions are detailed in Table III.1 and Table III.2 (see APPENDIX III).

The following changes were added to the ASM2d:

(1) Switching functions Sf/(Sf+Sac+Sprop), Sac/(Sf+Sac+Sprop) and Sprop/(Sf+Sac+Sprop) were added to the processes of aerobic and anoxic growth of heterotrophs on Sf (r5, r8, r11), Sac (r6, r9, r12) and Sprop (r7, r10 r13), respectively, in order to prevent the heterotrophic maximum specific growth rate (muh) from tripling, when the three substrates are present concurrently.

(2) Switching functions Sac/(Sac+Sprop) and Sprop/(Sac+Sprop) were added to the processes of acetate (r14) and propionate (r15) production from fermentation of Sf, respectively, in order to prevent the fermentation maximum rate on acetate (qh_ac) and on propionate (qh_prop) from doubling, when both substrates are present concurrently.

(3) Switching functions Sno3/(Sno2+Sno3) and Sno2/(Sno2+Sno3) were added to the processes of anoxic hydrolysis of Xs on NO_3 (r2) and on NO_2 (r3), respectively, and also to the NO_3 (r8-r10) and NO_2 (r11-r13) denitrification processes, respectively. This type of switching functions were also used by Sin et al., (2006) in order to model the kinetics of multi-step denitrification.

(4) A inhibition function kno2/(kno2+sno2) was added to the processes of anaerobic hydrolysis of Xs (r4) and also in the acetate and propionate production from fermentation of Sf (r14 and r15, respectively). This function was added in order to follow the same logic of existing functions ko2/(ko2+so2) and kno3/(kno3+sno3) in these processes, since anaerobic hydrolysis will also be inhibited by nitrite, in addition to nitrate and oxygen.

Relative to the metabolic model, the kinetic parameters for PAOs and GAOs are a function of temperature, and in some processes, for the same parameter there are two different expressions that depend on the temperature range. One way to implement this would be through conditional statements (like if and else), but in the MD it is not possible to use it. Although these technical issues have yet to be discussed with Hydromantis, an alternative method was developed in order to solve this problem (see Equation 3.6).

$$\left(kinetic\ parameter\ (A).\frac{T_1}{T_1+T_2}+kinetic\ parameter\ (B).\frac{T_2}{T_1+T_2}\right)\times kinetic\ expression_{\ j} \qquad \textbf{Equation 3.6}$$

Where,

T1 = any value of temperature defined in the following range $10 \leq T \leq 20$ºC;

T2 = any value of temperature defined in the following range: $20 < T2 \leq 30$ºC;

Kinetic parameter (A) = kinetic parameter used when T=T1;

Kinetic parameter (B) = kinetic parameter used when T=T2;

Kinetic expression $_j$ = kinetic expression for the process j.

Two parameters (T1 and T2) must be defined by the practitioners, according to the following condition. For example, if the practitioners are interested to model the process for any value of T1, they must define T1 with this value and T2 with zero. Thus, $kinetic\ parameter\ (B).\frac{T_2}{T_1+T_2}$ is equal to zero. The same logic must be employed by the practitioners, if they are interested to model for any value of T2 (it means that T1 must be set to the value zero). However, as already mentioned, these issues have to be discussed with Hydromantis in order to find an optimal solution.

The kinetic parameters and coefficients for the expressions of Table III.2 are detailed in Table IV.2 (see APPENDIX IV). The anoxic kinetic parameters assumed for PAOs were equal to the aerobic conditions and the same was done for GAOs.

3.4 Conclusions and recommendations for future research

A combined PAO-GAO metabolic-ASM2d model was successfully implemented in GPS-X 6.2. The model presents some modifications with respect to the metabolic model described by Oehmen et al. (2010) and also ASM2d (Henze et al. 1999) in order to successfully integrate the 2 models into one complete biological nutrient removal model. Some minor programming issues will still be solved in collaboration with Hydromantis Environmental Software Solutions, Inc., such as model the effect of temperature on the process kinetics. Then, the next steps will be model calibration and validation through experimental data of full-scale EBPR processes.

4 REFERENCES

AMANN, R. I. 1995. *In situ identification of micro-organisms by whole cell hybridization with rRNA-targeted nucleic acid probes,* Netherlands, Kluwer Academic Publishers.

AMANN, R. I., BINDER, B. J., OLSON, R. J., CHISHOLM, S. W., DEVEREUX, R. & STAHL, D. A. 1990. COMBINATION OF 16S RIBOSOMAL-RNA-TARGETED OLIGONUCLEOTIDE PROBES WITH FLOW-CYTOMETRY FOR ANALYZING MIXED MICROBIAL-POPULATIONS. *Applied and Environmental Microbiology,* 56**,** 1919-1925.

APHA-AMERICAN PUBLIC HEALTH ASSOCIATION 1995. *Standard methods for the examination for water and wastewater,* Washington, D.C., APHA.

BRDJANOVIC, D., LOGEMANN, S., VAN LOOSDRECHT, M. C. M., HOOIJMANS, C. M., ALAERTS, G. J. & HEIJNEN, J. J. 1998. Influence of temperature on biological phosphorus removal: Process and molecular ecological studies. *Water Research,* 32**,** 1035-1048.

BRDJANOVIC, D., VAN LOOSDRECHT, M. C. M., VERSTEEG, P., HOOIJMANS, C. M., ALAERTS, G. J. & HEIJNEN, J. J. 2000. Modeling COD, N and P removal in a full-scale wwtp Haarlem Waarderpolder. *Water Research,* 34**,** 846-858.

BUROW, L. C., KONG, Y., NIELSEN, J. L., BLACKALL, L. L. & NIELSEN, P. H. 2007. Abundance and ecophysiology of Defluviicoccus spp., glycogen-accumulating organisms in full-scale wastewater treatment processes. *Microbiology-Sgm,* 153**,** 178-185.

CARRETTE, R., BIXIO, D., THOEYE, C. & OCKLER, P. 2001. Full-scale application of the IAWQ ASM No. 2d model. *Water Science and Technology,* 44**,** 17-24.

CARVALHO, G., LEMOS, P. C., OEHMEN, A. & REIS, M. A. M. 2007. Denitrifying phosphorus removal: Linking the process performance with the microbial community structure. *Water Research,* 41**,** 4383-4396.

COMEAU, Y., HALL, K. J., HANCOCK, R. E. W. & OLDHAM, W. K. 1986. BIOCHEMICAL-MODEL FOR ENHANCED BIOLOGICAL PHOSPHORUS REMOVAL. *Water Research,* 20**,** 1511-1521.

CROCETTI, G. R., BANFIELD, J. F., KELLER, J., BOND, P. L. & BLACKALL, L. L. 2002. Glycogen-accumulating organisms in laboratory-scale and full-scale wastewater treatment processes. *Microbiology-Sgm,* 148**,** 3353-3364.

CROCETTI, G. R., HUGENHOLTZ, P., BOND, P. L., SCHULER, A., KELLER, J., JENKINS, D. & BLACKALL, L. L. 2000. Identification of polyphosphate-accumulating organisms and design of 16S rRNA-directed probes for their detection and quantitation. *Applied and Environmental Microbiology,* 66**,** 1175-1182.

DAIMS, H., BRUHL, A., AMANN, R., SCHLEIFER, K. H. & WAGNER, M. 1999. The domain-specific probe EUB338 is insufficient for the detection of all Bacteria: Development and evaluation of a more comprehensive probe set. *Systematic and Applied Microbiology,* 22**,** 434-444.

FILIPE, C. D. M., DAIGGER, G. T. & GRADY, C. P. L. 2001a. A metabolic model for acetate uptake under anaerobic conditions by glycogen accumulating organisms: Stoichiometry, kinetics, and the effect of pH. *Biotechnology and Bioengineering,* 76**,** 17-31.

FILIPE, C. D. M., DAIGGER, G. T. & GRADY, C. P. L. 2001b. pH as a key factor in the competition between glycogen-accumulating organisms and phosphorus-accumulating organisms. *Water Environment Research,* 73**,** 223-232.

FILIPE, C. D. M., DAIGGER, G. T. & GRADY, C. P. L. 2001c. Stoichiometry and kinetics of acetate uptake under anaerobic conditions by an enriched culture of phosphorus-accumulating organisms at different pHs. *Biotechnology and Bioengineering,* 76**,** 32-43.

GERNAEY, K. V., VAN LOOSDRECHT, M. C. M., HENZE, M., LIND, M. & JORGENSEN, S. B. 2004. Activated sludge wastewater treatment plant modelling and simulation: state of the art. *Environmental Modelling & Software,* 19**,** 763-783.

HE, S., GALL, D. L. & MCMAHON, K. D. 2007. "Candidatus accumulibacter" population structure in enhanced biological phosphorus removal Sludges as revealed by polyphosphate kinase genes. *Applied and Environmental Microbiology,* 73**,** 5865-5874.

HENZE, M., GUJER, W., MINO, T., MATSUO, T., WENTZEL, M. C., MARAIS, G. V. R. & VAN LOOSDRECHT, M. C. M. 1999. Activated Sludge Model No.2d, ASM2d. *Water Science and Technology,* 39**,** 165-182.

HESSELMANN, R. P. X., VON RUMMELL, R., RESNICK, S. M., HANY, R. & ZEHNDER, A. J. B. 2000. Anaerobic metabolism of bacteria performing enhanced biological phosphate removal. *Water Research,* 34**,** 3487-3494.

HESSELMANN, R. P. X., WERLEN, C., HAHN, D., VAN DER MEER, J. R. & ZEHNDER, A. J. B. 1999. Enrichment, Phylogenetic Analysis and Detection of a Bacterium That Performs Enhanced Biological Phosphate Removal in Activated Sludge. *Systematic and Applied Microbiology,* 22**,** 454-465.

HIEN, T. T. N., LE, V. Q., HANSEN, A. A., NIELSEN, J. L. & NIELSEN, P. H. 2011. High diversity and abundance of putative polyphosphate-accumulating Tetrasphaera-related bacteria in activated sludge systems. *Fems Microbiology Ecology,* 76**,** 256-267.

INGILDSEN, P., ROSEN, C., GERNAEY, K. V., NIELSEN, M. K., GUILDAL, T. & JACOBSEN, B. N. 2006. Modelling and control strategy testing of biological and chemical phosphorus removal at Avedore WWTP. *Water Science and Technology,* 53**,** 105-113.

KONG, Y., XIA, Y. & NIELSEN, P. H. 2008. Activity and identity of fermenting microorganisms in full-scale biological nutrient removing wastewater treatment plants. *Environmental Microbiology,* 10**,** 2008-2019.

KONG, Y. H., NIELSEN, J. L. & NIELSEN, P. H. 2004. Microautoradiographic study of Rhodocyclus-related polyphosphate accumulating bacteria in full-scale enhanced biological phosphorus removal plants. *Applied and Environmental Microbiology,* 70**,** 5383-5390.

KONG, Y. H., NIELSEN, J. L. & NIELSEN, P. H. 2005. Identity and ecophysiology of uncultured actinobacterial polyphosphate-accumulating organisms in full-scale enhanced biological phosphorus removal plants. *Applied and Environmental Microbiology,* 71**,** 4076-4085.

KONG, Y. H., ONG, S. L., NG, W. J. & LIU, W. T. 2002. Diversity and distribution of a deeply branched novel proteobacterial group found in anaerobic-aerobic activated sludge processes. *Environmental Microbiology,* 4**,** 753-757.

KONG, Y. H., XIA, Y., NIELSEN, J. L. & NIELSEN, P. H. 2006. Ecophysiology of a group of uncultured Gammaproteobacterial glycogen-accumulating organisms in full-scale enhanced biological phosphorus removal wastewater treatment plants. *Environmental Microbiology,* 8**,** 479-489.

KRISTIANSEN, R., NGUYEN, H. T. T., SAUNDERS, A. M., NIELSEN, J. L., WIMMER, R., LE, V. Q., MCILROY, S. J., PETROVSKI, S., SEVIOUR, R. J., CALTEAU, A., NIELSEN, K. L. & NIELSEN, P. H. 2013. A metabolic model for members of the genus Tetrasphaera involved in enhanced biological phosphorus removal. *Isme Journal,* 7**,** 543-554.

KUBA, T., MURNLEITNER, E., VANLOOSDRECHT, M. C. M. & HEIJNEN, J. J. 1996. A metabolic model for biological phosphorus removal by denitrifying organisms. *Biotechnology and Bioengineering,* 52**,** 685-695.

KY, R. C., COMEAU, Y., PERRIER, M. & TAKACS, I. 2001. Modelling biological phosphorus removal from a cheese factory effluent by an SBR. *Water Science and Technology,* 43**,** 257-264.

LANHAM, A. B., RICARDO, A. R., ALBUQUERQUE, M. G. E., PARDELHA, F., CARVALHEIRA, M., COMA, M., FRADINHO, J., CARVALHO, G., OEHMEN, A. & REIS, M. A. M. Determination of the extraction kinetics for the quantification of polyhydroxyalkanoate monomers in mixed microbial systems. *Process Biochemistry*.

LANHAM, A. B., RICARDO, A. R., COMA, M., FRADINHO, J., CARVALHEIRA, M., OEHMEN, A., CARVALHO, G. & REIS, M. A. M. 2012. Optimisation of glycogen quantification in mixed microbial cultures. *Bioresource Technology,* 118**,** 518-525.

LEE, S. H., KO, J. H., PARK, J. B., IM, J. H., KIM, J. R., LEE, J. J. & KIM, C. W. 2006. Use of activate sludge model No. 3 and Bio-P module for simulating five-stage step-feed enhanced biological phosphorous removal process. *Korean Journal of Chemical Engineering,* 23**,** 203-208.

LEMOS, P. C., DAI, Y., YUAN, Z., KELLER, J., SANTOS, H. & REIS, M. A. M. 2007. Elucidation of metabolic pathways in glycogen-accumulating organisms with in vivo C-13 nuclear magnetic resonance. *Environmental Microbiology,* 9**,** 2694-2706.

LIU, W. T., NIELSEN, A. T., WU, J. H., TSAI, C. S., MATSUO, Y. & MOLIN, S. 2001. In situ identification of polyphosphate- and polyhydroxyalkanoate-accumulating traits for microbial populations in a biological phosphorus removal process. *Environmental Microbiology,* 3**,** 110-122.

LOPEZ-VAZQUEZ, C. M., OEHMEN, A., HOOIJMANS, C. M., BRDJANOVIC, D., GIJZEN, H. J., YUAN, Z. G. & VAN LOOSDRECHT, M. C. M. 2009. Modeling the PAO-GAO competition: Effects of carbon source, pH and temperature. *Water Research,* 43**,** 450-462.

LOPEZ-VAZQUEZ, C. M., SONG, Y.-I., HOOIJMANS, C. M., BRDJANOVIC, D., MOUSSA, M. S., GIJZEN, H. J. & VAN LOOSDRECHT, M. C. M. 2008. Temperature effects on the aerobic

metabolism of glycogen-accumulating organisms. *Biotechnology and Bioengineering,* 101**,** 295-306.

LOPEZ-VAZQUEZ, C. M., SONG, Y.-I., HOOIJMANS, C. M., BRDJANOVIC, D., MOUSSA, M. S., GIJZEN, H. J. & VAN LOOSDRECHT, M. M. C. 2007. Short-term temperature effects on the anaerobic metabolism of glycogen accumulating organisms. *Biotechnology and Bioengineering,* 97**,** 483-495.

LOUIE, T. M., MAH, T. J., OLDHAM, W. & RAMEY, W. D. 2000. Use of metabolic inhibitors end gas chromatography/mass spectrometry to study poly-beta-hydroxyalkanoates metabolism involving cryptic nutrients in enhanced biological phosphorus removal systems. *Water Research,* 34**,** 1507-1514.

MARTIN, H. G., IVANOVA, N., KUNIN, V., WARNECKE, F., BARRY, K. W., MCHARDY, A. C., YEATES, C., HE, S., SALAMOV, A. A., SZETO, E., DALIN, E., PUTNAM, N. H., SHAPIRO, H. J., PANGILINAN, J. L., RIGOUTSOS, I., KYRPIDES, N. C., BLACKALL, L. L., MCMAHON, K. D. & HUGENHOLTZ, P. 2006. Metagenomic analysis of two enhanced biological phosphorus removal (EBPR) sludge communities. *Nature Biotechnology,* 24**,** 1263-1269.

MAURER, M., GUJER, W., HANY, R. & BACHMANN, S. 1997. Intracellular carbon flow in phosphorus accumulating organisms from activated sludge systems. *Water Research,* 31**,** 907-917.

MCKENZIE, C. M., SEVIOUR, E. M., SCHUMANN, P., MASZENAN, A. M., LIU, J. R., WEBB, R. I., MONIS, P., SAINT, C. P., STEINER, U. & SEVIOUR, R. J. 2006. Isolates of 'Candidatus Nostocoida limicola' Blackall et al. 2000 should be described as three novel species of the genus Tetrasphaera, as Tetrasphaera jenkinsii sp nov., Tetrasphaera vanveenii sp nov and Tetrasphaera veronensis sp nov. *International Journal of Systematic and Evolutionary Microbiology,* 56**,** 2279-2290.

MEIJER, S. 2004. *Theoretical and practical aspects of medelling activated sludge processes*.

MEIJER, S. C. F., VAN LOOSDRECHT, M. C. M. & HEIJNEN, J. J. 2002. Modelling the start-up of a full-scale biological phosphorous and nitrogen removing WWTP. *Water Research,* 36**,** 4667-4682.

MEYER, R. L., SAUNDERS, A. M. & BLACKALL, L. L. 2006. Putative glycogen-accumulating organisms belonging to the Alphaproteobacteria identified through rRNA-based stable isotope probing. *Microbiology-Sgm,* 152**,** 419-429.

MINO, T., ARUN, V., TSUZUKI, Y. & MATSUO, T. 1987. *Effect of phosphorus accumulation on acetate metabolism in the biological phosphorus removal process,* Oxford, Pergamon Press.

MINO, T., VAN LOOSDRECHT, M. C. M. & HEIJNEN, J. J. 1998. Microbiology and biochemistry of the enhanced biological phosphate removal process. *Water Research,* 32**,** 3193-3207.

MOUSSA, M. S., HOOIJMANS, C. M., LUBBERDING, H. J., GIJZEN, H. J. & VAN LOOSDRECHT, M. C. M. 2005. Modelling nitrification, heterotrophic growth and predation in activated sludge. *Water Research,* 39**,** 5080-5098.

MURNLEITNER, E., KUBA, T., VANLOOSDRECHT, M. C. M. & HEIJNEN, J. J. 1997. An integrated metabolic model for the aerobic and denitrifying biological phosphorus removal. *Biotechnology and Bioengineering,* 54**,** 434-450.

OEHMEN, A. 2004. The Competition Between Polyphosphate Accumulating Organisms and Glycogen Accumulating Organisms in the Enhanced Biological Phosphorous Removal Process. Brisbane, Australia: The University of Queensland.

OEHMEN, A., CARVALHO, G., FREITAS, F. & REIS, M. A. M. 2010a. Assessing the abundance and activity of denitrifying polyphosphate accumulating organisms through molecular and chemical techniques. *Water Science and Technology,* 61**,** 2061-2068.

OEHMEN, A., CARVALHO, G., LOPEZ-VAZQUEZ, C. M., VAN LOOSDRECHT, M. C. M. & REIS, M. A. M. 2010b. Incorporating microbial ecology into the metabolic modelling of polyphosphate accumulating organisms and glycogen accumulating organisms. *Water Research,* 44**,** 4992-5004.

OEHMEN, A., LEMOS, P. C., CARVALHO, G., YUAN, Z., KELLER, J., BLACKALL, L. L. & REIS, M. A. M. 2007a. Advances in enhanced biological phosphorus removal: From micro to macro scale. *Water Research,* 41**,** 2271-2300.

OEHMEN, A., LOPEZ-VAZQUEZ, C. M., CARVALHO, G., REIS, M. A. M. & VAN LOOSDRECHT, M. C. M. 2010c. Modelling the population dynamics and metabolic diversity of organisms relevant in anaerobic/anoxic/aerobic enhanced biological phosphorus removal processes. *Water Research,* 44**,** 4473-4486.

OEHMEN, A., SAUNDERS, A. M., VIVES, M. T., YUAN, Z. G. & KELLER, H. 2006a. Competition between polyphosphate and glycogen accumulating organisms in enhanced biological

phosphorus removal systems with acetate and propionate as carbon sources. *Journal of Biotechnology,* 123**,** 22-32.

OEHMEN, A., VIVES, M. T., LU, H. B., YUAN, Z. G. & KELLER, J. 2005a. The effect of pH on the competition between polyphosphate-accumulating organisms and glycogen-accumulating organisms. *Water Research,* 39**,** 3727-3737.

OEHMEN, A., YUAN, Z. G., BLACKALL, L. L. & KELLER, J. 2005b. Comparison of acetate and propionate uptake by polyphosphate accumulating organisms and glycogen accumulating organisms. *Biotechnology and Bioengineering,* 91**,** 162-168.

OEHMEN, A., ZENG, R. J., KELLER, J. & YUAN, Z. G. 2007b. Modeling the aerobic metabolism of polyphosphate-accumulating organisms enriched with propionate as a carbon source. *Water Environment Research,* 79**,** 2477-2486.

OEHMEN, A., ZENG, R. J., SAUNDERS, A. M., BLACKALL, L. L., KELLER, J. & YUAN, Z. G. 2006b. Anaerobic and aerobic metabolism of glycogen-accumulating organisms selected with propionate as the sole carbon source. *Microbiology-Sgm,* 152**,** 2767-2778.

OEHMEN, A., ZENG, R. J., YUAN, Z. G. & KELLER, J. 2005c. Anaerobic metabolism of propionate by polyphosphate-accumulating organisms in enhanced biological phosphorus removal systems. *Biotechnology and Bioengineering,* 91**,** 43-53.

PEREIRA, H., LEMOS, P. C., REIS, M. A. M., CRESPO, J., CARRONDO, M. J. T. & SANTOS, H. 1996. Model for carbon metabolism in biological phosphorus removal processes based on in vivo C-13-NMR labelling experiments. *Water Research,* 30**,** 2128-2138.

PETERSON, S. B., WARNECKE, F., MADEJSKA, J., MCMAHON, K. D. & HUGENHOLTZ, P. 2008. Environmental distribution and population biology of Candidatus Accumulibacter, a primary agent of biological phosphorus removal. *Environmental Microbiology,* 10**,** 2692-2703.

RIEGER, L., KOCH, G., KUHNI, M., GUJER, W. & SIEGRIST, H. 2001. The EAWAG Bio-P module for activated sludge model No. 3. *Water Research,* 35**,** 3887-3903.

SAUNDERS, A. M., OEHMEN, A., BLACKALL, L. L., YUAN, Z. & KELLER, J. 2003. The effect of GAOs (glycogen accumulating organisms) on anaerobic carbon requirements in full-scale Australian EBPR (enhanced biological phosphorus removal) plants. *Water Science and Technology,* 47**,** 37-43.

SERAFIM, L. S., LEMOS, P. C., OLIVEIRA, R. & REIS, M. A. M. 2004. Optimization of polyhydroxybutyrate production by mixed cultures submitted to aerobic dynamic feeding conditions. *Biotechnology and Bioengineering,* 87**,** 145-160.

SIN, G., GOVOREANU, R., BOON, N., SCHELSTRAETE, G. & VANROLLEGHEM, P. A. 2006. Evaluation of the impacts of model-based operation of SBRs on activated sludge microbial community. *Water Science and Technology,* 54**,** 157-166.

SMOLDERS, G. J. F., VANDERMEIJ, J., VANLOOSDRECHT, M. C. M. & HEIJNEN, J. J. 1994a. MODEL OF THE ANAEROBIC METABOLISM OF THE BIOLOGICAL PHOSPHORUS REMOVAL PROCESS - STOICHIOMETRY AND PH INFLUENCE. *Biotechnology and Bioengineering,* 43**,** 461-470.

SMOLDERS, G. J. F., VANDERMEIJ, J., VANLOOSDRECHT, M. C. M. & HEIJNEN, J. J. 1994b. STOICHIOMETRIC MODEL OF THE AEROBIC METABOLISM OF THE BIOLOGICAL PHOSPHORUS REMOVAL PROCESS. *Biotechnology and Bioengineering,* 44**,** 837-848.

SMOLDERS, G. J. F., VANDERMEIJ, J., VANLOOSDRECHT, M. C. M. & HEIJNEN, J. J. 1995. A STRUCTURED METABOLIC MODEL FOR ANAEROBIC AND AEROBIC STOICHIOMETRY AND KINETICS OF THE BIOLOGICAL PHOSPHORUS REMOVAL PROCESS. *Biotechnology and Bioengineering,* 47**,** 277-287.

VAN VELDHUIZEN, H. M., VAN LOOSDRECHT, M. C. M. & HEIJNEN, J. J. 1999. Modelling biological phosphorus and nitrogen removal in a full scale activated sludge process. *Water Research,* 33**,** 3459-3468.

WANG, X., ZENG, R. J., DAI, Y., PENG, Y. & YUAN, Z. 2008. The denitrification capability of cluster 1 Defluviioccus vanus-related glycogen-accumulating organisms. *Biotechnology and Bioengineering,* 99**,** 1329-1336.

WEXLER, M., RICHARDSON, D. J. & BOND, P. L. 2009. Radiolabelled proteomics to determine differential functioning of Accumulibacter during the anaerobic and aerobic phases of a bioreactor operating for enhanced biological phosphorus removal. *Environmental Microbiology,* 11**,** 3029-3044.

WICHERN, M., OBENAUS, F., WULF, P. & ROSENWINKEL, K. H. 2001. Modelling of full-scale wastewater treatment plants with different treatment processes using the Activated Sludge Model no. 3. *Water Science and Technology,* 44**,** 49-56.

WONG, M. T., TAN, F. M., NG, W. J. & LIU, W. T. 2004. Identification and occurrence of tetrad-forming Alphaproteobacteria in anaerobic-aerobic activated sludge processes. *Microbiology-Sgm,* 150**,** 3741-3748.

XIA, Y., KONG, Y., THOMSEN, T. R. & NIELSEN, P. H. 2008. Identification and ecophysiological characterization of epiphytic protein-hydrolyzing Saprospiraceae ("Candidatus epiflobacter" spp.) in activated sludge. *Applied and Environmental Microbiology,* 74**,** 2229-2238.

YEOMAN, S., STEPHENSON, T., LESTER, J. N. & PERRY, R. 1988. The removal of phosphorus during wastewater treatment: A review. *Environmental Pollution,* 49**,** 183-233.

ZENG, R. J., VAN LOOSDRECHT, M. C. M., YUAN, Z. G. & KELLER, J. 2003a. Metabolic model for glycogen-accumulating organisms in anaerobic/aerobic activated sludge systems. *Biotechnology and Bioengineering,* 81**,** 92-105.

ZENG, R. J., YUAN, Z. G. & KELLER, J. 2003b. Model-based analysis of anaerobic acetate uptake by a mixed culture of polyphosphate-accumulating and glycogen-accumulating organisms. *Biotechnology and Bioengineering,* 83**,** 293-302.

ZHOU, Y., PIJUAN, M. & YUAN, Z. 2007. Free nitrous acid inhibition on anoxic phosphorus uptake and denitrification by poly-phosphate accumulating organisms. *Biotechnology and Bioengineering,* 98**,** 903-912.

ZHOU, Y., PIJUAN, M., ZENG, R. J. & YUAN, Z. 2008. Free Nitrous Acid Inhibition on Nitrous Oxide Reduction by a Denitrifying-Enhanced Biological Phosphorus Removal Sludge. *Environmental Science & Technology,* 42**,** 8260-8265.

ZHOU, Y., PIJUAN, M., ZENG, R. J. & YUAN, Z. 2009. Involvement of the TCA cycle in the anaerobic metabolism of polyphosphate accumulating organisms (PAOs). *Water Research,* 43**,** 1330-1340.

ZILLES, J. L., PECCIA, J., KIM, M. W., HUNG, C. H. & NOGUERA, D. R. 2002. Involvement of Rhodocyclus-related organisms in phosphorus removal in full-scale wastewater treatment plants. *Applied and Environmental Microbiology,* 68**,** 2763-2769.

APPENDIX I – GPS-X LIBRARIES

Table I.1: Library (cnpiplib) state variables.

Cryptic Name	Description	
Inorganic Suspended Solids		
Xii	inert inorganic suspended solids	g/m3
Organic Variables		
Si	soluble inert organic material	gCOD/m3
Ss	readily biodegradable substrate	gCOD/m3
Sf	fermentable readily biodegradable substrate	gCOD/m3
Slf	volatile fatty acids	gCOD/m3
Sac	acetate	gCOD/m3
Sprop	propionate	gCOD/m3
Xi	particulate inert organic material	gCOD/m3
Xs	slowly biodegradable substrate	gCOD/m3
Xh	active heterotrophic biomass	gCOD/m3
Xaut	active autotrophic biomass	gCOD/m3
Xpao	active accumulibacter biomass, a poly-P accumulating organism	gCOD/m3
Xu	unbiodegradable particulates from cell decay	gCOD/m3
Xsto	internal cell storage product	gCOD/m3
Xpao_pha	cell-internal storage of poly-hydroxy-alkanoates (PHA) in PAOs	gCOD/m3
Xpao_gly	cell-internal storage of glycogen in PAOs	gCOD/m3
Xgb	active competibacter biomass, a gly accumulating organism	gCOD/m3
Xgb_pha	cell-internal storage of poly-hydroxy-alkanoates (PHA) in GB	gCOD/m3
Xgb_gly	cell-internal storage of glycogen in GB	gCOD/m3
Xdef	active defluviicoccus biomass, a gly accumulating organism	gCOD/m3
Xdef_pha	cell-internal storage of poly-hydroxy-alkanoates (PHA) in DEF	gCOD/m3
Xdef_gly	cell-internal storage of glycogen in DEF	gCOD/m3
Xnh	active autotrophic ammonia oxidisers	gCOD/m3
Xno2	active autotrophic nitrite oxidisers	gCOD/m3
Dissolved Oxygen		
So	dissolved oxygen	gO2/m3
Phosphorus Compounds		
Spo4	soluble ortho-phosphate	gP/m3
Xpp	stored polyphosphate	gP/m3
Xppr	stored polyphosphate (releasable)	gP/m3
Nitrogen Compounds		
Snh	free and ionized ammonia	gN/m3
Snd	soluble biodegradable organic nitrogen	gN/m3
Xnd	particulate biodegradable organic nitrogen	gN/m3
Sno3	nitrate	gN/m3
Sno2	nitrite	gN/m3
Sno	nitrate and nitrite	gN/m3
Sni	soluble unbiodegradable organic nitrogen	gN/m3
Sn2	dinitrogen	gN/m3

Table I.1: (cont.).

Alkalinity		
Salk	alkalinity	mole/m3
Metal Precipitates		
Xmeoh	metal-hydroxides	g/m3
Xmep	metal-phosphates	g/m3

Table I.2: Library (cnpiplib) stoichiometry variables.

Cryptic Name	Description	
Organic Fractions		
icv	XCOD/VSS ratio	gCOD/gVSS
fbod	BOD5/BODultimate ratio	-
Nutrient Fractions		
insi	N content of soluble inert organic material	gN/gCOD
inss	N content of readily biodegradable substrate	gN/gCOD
insf	N content of fermentable readily biodegradable substrate	gN/gCOD
inxi	N content of particulate inert organic material	gN/gCOD
inxs	N content of slowly biodegradable substrate	gN/gCOD
inxu	N content of unbiodegradable particulates from cell decay	gN/gCOD
inxh	N content of active heterotrophic biomass	gN/gCOD
inxnh	N content of active autotrophic ammonia oxidisers biomass	gN/gCOD
inxno2	N content of active autotrophic nitrite oxidisers biomass	gN/gCOD
inxpao	N content of active poly-P accumulating biomass	gN/gCOD
inxgb	N content of active Competibacter biomass	gN/gCOD
inxdef	N content of active Defluviicoccus biomass	gN/gCOD
ipsi	P content of soluble inert organic material	gP/gCOD
ipss	P content of readily biodegradable substrate	gP/gCOD
ipsf	P content of fermentable readily biodegradable substrate	gP/gCOD
ipxi	P content of particulate inert organic material	gP/gCOD
ipxs	P content of slowly biodegradable substrate	gP/gCOD
ipxu	P content of unbiodegradable particulates from cell decay	gP/gCOD
ipxh	P content of active heterotrophic biomass	gP/gCOD
ipxnh	P content of active autotrophic ammonia oxidisers biomass	gP/gCOD
ipxno2	P content of active autotrophic nitrite oxidisers biomass	gP/gCOD
ipxpao	P content of active poly-P accumulating biomass	gP/gCOD
ipxgb	P content of active Competibacter biomass	gP/gCOD
ipxdef	P content of active Defluviicoccus biomass	gP/gCOD

Table I. 3: Library (cnpiplib) composite variable calculations.

Cryptic Name	Variable Name	Definition	
Volatile Fraction			
ivt	VSS/TSS ratio	vss/(x)	gTSS/gVSS
Composite Variables			
scod	filtered COD	sbodu+Si	gCOD/m3
xcod	particulate COD	xbodu+Xi+Xu	gCOD/m3
cod	total COD	scod+xcod	gCOD/m3
sbod	filtered carbonaceous BOD5	fbod*sbodu	gO2/m3
xbod	particulate carbonaceous BOD5	fbod*xbodu	gO2/m3
bod	total carbonaceous BOD5	sbod+xbod	gO2/m3
sbodu	filtered ultimate carbonaceous BOD	Ss+Slf+Sf+Sac+Sprop	gO2/m3
xbodu	particulate ultimate carbonaceous BOD ...	Xs+Xh+Xaut+Xnh+Xno2+Xsto+Xpao+Xpao_pha+Xpao_gly+Xgb+Xgb_pha+Xgb_gly+Xdef+Xdef_pha+Xdef_gly	gO2/m3
bodu	total ultimate carbonaceous BOD	sbodu+xbodu	gO2/m3
vss	volatile suspended solids	(xcod)/(icv)	g/m3
x	total suspended solids	vss + xiss	g/m3
xiss	inert inorganic suspended solids	Xii+Xmeoh+Xmep+0.205*(Xpp+Xppr)	g/m3
stkn	filtered TKN	Snh+Snd+Sni+insi*Si+inss*Ss+insf*Sf	gN/m3
xtkn	particulate TKN	tkn - stkn	gN/m3
tkn	total TKN	stkn+Xnd+inxh*Xh+inxnh*Xnh+inxno2*Xno2+inxpao*Xpao+inxgb*Xgb+inxdef*Xdef+inxi*Xi+inxu*Xu+inxs*Xs	gN/m3
tn	total nitrogen	tkn+Sno3+Sno2+Sno	gN/m3
stp	filtered phosphorus	Spo4+ipsi*Si+ipss*Ss&o+ipsf*Sf	gP/m3
xtp	particulate phosphorus	ipxh*Xh+ipxnh*Xnh+ipxno2*Xno2+ipxpao*Xpao+ipxgb*Xgb+ipxdef*Xdef+ipxi*Xi+ipxu*Xu+ipxs*Xs+Xpp+Xppr+0.205*Xmep	gP/m3
tp	total phosphorus	xtp + stp	gP/m3

APPENDIX II - STOICHIOMETRIC MATRIX

Table II.1: Model stoichiometry matrix. Adapted from (Oehmen et al., 2010c, Henze et al., 1999, Sin et al., 2006, Moussa et al., 2005).

Process (j)			Component (i)																											
			So	Sf	Sac	Sprop	Si	Snh	Sno3	Sno2	Sn2	Spo4	Salk	Xi	Xs	Xh	Xpao	Xpp	Xpao_pha	Xpao_gly	Xgb	Xgb_pha	Xgb_gly	Xdef	Xdef_pha	Xdef_gly	Xnh	Xno2	Xmeoh	Xmep
Hydrolysis:																														
r1	Aerobic hydrolysis of Xs	g COD/m^3/d		1-prodfsi			prodfsi	@N				@P	@CH		-1															
r2	Anoxic hydrolysis of Xs (on NO_3)	g COD/m^3/d		1-prodfsi			prodfsi	@N				@P	@CH		-1															
r3	Anoxic hydrolysis of Xs (on NO_2)	g COD/m^3/d		1-prodfsi			prodfsi	@N				@P	@CH		-1															
r4	Anaerobic hydrolysis of Xs	g COD/m^3/d		1-prodfsi			prodfsi	@N				@P	@CH		-1															
Heterotrophic organisms:																														
r5	Aerobic growth of Xh on Sf	g COD/m^3/d	@COD	-1/yh				@N				@P	@CH			1														
r6	Aerobic growth of Xh on Sac	g COD/m^3/d	@COD		-1/yh			@N				@P	@CH			1														
r7	Aerobic growth of Xh on Sprop	g COD/m^3/d	@COD			-1/yh		@N				@P	@CH			1														
r8	Anoxic growth (on NO_3) of Xh on Sf	g COD/m^3/d		-1/yh				@N	-(1-yh)/(1.14*yh)	(1-yh)/(1.14*yh)		@P	@CH			1														
r9	Anoxic growth (on NO_3) of Xh on Sac	g COD/m^3/d			-1/yh			@N	-(1-yh)/(1.14*yh)	(1-yh)/(1.14*yh)		@P	@CH			1														

Table II.1: (cont.)

Process (j)			Component (i)																												
			So	Sf	Sac	Sprop	Si	Snh	Sno3	Sno2	Sn2	Spo4	Salk	Xi	Xs	Xh	Xpao	Xpp	Xpao_pha	Xpao_gly	Xgb	Xgb_pha	Xgb_gly	Xdef	Xdef_pha	Xdef_gly	Xnh	Xno2	Xmeoh	Xmep
r10	Anoxic growth (on NO_3) of Xh on Sprop	g COD/m^3/d				-1/yh		@N	-(1-yh)/(1.14*yh)	(1-yh)/(1.14*yh)		@P	@CH			1															
r11	Anoxic growth (on NO_2) of Xh on Sf	g COD/m^3/d		-1/yh				@N		-(1-yh)/(1.72*yh)	(1-yh)/(1.72*yh)	@P	@CH			1															
r12	Anoxic growth (on NO_2) of Xh on Sac	g COD/m^3/d			-1/yh			@N		-(1-yh)/(1.72*yh)	(1-yh)/(1.72*yh)	@P	@CH			1															
r13	Anoxic growth (on NO_2) of Xh on Sprop	g COD/m^3/d				-1/yh		@N		-(1-yh)/(1.72*yh)	(1-yh)/(1.72*yh)	@P	@CH			1															
r14	Sac production from fermentation of Sf	g COD/m^3/d		-1	1			@N				@P	@CH																		
r15	Sprop production from fermentation of Sf	g COD/m^3/d		-1		1		@N				@P	@CH																		
r16	Lysis of Xh	g COD/m^3/d						@N				@P	@CH	prodfxi	1- prodfxi	-1															

Table II.1: (cont.)

Process (j)			Component (i)																											
			So	Sf	Sac	Sprop	Si	Snh	Sno3	Sno2	Sn2	Spo4	Salk	Xi	Xs	Xh	Xpao	Xpp	Xpao_pha	Xpao_gly	Xgb	Xgb_pha	Xgb_gly	Xdef	Xdef_pha	Xdef_gly	Xnh	Xno2	Xmeoh	Xmep
Polyphosphate accumulating organisms:																														
r17	Anaerobic Sac uptake by PAOs	g COD/m^3/d			-1							ypo4_ac_pao	@CH					-ypo4_ac_pao	yac_pha_pao	-ygly_ac_pao										
r18	Anaerobic Sprop uptake by PAOs	g COD/m^3/d				-1						ypo4_prop_pao	@CH					-ypo4_prop_pao	yprop_pha_pao	-ygly_prop_pao										
r19	Anaerobic maintenance by PAOs	g P/m^3/d										1	@CH					-1												
r20	Aerobic Xpao_pha degradation by PAOs	g COD/m^3/d	-ypha_x_pao/yo2_x_pao					@N				-ipbm*ypha_x_pao	@CH				ypha_x_pao		-1											
r21	Aerobic Xpao_gly production by PAOs	g COD/m^3/d	(ypha_x_pao/(yo2_x_pao*ypha_gly_pao))-(1/yo2_gly_pao)					@N				ipbm*ypha_x_pao/ypha_gly_pao	@CH				-ypha_x_pao/ypha_gly_pao			1										
r22	Aerobic Xpp formation by PAOs	g P/m^3/d	(ypha_x_pao/(yo2_x_pao*ypha_pp_pao))-(1/yo2_pp_pao)					@N				-(ipbm*(ypha_x_pao/ypha_pp_pao)-1)	@CH				-ypha_x_pao/ypha_pp_pao	1												
r23	Aerobic maintenance by PAOs	g COD/m^3/d	((ypha_x_pao/yo2_x_pao)-1)					@N				ipbm*ypha_x_pao	@CH				-ypha_x_pao													
r24	Anoxic Xpao_pha degradation by PAO I (on NO_3)	g COD/m^3/d						@N	-fpaoI*((yno_pha_x_pao)/(1.14*yno3_x_pao))	fpaoI*((yno_pha_x_pao)/(1.14*yno3_x_pao))		-fpaoI*ipbm*yno_pha_x_pao	@CH				fpaoI*yno_pha_x_pao		-fpaoI											
r25	Anoxic Xpao_gly production by PAO I (on NO_3)	g COD/m^3/d						@N	fpaoI*((yno_pha_x_pao/(yno3_x_pao*yno_pha_gly_pao))-(1/yno3_gly_pao))/(1.14)	-fpaoI(((yno_pha_x_pao/(yno3_x_pao*yno_pha_gly_pao))-(1/yno3_gly_pao))/(1.14))		fpaoI*(ipbm*yno_pha_x_pao/yno_pha_gly_pao)	@CH				-fpaoI*(yno_pha_x_pao/yno_pha_gly_pao)			fpaoI										
r26	Anoxic Xpp formation by PAO I (on NO_3)	g P/m^3/d						@N	fpaoI*(((yno_pha_x_pao)/(yno3_x_pao*yno_pha_pp_pao))-(1/yno3_pp_pao))/1.14	-fpaoI*(((yno_pha_x_pao)/(yno3_x_pao*yno_pha_pp_pao))-(1/yno3_pp_pao))/1.14		-fpaoI*((ipbm*(yno_pha_x_pao/yno_pha_pp_pao))-1)	@CH				-fpaoI*(yno_pha_x_pao/yno_pha_pp_pao)	fpaoI												

Table II.1: (cont.)

Process (j)			Component (i)																										
			So	Sf	Sac	Sprop	Si	Snh	Sno3	Sno2	Sn2	Spo4	Salk	Xi	Xs	Xh	Xpao	Xpp	Xpao_pha	Xpao_gly	Xgb	Xgb_pha	Xgb_gly	Xdef	Xdef_pha	Xdef_gly	Xnh	Xno2	Xmeoh	Xmep
r27	Anoxic maintenance by PAO I (on NO_3)	g COD/m^3/d						@N	fpaoI*((yno_pha_x_pao /yno3_x_pao)-1)/1.14	- fpaoI*((yno_pha_x_pao/yno3_x_pao)-1)/1.14		fpaoI*ipbm*yno_pha_x _pao	@CH				-fpaoI*yno_pha_x_pao													
r28	Anoxic Xpao_pha degradation by PAO (on NO_2)	g COD/m^3/d						@N		- ((yno_pha_x_pao)/(1.72*yno2_x_pao))	((yno_pha_x_pao)/(1.72*yno2_x_pao))	-ipbm*yno_pha_x_pao	@CH				yno_pha_x_pao		-1											
r29	Anoxic Xpao_gly production by PAO (on NO_2)	g COD/m^3/d						@N		((yno_pha_x_pao/(yno2_x _pao*yno_pha_gly_pao))-(1/yno2_gly_pao))/(1.72)	- (((yno_pha_x_pao/(yno2_x_pao*yno_pha_gly_pao))-(1/yno2_gly_pao))/(1.72))	(ipbm*yno_pha_x_pao/ yno_pha_gly_pao)	@CH				- (yno_pha_x_pao/yno_pha_gly_pao)			1										
r30	Anoxic Xpp formation by PAO (on NO_2)	g P/m^3/d						@N		(((yno_pha_x_pao)/(yno2_x_pao*yno_pha_pp_pao))-(1/yno2_pp_pao))/1.72	- (((yno_pha_x_pao)/(yno2_x _pao*yno_pha_pp_pao))-(1/yno2_pp_pao))/1.72	- ((ipbm*(yno_pha_x_pao/yno_pha_pp_pao))-1)	@CH				- (yno_pha_x_pao/yno_pha_pp_pao)	1												
r31	Anoxic maintenance by PAO (on NO_2)	g COD/m^3/d						@N		((yno_pha_x_pao/yno2_x_pao)-1)/1.72	- ((yno_pha_x_pao/yno2_x_pao)-1)/1.72	ipbm*yno_pha_x_pao	@CH				-yno_pha_x_pao													

Table II.1: (cont.)

Process (j)		Component (i)																														
		So	Sf	Sac	Sprop	Si	Snh	Sno3	Sno2	Sn2	Spo4	Salk	Xi	Xs	Xh	Xpao	Xpp	Xpao_pha	Xpao_gly	Xgb	Xgb_pha	Xgb_gly	Xdef	Xdef_pha	Xdef_gly	Xhh	Xno2	Xmeoh	Xmep
Glycogen accumulating organisms:																																
r32	Anaerobic Sac uptake by GB and DGB	g COD/m^3/d			-1							@CH									yac_pha_gao	-ygly_ac_gao										
r33	Anaerobic Sprop uptake by GB and DGB	g COD/m^3/d				-1						@CH									yprop_pha_gao	-ygly_prop_gao										
r34	Anaerobic maintenance by GB and DGB	g COD/m^3/d										@CH									mpha_an_gao	-1										
r35	Aerobic Xgb_pha degradation by GB and DGB	g COD/m^3/d	-ypha_x_gao/yo2_x_gao				@N				-ipbm*ypha_x_gao	@CH								ypha_x_gao	-1										
r36	Aerobic Xgb_gly production by GB and DGB	g COD/m^3/d	(ypha_x_gao/(yo2_x_gao*ypha_gly_gao))-(1/yo2_gly_gao)				@N				ipbm*ypha_x_gao/ypha_gly_gao	@CH								-ypha_x_gao/ypha_gly_gao		1									
r37	Aerobic maintenance by GB and DGB	g COD/m^3/d	((ypha_x_gao/yo2_x_gao)-1)				@N				ipbm*ypha_x_gao	@CH								-ypha_x_gao											
r38	Anoxic Xgb_pha degradation by DGB (on NO_3)	g COD/m^3/d					@N	-fdgb*((yno_pha_x_gao)/(1.14*yno3_x_gao))	fdgb*((yno_pha_x_gao)/(1.14*yno3_x_gao))		-fdgb*ipbm*yno_pha_x_gao	@CH								fdgb*yno_pha_x_gao	-fdgb									
r39	Anoxic Xgb_gly production by DGB (on NO_3)	g COD/m^3/d					@N	fdgb*((yno_pha_x_gao/(yno3_x_gao*yno_pha_gly_gao))-(1/yno3_gly_gao))/(1.14)	-fdgb*(((yno_pha_x_gao/(yno3_x_gao*yno_pha_gly_gao))-(1/yno3_gly_gao))/(1.14))		fdgb*(ipbm*yno_pha_x_gao/yno_pha_gly_gao)	@CH								-fdgb*(yno_pha_x_gao/yno_pha_gly_gao)		fdgb							
r40	Anoxic maintenance by DGB (on NO_3)	g COD/m^3/d					@N	fdgb*((yno_pha_x_gao/yno3_x_gao)-1)/1.14	-fdgb*((yno_pha_x_gao/yno3_x_gao)-1)/1.14		fdgb*ipbm*yno_pha_x_gao	@CH								-fdgb*yno_pha_x_gao										
r41	Anoxic Xgb_pha degradation by DGB (on NO_2)	g COD/m^3/d					@N		-fdgb*((yno_pha_x_gao)/(1.72*yno2_x_gao))	fdgb*((yno_pha_x_gao)/(1.72*yno2_x_gao))	-fdgb*ipbm*yno_pha_x_gao	@CH								fdgb*yno_pha_x_gao	-fdgb									

Table II.1: (cont.)

Process (j)		Component (i)																														
		So	Sf	Sac	Sprop	Si	Snh	Sno3	Sno2	Sn2	Spo4	Salk	Xi	Xs	Xh	Xpao	Xpp	Xpao_pha	Xpao_gly	Xgb	Xgb_pha	Xgb_gly	Xdef	Xdef_pha	Xdef_gly	Xnh	Xno2	Xmeoh	Xmep
r42	Anoxic Xgb_gly production by DGB (on NO_2)	g COD/m³/d					@N		fdgb*((yno_pha_x_gao/(yno2_x_gao*yno_pha_gly_gao))-(1/yno2_gly_gao))/(1.72)	-fdgb*(((yno_pha_x_gao/(yno2_x_gao*yno_pha_gly_gao))-(1/yno2_gly_gao))/(1.72))	fdgb*(ipbm*yno_pha_x_gao/yno_pha_gly_gao)	@CH								-fdgb*(yno_pha_x_gao/yno_pha_gly_gao)		fdgb								
r43	Anoxic maintenance by DGB (on NO_2)	g COD/m³/d					@N		fdgb*((yno_pha_x_gao/yno2_x_gao)-1)/1.72	-fdgb*((yno_pha_x_gao/yno2_x_gao)-1)/1.72	fdgb*ipbm*yno_pha_x_gao	@CH								-fdgb*yno_pha_x_gao									

Table II.1: (cont.)

	Process (j)		Components (i)																														
			So	Sf	Sac	Sprop	Si	Snh	Sno3	Sno2	Sn2	Spo4	Salk	Xi	Xs	Xh	Xpao	Xpp	Xpao_pha	Xpao_gly	Xgb	Xgb_pha	Xgb_gly	Xdef	Xdef_pha	Xdef_gly	Xnh	Xno2	Xmeoh	Xmep
r44	Anaerobic Sac uptake by DEF and DDEF	g COD/m^3/d			-1								@CH												yac_pha_gao	-ygly_ac_gao				
r45	Anaerobic Sprop uptake by DEF and DDEF	g COD/m^3/d				-1							@CH												yprop_pha_gao	-ygly_prop_gao				
r46	Anaerobic maintenance by DEF and DDEF	g COD/m^3/d											@CH												mpha_an_gao	-1				
r47	Aerobic Xdef_pha degradation by DEF and DDEF	g COD/m^3/d	-ypha_x_gao/yo2_x_gao					@N				-ipbm*ypha_x_gao	@CH											ypha_x_gao	-1					
r48	Aerobic Xdef_gly production by DEF and DDEF	g COD/m^3/d	(ypha_x_gao/(yo2_x_gao*ypha_gly_gao))-(1/yo2_gly_gao)					@N				ipbm*ypha_x_gao/ypha_gly_gao	@CH											-ypha_x_gao/ypha_gly_gao		1			
r49	Aerobic maintenance by DEF and DDEF	g COD/m^3/d	((ypha_x_gao/yo2_x_gao)-1)					@N				ipbm*ypha_x_gao	@CH											-ypha_x_gao						
r50	Anoxic Xdef_pha degradation by DDEF (on NO_3)	g COD/m^3/d						@N	-fddef*((yno_pha_x_gao)/(1.14*yno3_x_gao))		fddef*((yno_pha_x_gao)/(1.14*yno3_x_gao))	-fddef*ipbm*yno_pha_x_gao	@CH											fddef*yno_pha_x_gao	-fddef				
r51	Anoxic Xdef_gly production by DDEF (on NO_3)	g COD/m^3/d						@N	fddef*((yno_pha_x_gao/(yno3_x_gao*yno_pha_gly_gao))-(1/yno3_gly_gao))/(1.14)		-fddef*(((yno_pha_x_gao/(yno3_x_gao*yno_pha_gly_gao))-(1/yno3_gly_gao))/(1.14))	fddef*ipbm*yno_pha_x_gao/yno_pha_gly_gao	@CH											-fddef*(yno_pha_x_gao/yno_pha_gly_gao)		fddef			
r52	Anoxic maintenance by DDEF (on NO_3)	g COD/m^3/d						@N	fddef*((yno_pha_x_gao/yno3_x_gao)-1)/1.14		-fddef*((yno_pha_x_gao/yno3_x_gao)-1)/1.14	fddef*ipbm*yno_pha_x_gao	@CH											-fddef*yno_pha_x_gao					

Table II.1: (cont.)

Process (j)			Component (i)																											
			So	Sf	Sac	Sprop	Si	Snh	Sno3	Sno2	Sn2	Spo4	Salk	Xi	Xs	Xh	Xpao	Xpp	Xpao_pha	Xpao_gly	Xgb	Xgb_pha	Xgb_gly	Xdef	Xdef_pha	Xdef_gly	Xnh	Xno2	Xmeoh	Xmep
Autotrophic organisms:																														
r53	Aerobic growth of Xnh	g COD/m^3/d	@COD					@N		1/ynh		-ipbm	@CH														1			
r54	Aerobic growth of Xno2	g COD/m^3/d	@COD					@N	1/yno2	-1/yno2		-ipbm	@CH															1		
r55	Lysis of Xnh	g COD/m^3/d						@N				@P	@CH	prodfxi	1-prodfxi												-1			
r56	Lysis of Xno2	g COD/m^3/d						@N				@P	@CH	prodfxi	1-prodfxi													-1		
Simultaneous precipitation of P with $Fe(OH)_3$:																														
r57	Precipitation of phosphates with Xmeoh	g P/m^3/d										-1	@CH																-3.45	4.87
r58	Redissolution of Xmep	g P/m^3/d										1	@CH																3.45	-4.87

Table II.2: Conservation matrix. Adapted from (Moussa et al., 2005, Henze et al., 1999).

↓ Conservation for:		Component (i)																												
		So	Sf	Sac	Sprop	Si	Snh	Sno3	Sno2	Sn2	Spo4	Salk	Xi	Xs	Xh	Xpao	Xpp	Xpao_pha	Xpao_gly	Xgb	Xgb_pha	Xgb_gly	Xdef	Xdef_pha	Xdef_gly	Xnh	Xno2	Xmeoh	Xmep
		g O_2	g COD	g COD	g COD	g COD	g N	g N	g N	g N	g P	mol	g COD	g COD	g COD	g COD	g P	g COD	g COD	g COD	g COD	g COD	g COD	g COD	g COD	g COD	g COD	g TSS	g TSS
COD	g COD	-1	1	1	1	1		-4.57	-3.43	-1.71			1	1	1	1		1	1	1	1	1	1	1	1	1	1			
N	g N		insf			insi	1	1	1	1			inxi	inxs	inbm	inbm					inbm			inbm			inbm	inbm		
P	g P		ipsf			ipsi					1		ipxi	ipxs	ipbm	ipbm	1				ipbm			ipbm			ipbm	ipbm		0.205
CH	mole			-1/64	-1/112		1/14	-1/14	-1/14		-1.5/31	-1					-1/31													

APPENDIX III – MODEL KINETICS

Table III.1: Saturation/Inhibition functions used in the kinetic equations (Henze et al., 1999, Murnleitner et al., 1997, Meijer et al., 2002, Zhou et al., 2007, Zhou et al., 2008, Lopez-Vazquez et al., 2009).

Cryptic Name	Function Definition	Description	
airsat	oxygen saturation function for hydrolysis, non poly-P and poly-P heterotrophs growth	So/(ko+So)	-
airinhib	oxygen inhibition function for hydrolysis, non poly-P and poly-P heterotrophs growth	ko/(ko + So)	-
Sno3sat	nitrate saturation function for non poly-P and poly-P heterotrophs growth	Sno3/(kno3+Sno3)	-
Sno2sat	nitrite saturation function for non poly-P and poly-P heterotrophs growth	Sno2/(kno2+Sno2)	-
Sno3inhib	nitrate Inhibition function for non poly-P and poly-P heterotrophs growth	kno3/(Sno3+kno3)	-
Sno2inhib	nitrite Inhibition function for non poly-P and poly-P heterotrophs growth	kno2/(Sno2+kno2)	-
subsat	slowly biodegradable substrate saturation function for hydrolysis	(Xs/(Xh))/(kx+(Xs/(Xh)))	-
Sfsat1	fermentable substrate saturation function for heterotrophs growth	Sf/(kf+Sf)	-
Snhsat	ammonia (as nutrient) saturation function for non poly-P and poly-P heterotrophs growth	Snh/(knh+Snh)	-
Spo4sat	phosphorus (as nutrient) saturation function for heterotrophs growth	Spo4/(kpo4 +Spo4)	-
SalksatHET	alkalinity saturation function for heterotrophs growth	Salk/(kalk+Salk)	-
SacsatHET	acetate saturation function for heterotrophs	Sac/(kacHET+Sac)	-
SpropsatHET	propionate saturation function for heterotrophs	Sprop/(kpropHET+Sprop)	-
Sfsat2	fermentable substrate saturation function for fermentation	Sf/(kfe + Sf)	-
SacsatPAO	acetate saturation function for PAOs	Sac/(kacPAO+Sac)	-
Xppsat	poly-P saturation function for PAOs	Xpp/(Xpp+kpp)	-
Xpao_glysat	glycogen saturation function for PAOs	Xpao_gly/(Xpao_gly+kgly)	-
SalksatPAO	alkalinity saturation function for PAOs	Salk/(kalkPAO+Salk)	-
SpropsatPAO	propionate saturation function for PAOs	Sprop/(kpropPAO+Sprop)	-
Xpao_phafsat	saturation function for the fraction of PHA in biomass in PAOs	Xpao_pha/(Xpao_pha+kfphaPAO)	-
Xpao_phasat	PHA saturation function for PAOs	Xpao_pha/(Xpao_pha+kphaPAO)	-
Spo4satPAO	orthophosphate saturation function for PAOs	Spo4/(Spo4+kpo4PAO)	-
SHno2	inhibition by free nitrous acid function in PAOs	(14*Sno2)/((e^((-2300)/(273+T1+T2)))*10^pH)	gN/m3

Table III.1: (cont.)

Cryptic Name	Function Definition	Description	
SacsatGAO	acetate saturation function for GAOs	Sac/(kacGAO+Sac)	-
Xgb_glysat	glycogen saturation function for GB (GAOs)	Xgb_gly/(Xgb_gly+kgly)	-
SalksatGAO	alkalinity saturation function for GAOs	Salk/(kalkGAO+Salk)	-
SpropsatGAO	propionate saturation function for GAOs	Sprop/(kpropGAO+Sprop)	-
Xgb_phafsat	Saturation function for the fraction of PHA in biomass in GB (GAOs)	Xgb_pha/(Xgb_pha+kfphaGAO)	-
Xgb_phasat	PHA saturation function for GB (GAOs)	Xgb_pha/(Xgb_pha+kphaGAO)	-
Xdef_glysat	glycogen saturation function for DEF (GAOs)	Xdef_gly/(Xdef_gly+kgly)	-
Xdef_phafsat	Saturation function for the fraction of PHA in biomass in DEF (GAOs)	Xdef_pha/(Xdef_pha+kfphaGAO)	-
Xdef_phasat	PHA saturation function for DEF (GAOs)	Xdef_pha/(Xdef_pha+kphaGAO)	-
airsatautnh	oxygen saturation function for autotrophic ammonia oxidisers growth	(So/(koanh+So))	-
Snhsataut	ammonia (as substrate) saturation function for autotrophic ammonia oxidisers growth	(Snh/(Snh+knha))	-
Salksatautnh	alkalinity saturation function for autotrophic ammonia oxidisers growth	(Salk/(kalknha+Salk))	-
airsatautno2	oxygen saturation function for autotrophic nitrite oxidisers growth	(So/(koano2+So))	-
Sno2sataut	nitrite (as substrate) saturation function for autotrophic nitrite oxidisers growth	(Sno2/(Sno2+kno2a))	-
Salksatautno2	alkalinity saturation function for autotrophic nitrite oxidisers growth	(Salk/(kalkno2a+Salk))	-
SalksatHETprec	alkalinity saturation function for redissolution of phosphates	(Salk/(kalkpre+Salk))	-
MXh	high-concentration inhibition for heterotrophs	(kXh/(kXh+Xh))	-
MXnh	high concentration inhibition for autotrophic ammonia oxidisers	(kXnh/(kXnh+Xnh))	-
MXno2	high concentration inhibition for autotrophic nitrite oxidisers	(kXno2/(kXno2+Xno2))	-

Table III.2: Kinetic equations (Henze et al., 1999, Murnleitner et al., 1997, Meijer et al., 2002, Zhou et al., 2007, Zhou et al., 2008, Lopez-Vazquez et al., 2009, Meijer, 2004).

Process		Expression
Hydrolysis:		
r1	Aerobic hydrolysis of Xs	$kh * airsat * subsat * Xh$
r2	Anoxic hydrolysis of Xs (on NO_3)	$kh * nno3hydrol * airinhib * Sno3sat * \left(\frac{Sno3}{Sno2 + Sno3}\right) * subsat * Xh$
r3	Anoxic hydrolysis of Xs (on NO_2)	$kh * nno2hydrol * airinhib * Sno2sat * \left(\frac{Sno2}{Sno2 + Sno3}\right) * subsat * Xh$
r4	Anaerobic hydrolysis of Xs	$kh * nfe * airinhib * Sno3inhib * Sno2inhib * subsat * Xh$
Heterotrophic organisms:		
r5	Aerobic growth of Xh on Sf	$muh * airsat * Sfsat1 * \left(\frac{Sf}{Sf + Sac + Sprop}\right) * Snhsat * Spo4sat * SalksatHET * Xh$
r6	Aerobic growth of Xh on Sac	$muh * airsat * SacsatHET * \left(\frac{Sac}{Sf + Sac + Sprop}\right) * Snhsat * Spo4sat * SalksatHET * Xh$
r7	Aerobic growth of Xh on Sprop	$muh * airsat * SpropsatHET * \left(\frac{Sprop}{Sf + Sac + Sprop}\right) * Snhsat * Spo4sat * SalksatHET * Xh$
r8	Anoxic growth (on NO_3) of Xh on Sf	$muh * nno3HET * airinhib * Sno3sat * Sfsat1 * \left(\frac{Sf}{Sf + Sac + Sprop}\right) * \left(\frac{Sno3}{Sno2 + Sno3}\right) * Snhsat * Spo4sat * SalksatHET * Xh$
r9	Anoxic growth (on NO_3) of Xh on Sac	$muh * nno3HET * airinhib * Sno3sat * SacsatHET * \left(\frac{Sac}{Sf + Sac + Sprop}\right) * \left(\frac{Sno3}{Sno2 + Sno3}\right) * Snhsat * Spo4sat * SalksatHET * Xh$
r10	Anoxic growth (on NO_3) of Xh on Sprop	$muh * nno3HET * airinhib * Sno3sat * SpropsatHET * \left(\frac{Sprop}{Sf + Sac + Sprop}\right) * \left(\frac{Sno3}{Sno2 + Sno3}\right) * Snhsat * Spo4sat * SalksatHET * Xh$
r11	Anoxic growth (on NO_2) of Xh on Sf	$muh * nno2HET * airinhib * Sno2sat * Sfsat1 * \left(\frac{Sf}{Sf + Sac + Sprop}\right) * \left(\frac{Sno2}{Sno2 + Sno3}\right) * Snhsat * Spo4sat * SalksatHET * Xh$
r12	Anoxic growth (on NO_2) of Xh on Sac	$muh * nno2HET * airinhib * Sno2sat * SacsatHET * \left(\frac{Sac}{Sf + Sac + Sprop}\right) * \left(\frac{Sno2}{Sno2 + Sno3}\right) * Snhsat * Spo4sat * SalksatHET * Xh$
r13	Anoxic growth (on NO_2) of Xh on Sprop	$muh * nno2HET * airinhib * Sno2sat * SpropsatHET * \left(\frac{Sprop}{Sf + Sac + Sprop}\right) * \left(\frac{Sno2}{Sno2 + Sno3}\right) * Snhsat * Spo4sat * SalksatHET * Xh$

Table III.2: (cont.)

	Process	Expression
r14	Sac production from fermentation of Sf	$qh\_ac * airinhib * Sno3inhib * Sno2inhib * \left(\frac{Sac}{Sac + Sprop}\right) * Sfsat2 * SalksatHET * Xh$
r15	Sprop production from fermentation of Sf	$qh\_prop * airinhib * Sno3inhib * Sno2inhib * \left(\frac{Sprop}{Sac + Sprop}\right) * Sfsat2 * SalksatHET * Xh$
r16	Lysis of Xh	$bh * Xh$
Polyphosphate accumulating organisms:		
r17	Anaerobic Sac uptake by PAOs	$\left(\left(qacphaPAO * 1.095^{T1-20} * \left(\frac{T1}{T1+T2}\right)\right) + \left(qacphaPAO * \left(\frac{T2}{T1+T2}\right)\right)\right) * \left(SacsatPAO * \left(\frac{Sac}{Sac+Sprop}\right) * Xppsat * Xpao\_glysat * \left(\frac{fphamaxPAO - \left(\frac{Xpao\_pha}{Xpao}\right)}{fphamaxPAO - \left(\frac{Xpao\_pha}{Xpao}\right) + kfphaPAO}\right) * airinhib * Xpao\right)$
r18	Anaerobic Sprop uptake by PAOs	$\left(\left(qpropphaPAO * 1.095^{T1-20} * \left(\frac{T1}{T1+T2}\right)\right) + \left(qpropphaPAO * \left(\frac{T2}{T1+T2}\right)\right)\right) * \left(SpropsatPAO * \left(\frac{Sprop}{Sac+Sprop}\right) * Xppsat * Xpao\_glysat * \left(\frac{fphamaxPAO - \left(\frac{Xpao\_pha}{Xpao}\right)}{fphamaxPAO - \left(\frac{Xpao\_pha}{Xpao}\right) + kfphaPAO}\right) * airinhib * Xpao\right)$
r19	Anaerobic maintenance by PAOs	$manPAO * 1.096^{(T1+T2)-20} * Xppsat * airinhib * Sno3inhib * Sno2inhib * Xpao$
r20	Aerobic Xpao_pha degradation by PAOs	$\left(\left(kphaoxacPAO * 1.129^{T1-20} * \left(\frac{T1}{T1+T2}\right)\right) + \left(kphaoxacPAO * \left(\frac{T2}{T1+T2}\right)\right)\right) * \left(\left(\frac{Xpao\_pha}{Xpao}\right)^{\frac{2}{3}}\right) * Xpao\_phafsat * airsat * Snhsat * SalksatPAO * Spo4sat * Xpao$

Table III.2: (cont.)

	Process	Expression
r21	Aerobic Xpao_gly production by PAOs	$\left(\left(kglyoxacPAO * 1.125^{T1-20} * \left(\frac{T1}{T1+T2}\right)\right) + \left(kglyoxacPAO * \left(\frac{T2}{T1+T2}\right)\right)\right) * \left(\left(\frac{Xpao\_pha}{Xpao}\right)^{\frac{2}{3}}\right) * \left(\frac{1}{\frac{Xpao\_gly}{Xpao}}\right) * \left(\frac{fglymaxPAO - \left(\frac{Xpao\_gly}{Xpao}\right)}{fglymaxPAO - \left(\frac{Xpao\_gly}{Xpao}\right) + kgly}\right) * Xpao\_phasat * airsat * Xpao$
r22	Aerobic Xpp formation by PAOs	$\left(\left(kppoxacPAO * 1.031^{T1-20} * \left(\frac{T1}{T1+T2}\right)\right) + \left(kppoxacPAO * \left(\frac{T2}{T1+T2}\right)\right)\right) * \left(\frac{1}{\frac{Xpp}{Xpao}}\right) * \left(\frac{fppmaxPAO - \left(\frac{Xpp}{Xpao}\right)}{fppmaxPAO - \left(\frac{Xpp}{Xpao}\right) + kpp}\right) * Xpao\_phasat * Spo4satPAO * airsat * Xpao$
r23	Aerobic maintenance by PAOs	$mphaoxPAO * 1.064^{(T1+T2)-20} * airsat * Xpao$
r24	Anoxic Xpao_pha degradation by PAO I (on NO_3)	$\left(\left(kphaaxacPAO * 1.129^{T1-20} * \left(\frac{T1}{T1+T2}\right)\right) + \left(kphaaxacPAO * \left(\frac{T2}{T1+T2}\right)\right)\right) * \left(\left(\frac{Xpao\_pha}{Xpao}\right)^{\frac{2}{3}}\right) * Xpao\_phafsat * Sno3sat * airinhib * Snhsat * SalksatPAO * Spo4sat * Xpao$
r25	Anoxic Xpao_gly production by PAO I (on NO_3)	$\left(\left(kglyaxacPAO * 1.125^{T1-20} * \left(\frac{T1}{T1+T2}\right)\right) + \left(kglyaxacPAO * \left(\frac{T2}{T1+T2}\right)\right)\right) * \left(\left(\frac{Xpao\_pha}{Xpao}\right)^{\frac{2}{3}}\right) * \left(\frac{1}{\frac{Xpao\_gly}{Xpao}}\right) * \left(\frac{fglymaxPAO - \left(\frac{Xpao\_gly}{Xpao}\right)}{fglymaxPAO - \left(\frac{Xpao\_gly}{Xpao}\right) + kgly}\right) * Xpao\_phasat * Sno3sat * airinhib * Xpao$
r26	Anoxic Xpp formation by PAO I (on NO_3)	$\left(\left(kppaxacPAO * 1.031^{T1-20} * \left(\frac{T1}{T1+T2}\right)\right) + \left(kppaxacPAO * \left(\frac{T2}{T1+T2}\right)\right)\right) * \left(\frac{1}{\frac{Xpp}{Xpao}}\right) * (e^{-170*SHno2}) * \left(\frac{fppmaxPAO - \left(\frac{Xpp}{Xpao}\right)}{fppmaxPAO - \left(\frac{Xpp}{Xpao}\right) + kpp}\right) * Xpao\_phasat * Spo4satPAO * Sno3sat * airinhib * Xpao$

Table III.2: (cont.)

	Process	Expression
r27	Anoxic maintenance by PAO I (on NO_3)	$mphaaxPAO * 1.064^{(T1+T2)-20} * Sno3sat * airinhib * Xpao$
r28	Anoxic Xpao_pha degradation by PAO (on NO_2)	$\left(\left(kphaaxacPAO * 1.129^{T1-20} * \left(\frac{T1}{T1+T2}\right)\right) + \left(kphaaxacPAO * \left(\frac{T2}{T1+T2}\right)\right)\right) * \left(\left(\frac{Xpao\_pha}{Xpao}\right)^{\frac{2}{3}}\right) * Xpao\_phafsat * Sno2sat * airinhib * Snhsat * SalksatPAO * Spo4sat * Xpao$
r29	Anoxic Xpao_gly production by PAO (on NO_2)	$\left(\left(kglyaxacPAO * 1.125^{T1-20} * \left(\frac{T1}{T1+T2}\right)\right) + \left(kglyaxacPAO * \left(\frac{T2}{T1+T2}\right)\right)\right) * \left(\left(\frac{Xpao\_pha}{Xpao}\right)^{\frac{2}{3}}\right) * \left(\frac{1}{\frac{Xpao\_gly}{Xpao}}\right) * \left(\frac{fglymaxPAO - \left(\frac{Xpao\_gly}{Xpao}\right)}{fglymaxPAO - \left(\frac{Xpao\_gly}{Xpao}\right) + kgly}\right) * Xpao\_phasat * Sno2sat * airinhib * Xpao$
r30	Anoxic Xpp formation by PAO (on NO_2)	$\left(\left(kppaxacPAO * 1.031^{T1-20} * \left(\frac{T1}{T1+T2}\right)\right) + \left(kppaxacPAO * \left(\frac{T2}{T1+T2}\right)\right)\right) * \left(\frac{1}{\frac{Xpp}{Xpao}}\right) * (e^{-170*SHno2}) * \left(\frac{fppmaxPAO - \left(\frac{Xpp}{Xpao}\right)}{fppmaxPAO - \left(\frac{Xpp}{Xpao}\right) + kpp}\right) * Xpao\_phasat * Spo4satPAO * Sno2sat * airinhib * Xpao$
r31	Anoxic maintenance by PAO (on NO_2)	$mphaaxPAO * 1.064^{(T1+T2)-20} * Sno2sat * airinhib * Xpao$
Glycogen accumulating organisms:		
r32	Anaerobic Sac uptake by GB and DGB	$\left(\left(qacphaGBa * 1.211^{T1-20} * \left(\frac{10^{-pH}}{1.2*10^{-8}+10^{-pH}}\right) * \left(\frac{T1}{T1+T2}\right)\right) + \left(qacphaGBb * \left(\frac{10^{-pH}}{1.2*10^{-8}+10^{-pH}}\right) * \left(\frac{T2}{T1+T2}\right)\right)\right) * SacsatGAO * \left(\frac{Sac}{Sac+Sprop}\right) * Xgb\_glysat * \left(\frac{fphamaxGAO - \left(\frac{Xgb\_pha}{Xgb}\right)}{fphamaxGAO - \left(\frac{Xgb\_pha}{Xgb}\right) + kfphaGAO}\right) * airinhib * Xgb$

Table III.2: (cont.)

	Process	Expression
r33	Anaerobic Sprop uptake by GB and DGB	$\left(\left(qpropphaGB * 1.211^{T1-20} * \left(\frac{10^{-pH}}{1.2*10^{-8}+10^{-pH}}\right) * \left(\frac{T1}{T1+T2}\right)\right) + \left(qpropphaGB * \left(\frac{10^{-pH}}{1.2*10^{-8}+10^{-pH}}\right) * \left(\frac{T2}{T1+T2}\right)\right)\right) * SpropsatGAO * \left(\frac{Sprop}{Sac+Sprop}\right) * Xgb\_glysat * \left(\frac{fphamaxGAO - \left(\frac{Xgb\_pha}{Xgb}\right)}{fphamaxGAO - \left(\frac{Xgb\_pha}{Xgb}\right) + kfphaGAO}\right) * airinhib * Xgb$
r34	Anaerobic maintenance by GB and DGB	$manGB * 1.028^{(T1+T2)-20} * Xgb\_glysat * airinhib * Sno3inhib * Sno2inhib * Xgb$
r35	Aerobic Xgb_pha degradation by GB and DGB	$qphaoxGB * 1.109^{(T1+T2)-20} * \left(\left(\frac{Xgb\_pha}{Xgb}\right)^{\frac{2}{3}}\right) * Xgb\_phafsat * airsat * Snhsat * SalksatGAO * Spo4sat * Xgb$
r36	Aerobic Xgb_gly production by GB and DGB	$qglyoxGB * 1.071^{(T1+T2)-20} * \left(\left(\frac{Xgb\_pha}{Xgb}\right)^{\frac{2}{3}}\right) * \left(\frac{1}{\frac{Xgb\_gly}{Xgb}}\right) * \left(\frac{fglymaxGAO - \left(\frac{Xgb\_gly}{Xgb}\right)}{fglymaxGAO - \left(\frac{Xgb\_gly}{Xgb}\right) + kgly}\right) * Xgb\_phasat * airsat * Xgb$
r37	Aerobic maintenance by GB and DGB	$mphaoxGB * 1.046^{(T1+T2)-20} * airsat * Xgb$
r38	Anoxic Xgb_pha degradation by DGB (on NO_3)	$qphaaxGB * 1.109^{(T1+T2)-20} * \left(\left(\frac{Xgb\_pha}{Xgb}\right)^{\frac{2}{3}}\right) * Xgb\_phafsat * Sno3sat * airinhib * Snhsat * SalksatGAO * Spo4sat * Xgb$
r39	Anoxic Xgb_gly production by DGB (on NO_3)	$qglyaxGB * 1.071^{(T1+T2)-20} * \left(\left(\frac{Xgb\_pha}{Xgb}\right)^{\frac{2}{3}}\right) * \left(\frac{1}{\frac{Xgb\_gly}{Xgb}}\right) * \left(\frac{fglymaxGAO - \left(\frac{Xgb\_gly}{Xgb}\right)}{fglymaxGAO - \left(\frac{Xgb\_gly}{Xgb}\right) + kgly}\right) * Xgb\_phasat * Sno3sat * airinhib * Xgb$
r40	Anoxic maintenance by DGB (on NO_3)	$mphaaxGB * 1.046^{(T1+T2)-20} * Sno3sat * airinhib * Xgb$
r41	Anoxic Xgb_pha degradation by DGB (on NO_2)	$qphaaxGB * 1.109^{(T1+T2)-20} * \left(\left(\frac{Xgb\_pha}{Xgb}\right)^{\frac{2}{3}}\right) * Xgb\_phafsat * Sno2sat * \left(\frac{Sno2}{Sno2+Sno3}\right) * airinhib * Snhsat * SalksatGAO * Spo4sat * Xgb$

Table III.2: (cont.)

	Process	Expression
r42	Anoxic Xgb_gly production by DGB (on NO_2)	$qglyaxGB * 1.071^{(T1+T2)-20} * \left(\left(\frac{Xgb\_pha}{Xgb}\right)^{\frac{2}{3}}\right) * \left(\frac{1}{\frac{Xgb\_gly}{Xgb}}\right) * \left(\frac{fglymaxGAO - \left(\frac{Xgb\_gly}{Xgb}\right)}{fglymaxGAO - \left(\frac{Xgb\_gly}{Xgb}\right) + kgly}\right) * Xgb\_phasat * \left(\frac{Sno2}{Sno2 + Sno3}\right) * Sno2sat * airinhib * Xgb$
r43	Anoxic maintenance by DGB (on NO_2)	$mphaaxGB * 1.046^{(T1+T2)-20} * \left(\frac{Sno2}{Sno2 + Sno3}\right) * Sno2sat * airinhib * Xgb$
r44	Anaerobic Sac uptake by DEF and DDEF	$\left(\left(qacphaDEFa * 1.211^{T1-20} * \left(\frac{10^{-pH}}{1.2 * 10^{-8} + 10^{-pH}}\right) * \left(\frac{T1}{T1 + T2}\right)\right) + \left(qacphaDEFb * \left(\frac{10^{-pH}}{1.2 * 10^{-8} + 10^{-pH}}\right) * \left(\frac{T2}{T1 + T2}\right)\right)\right) * SacsatGAO * \left(\frac{Sac}{Sac + Sprop}\right) * Xdef\_glysat * \left(\frac{fphamaxGAO - \left(\frac{Xdef\_pha}{Xdef}\right)}{fphamaxGAO - \left(\frac{Xdef\_pha}{Xdef}\right) + kfphaGAO}\right) * airinhib * Xdef$
r45	Anaerobic Sprop uptake by DEF and DDEF	$\left(\left(qpropphaDEFa * 1.211^{T1-20} * \left(\frac{10^{-pH}}{1.2 * 10^{-8} + 10^{-pH}}\right) * \left(\frac{T1}{T1 + T2}\right)\right) + \left(qpropphaDEFb * \left(\frac{10^{-pH}}{1.2 * 10^{-8} + 10^{-pH}}\right) * \left(\frac{T2}{T1 + T2}\right)\right)\right) * SpropsatGAO * \left(\frac{Sprop}{Sac + Sprop}\right) * Xdef\_glysat * \left(\frac{fphamaxGAO - \left(\frac{Xdef\_pha}{Xdef}\right)}{fphamaxGAO - \left(\frac{Xdef\_pha}{Xdef}\right) + kfphaGAO}\right) * airinhib * Xdef$
r46	Anaerobic maintenance by DEF and DDEF	$manDEF * 1.028^{(T1+T2)-20} * Xdef\_glysat * airinhib * Sno3inhib * Xdef$
r47	Aerobic Xdef_pha degradation by DEF and DDEF	$qphaoxDEF * 1.109^{(T1+T2)-20} * \left(\left(\frac{Xdef\_pha}{Xdef}\right)^{\frac{2}{3}}\right) * Xdef\_phafsat * airsat * Snhsat * SalksatGAO * Spo4sat * Xdef$
r48	Aerobic Xdef_gly production by DEF and DDEF	$qglyoxDEF * 1.071^{(T1+T2)-20} * \left(\left(\frac{Xdef\_pha}{Xdef}\right)^{\frac{2}{3}}\right) * \left(\frac{1}{\frac{Xdef\_gly}{Xdef}}\right) * \left(\frac{fglymaxGAO - \left(\frac{Xdef\_gly}{Xdef}\right)}{fglymaxGAO - \left(\frac{Xdef\_gly}{Xdef}\right) + kgly}\right) * Xdef\_phasat * airsat * Xdef$
r49	Aerobic maintenance by DEF and DDEF	$mphaoxDEF * 1.046^{(T1+T2)-20} * airsat * Xdef$

Table III.2: (cont.)

	Process	Expression
r50	Anoxic Xdef_pha degradation by DDEF (on NO_3)	$qphaaxDEF * 1.109^{(T1+T2)-20} * \left(\left(\frac{Xdef\_pha}{Xdef}\right)^{\frac{2}{3}}\right) * Xdef\_phafsat * Sno3sat * airinhib * Snhsat * SalksatGAO * Spo4sat * Xdef$
r51	Anoxic Xdef_gly production by DDEF (on NO_3)	$qglyaxDEF * 1.071^{(T1+T2)-20} * \left(\left(\frac{Xdef\_pha}{Xdef}\right)^{\frac{2}{3}}\right) * \left(\frac{1}{\frac{Xdef\_gly}{Xdef}}\right) * \left(\frac{fglymaxGAO - \left(\frac{Xdef\_gly}{Xdef}\right)}{fglymaxGAO - \left(\frac{Xdef\_gly}{Xdef}\right) + kgly}\right) * Xdef\_phasat * Sno3sat * airinhib * Xdef$
r52	Anoxic maintenance by DDEF (on NO_3)	$mphaaxDEF * 1.046^{(T1+T2)-20} * Sno3sat * airinhib * Xdef$
	Autotrophic organisms:	
r53	Aerobic growth of Xnh	$muautnh * airsatautnh * Snhsataut * Spo4sat * Salksatautnh * Xnh$
r54	Aerobic growth of Xno2	$muautno2 * airsatautno2 * Sno2sataut * Spo4sat * Salksatautno2 * Xno2$
r55	Lysis of Xnh	$bautnh * Xnh$
r56	Lysis of Xno2	$bautno2 * Xno2$
	Simultaneous precipitation of P with $Fe(OH)_3$:	
r57	Precipitation of phosphates with Xmeoh	$kpre * Spo4 * Xmeoh$
r58	Redissolution of Xmep	$kred * Xmep * SalksatHETprec$

APPENDIX IV – MODEL PARAMETERS

Table IV. 1: Stoichiometric parameters.

Parameter	Value	Units	Description	Source
Hydrolysis:				
prodfsi	0.00	g COD/g COD	Production of soluble inerts in hydrolysis	(Henze et al., 1999)
Heterotrophic organisms:				
yh	0.63	g COD/g COD	Heterotrophic yield	(Henze et al., 1999)
prodfxi	0.10	g COD/g COD	Fraction of inert COD generated in biomass lysis	(Henze et al., 1999)
Autotrophic organisms:				
ynh	0.18	g COD/g N	Yield of ammonia oxidisers per NO2-N	Moussa et al., (2005)
yno2	0.06	g COD/g N	Yield of nitrite oxidisers per NO3-N	Moussa et al., (2005)
prodfxi	0.10	g COD/g COD	Fraction of inert COD generated in biomass lysis	(Henze et al., 1999)
Polyphosphate accumulating organisms:				
yac_pha_pao	1.50	g COD/g COD	Yield for anaerobic formation of PHA from S_{ac}	(Smolders et al., 1994a)
ygly_ac_pao	0.50	g COD/g COD	Yield for anaerobic consumption of glycogen from S_{ac}	(Smolders et al., 1994a)

Table IV.1: (cont.)

Parameter	Value	Units	Description	Source
ypo4_ac_pao	0.15.pH-0.53	g P/g COD	Anaerobic yield for phosphate release from S_{ac}	(Smolders et al., 1994a); (Filipe et al., 2001c)
yprop_pha_pao	1.29	g COD/g COD	Yield for anaerobic formation of PHA from S_{prop}	(Oehmen et al., 2005a)
ygly_prop_pao	2/7	g COD/g COD	Yield for anaerobic consumption of glycogen from S_{prop}	(Oehmen et al., 2005a)
ypo4_prop_pao	0.33	g P/g COD	Anaerobic yield for phosphate release from S_{prop}	(Oehmen et al., 2005a)
ypha_x_pao [A]	$\frac{\left(\frac{17340965703.ratio\_prop\_ac}{2861868800}+\frac{84646755}{14309344}\right)\left(\frac{90923236313895.ratio\_prop\_ac}{4790822947038016}+\frac{2650572433125}{149713217094938}\right)}{\left(\frac{5582601.ratio\_prop\_ac}{114474752}+\frac{378225}{7154672}\right)\left(\frac{1253263706243883.ratio\_prop\_ac}{207305190265600}+\frac{3023162031915}{518262975664}\right)}$	g COD/g COD	Maximum biomass growth yield on PHA (aerobic)	(Smolders et al., 1994b, Kuba et al., 1996, Zeng et al., 2003a, Lopez-Vazquez et al., 2009)
ypha_pp_pao [B]	$\frac{\frac{6605711406209493.ratio\_prop\_ac}{2645511518720000}+\frac{6448914605781}{2645511518720}}{\frac{2964361131.ratio\_prop\_ac}{2003308160}+\frac{40167495}{25041352}}$	g P/g COD	Maximum yield of poly-P stored on PHA (aerobic)	
ypha_gly_pao [C]	$\frac{\left(\frac{17340965703.ratio\_prop\_ac}{2861868800}+\frac{84646755}{14309344}\right)\left(\frac{138725773983.ratio\_prop\_ac}{195809513984}+\frac{29541263625}{48952378496}\right)}{\left(\frac{5582601.ratio\_prop\_ac}{3605504}+\frac{378225}{225344}\right)\left(\frac{1264890303.ratio\_prop\_ac}{211823360}+\frac{57111975}{10591168}\right)}$	g COD/g COD	Maximum yield of glycogen stored on PHA (aerobic)	
yo2_x_pao [D]	$\frac{\left(\frac{17340965703.ratio\_prop\_ac}{2861868800}+\frac{84646755}{14309344}\right)\left(\frac{739213303365.ratio\_prop\_ac}{16584415221248}+\frac{21549369375}{518262975664}\right)}{\frac{84396361654744704675513.ratio\_prop\_ac^2}{9492484097586949652480000}+\frac{178116561581996667897.ratio\_prop\_ac}{94924840975869496524800}+\frac{729556340882223375}{7416003201239804416}}$	g COD/g O2	Biomass growth per oxygen consumed	

Table IV.1: (cont.)

Parameter	Value	Units	Description	Source
yo2_pp_pao [E]	$\frac{\frac{53704970782191.ratio\_prop\_ac}{9157980160000}+\frac{52430200047}{9157980160}}{\frac{72759400443.ratio\_prop\_ac}{40066163200}+\frac{361507455}{200330816}}$	g P/g O2	Poly-P uptake per oxygen consumed	
yo2_gly_pao [F]	$\frac{\left(\frac{1127851821.ratio\_prop\_ac}{677834752}+\frac{240172875}{169458688}\right)\left(\frac{17340965703.ratio\_prop\_ac}{2861868800}+\frac{84646755}{14309344}\right)}{\frac{275988536191467.ratio\_prop\_ac^2}{218208563363840}+\frac{118054007261775.ratio\_prop\_ac}{38186498588672}+\frac{2145812259375}{1193328080896}}$	g COD/g O2	Glycogen produced per oxygen consumed	
yno_pha_x_pao [G]	$\frac{\left(\frac{680759613.ratio\_prop\_ac}{112672000}+\frac{4584087}{788704}\right)\left(\frac{454616181569475.ratio\_prop\_ac}{28857079025855552}+\frac{13252862165625}{901783719557986}\right)}{\left(\frac{5582601.ratio\_prop\_ac}{114474752}+\frac{378225}{7154672}\right)\left(\frac{417433571157231.ratio\_prop\_ac}{68825082771200}+\frac{1023797509155}{172062706928}\right)}$	g COD/g COD	Maximum biomass growth yield on PHA (anoxic)	
yno_pha_pp_pao [H]	$\frac{\frac{259322440139703.ratio\_prop\_ac}{104153996800000}+\frac{1746220844997}{729077977600}}{\frac{2964361131.ratio\_prop\_ac}{1104185600}+\frac{8033499}{2760464}}$	g P/g COD	Maximum yield of poly-P stored on PHA (anoxic)	
yno_pha_gly_pao [I]	$\frac{\left(\frac{680759613.ratio\_prop\_ac}{112672000}+\frac{4584087}{788704}\right)\left(\frac{5461644645.ratio\_prop\_ac}{8332319744}+\frac{1163041875}{2083079936}\right)}{\left(\frac{5582601.ratio\_prop\_ac}{3605504}+\frac{378225}{225344}\right)\left(\frac{27096039.ratio\_prop\_ac}{4506880}+\frac{17776575}{3154816}\right)}$	g COD/g COD	Maximum yield of glycogen stored on PHA (anoxic)	
yno3_x_pao [J]	$\frac{\left(\frac{680759613.ratio\_prop\_ac}{112672000}+\frac{4584087}{788704}\right)\left(\frac{3696066516825.ratio\_prop\_ac}{87407855119424}+\frac{107746846875}{2731495472482}\right)}{\frac{43207290995686453554741.ratio\_prop\_ac^2}{3151493712645037096960000}+\frac{91012957246249044129.ratio\_prop\_ac}{31514937126450370969 6}+\frac{372168219113663625}{2462104463003935232}}$	g COD/g N	Biomass growth per nitrate consumed	
yno3_pp_pao [K]	$\frac{\frac{2108312521461.ratio\_prop\_ac}{315481600000}+\frac{14196917439}{2208371200}}{\frac{72759400443.ratio\_prop\_ac}{22083712000}+\frac{72301491}{22083712}}$	g P/g N	Poly-P uptake per nitrate consumed	
yno3_gly_pao [L]	$\frac{\left(\frac{44403615.ratio\_prop\_ac}{25238528}+\frac{9455625}{6309632}\right)\left(\frac{680759613.ratio\_prop\_ac}{112672000}+\frac{4584087}{788704}\right)}{\frac{275988536191467.ratio\_prop\_ac^2}{129996590940160}+\frac{118054007261775.ratio\_prop\_ac}{22749403414528}+\frac{2145812259375}{710918856704}}$	g COD/g N	Glycogen produced per nitrate consumed	
yno2_x_pao [M]	$\frac{\left(\frac{680759613.ratio\_prop\_ac}{112672000}+\frac{4584087}{788704}\right)\left(\frac{11088199550475.ratio\_prop\_ac}{174815710238848}+\frac{323240540625}{5462990944964}\right)}{\frac{43207290995686453554741.ratio\_prop\_ac^2}{3151493712645037096960000}+\frac{91012957246249044129.ratio\_prop\_ac}{31514937126450370969 6}+\frac{372168219113663625}{2462104463003935232}}$	g COD/g N	Biomass growth per nitrite consumed	

Table IV.1: (cont.)

Parameter	Value	Units	Description	Source
yno2_pp_pao_N	$\frac{\frac{6324937564383.ratio\_prop\_ac}{630963200000}+\frac{42590752317}{4416742400}}{\frac{72759400443.ratio\_prop\_ac}{22083712000}+\frac{72301491}{22083712}}$	g P/g N	Poly-P uptake per nitrite consumed	
yno2_gly_pao_o	$\frac{\left(\frac{133210845.ratio\_prop\_ac}{50477056}+\frac{28366875}{12619264}\right)\left(\frac{680759613.ratio\_prop\_ac}{112672000}+\frac{4584087}{788704}\right)}{\frac{275988536191467.ratio\_prop\_ac^2}{129996590940160}+\frac{118054007261775.ratio\_prop\_ac}{22749403414528}+\frac{2145812259375}{710918856704}}$	g COD/g N	Glycogen produced per nitrite consumed	
Glycogen accumulating organisms:				
yac_pha_gao	$\frac{57.pH}{500}+\frac{33}{25}$	g COD/g COD	Yield for anaerobic formation of PHA from S_{ac}	(Zeng et al., 2003b)
ygly_ac_gao	0.114.pH+0.32	g COD/g COD	Yield for anaerobic consumption of glycogen from S_{ac}	(Filipe et al., 2001a)
yprop_pha_gao	1.57	g COD/g COD	Yield for anaerobic formation of PHA from S_{prop}	(Oehmen et al., 2006b)
ygly_prop_gao	0.57	g COD/g COD	Yield for anaerobic consumption of glycogen from S_{prop}	(Oehmen et al., 2006b)
mpha_an_gao	1.00	g COD/(g COD.)	Anaerobic maintenance coefficient on PHA	(Zeng et al., 2003b)

Table IV.1: (cont.)

Parameter	Value	Units	Description	Source
ypha_x_gao_P	$\left(\frac{19.pH}{6400}+\frac{71}{1920}\right)\left(\frac{4211844399.pH}{39062500000}+\frac{217590848613.ratio\_prop\_ac}{125000000000}+\frac{9607133799}{7812500000}\right)\left(\frac{568242435609.pH}{19531250000000}+\frac{925821105039.ratio\_prop\_ac}{1953125000000}+\frac{623081251767}{1953125000000}\right)}{\left(\frac{41401.pH}{180000}+\frac{149309}{54000}\right)\left(\frac{3518667.ratio\_prop\_ac}{31250000000}+\frac{22284891.pH}{3125000000000}+\frac{27758373}{312500000000}\right)\left(\frac{3929504275305117.ratio\_prop\_ac}{15625000000000}+\frac{4856384485036449\,.pH}{312500000000000}+\frac{5483156828651487}{31250000000000}\right)}$	g COD/g COD	Maximum biomass growth yield on PHA (aerobic)	(Smolders et al., 1994b, Kuba et al., 1996, Zeng et al., 2003a, Lopez-Vazquez et al., 2009)
ypha_gly_gao_Q	$\left(\frac{19.pH}{6400}+\frac{71}{1920}\right)\left(\frac{1270238787.pH}{4882812500000}+\frac{4211844399.ratio\_prop\_ac}{976562500000}+\frac{1285095381}{488281250000}\right)\left(\frac{26675014527.pH}{976562500000000}+\frac{1378075374549.ratio\_prop\_ac}{3125000000000000}+\frac{60845180727}{195312500000000}\right)}{\left(\frac{41401.pH}{180000}+\frac{149309}{54000}\right)\left(\frac{22284891.ratio\_prop\_ac}{3125000000000}+\frac{141137643.pH}{312500000000000}+\frac{175803029}{31250000000000}\right)\left(\frac{183337798257.pH}{390625000000000}+\frac{601224074289.ratio\_prop\_ac}{78125000000000}+\frac{195386495991}{39062500000000}\right)}$	g COD/g COD	Maximum yield of glycogen stored on PHA (aerobic)	
yo2_x_gao_R	$\left(\frac{4211844399.pH}{39062500000}+\frac{217590848613.ratio\_prop\_ac}{125000000000}+\frac{9607133799}{7812500000}\right)\left(\frac{568242435609.pH}{625000000000000}+\frac{925821105039.ratio\_prop\_ac}{62500000000000}+\frac{623081251767}{62500000000000}\right)}{\frac{842268825870275371308663.pH.ratio\_prop\_ac}{781250000000000000000000000}+\frac{207081143688001961548 53.pH^2}{610351562500000000000000000}+\frac{668902292330018979882 5379\,.ratio\_prop\_ac^2}{781250000000000000000000000}+\frac{403033076982025604464599.pH}{488281250000000000000000000}+\frac{102571538623101199720101 69.ratio\_prop\_ac}{781250000000000000000000000}+\frac{244042791451183639987281}{488281250000000000000000000}}$	g COD/g O2	Biomass growth per oxygen consumed	
yo2_gly_gao_S	$\left(\frac{1270238787.pH}{156250000000000}+\frac{4211844399.ratio\_prop\_ac}{31250000000000}+\frac{1285095381}{15625000000000}\right)\left(\frac{26675014527.pH}{976562500000000}+\frac{1378075374549.ratio\_prop\_ac}{3125000000000000}+\frac{60845180727}{195312500000000}\right)}{\frac{24315827171637539403.pH.ratio\_prop\_ac}{244140625000000000000000000}+\frac{1972063592887949451.pH^2}{610351562500000000000000000}+\frac{1868717726939830014 9.ratio\_prop\_ac^2}{244140625000000000000000000}+\frac{2676596678704377963.pH}{305175781250000000000000000}+\frac{3330756311040087678 9.ratio\_prop\_ac}{244140625000000000000000000}+\frac{3519961628862452319}{610351562500000000000000000}}$	g COD/g O2	Glycogen produced per oxygen consumed	

Table IV.1: (cont.)

Parameter	Value	Units	Description	Source
$y_{no\_pha\_x\_gao}^{r}$	$\left(\frac{19.pH}{6400}+\frac{71}{1920}\right)\left(\frac{4612972437.pH}{78125000000}+\frac{59757521661.ratio\_prop\_ac}{62500000000}+\frac{5194725381}{7812500000}\right)\left(\frac{568242435609.pH}{19531250000000}+\frac{925821105039.ratio\_prop\_ac}{1953125000000}+\frac{623081251767}{1953125000000}\right)$ $\left(\frac{41401.pH}{180000}+\frac{149309}{54000}\right)\left(\frac{3518667.ratio\_prop\_ac}{31250000000}+\frac{22284891.pH}{3125000000000}+\frac{27758373}{312500000000}\right)\left(\frac{1309736024639019.ratio\_prop\_ac}{7812500000000}+\frac{1624163481436293.pH}{156250000000000}+\frac{1860107807372859}{15625000000000}\right)$	g COD/g COD	Maximum biomass growth yield on PHA (anoxic)	
$y_{no\_pha\_gly\_gao}^{u}$	$\left(\frac{19.pH}{6400}+\frac{71}{1920}\right)\left(\frac{200564019.pH}{48828125000}+\frac{665028063.ratio\_prop\_ac}{9765625000}+\frac{202909797}{4882812500}\right)\left(\frac{4612972437.pH}{19531250000000}+\frac{59757521661.ratio\_prop\_ac}{15625000000000}+\frac{5194725381}{1953125000000}\right)$ $\left(\frac{41401.pH}{180000}+\frac{149309}{54000}\right)\left(\frac{3518667.ratio\_prop\_ac}{31250000000}+\frac{22284891.pH}{3125000000000}+\frac{27758373}{312500000000}\right)\left(\frac{8757962163.pH}{1953125000000}+\frac{28511758701.ratio\_prop\_ac}{390625000000}+\frac{9642320469}{195312500000}\right)$	g COD/g COD	Maximum yield of glycogen stored on PHA (anoxic)	
$y_{no3\_x\_gao}^{v}$	$\left(\frac{4612972437.pH}{78125000000}+\frac{59757521661.ratio\_prop\_ac}{62500000000}+\frac{5194725381}{7812500000}\right)\left(\frac{568242435609.pH}{546875000000000}+\frac{925821105039.ratio\_prop\_ac}{54687500000000}+\frac{623081251767}{54687500000000}\right)$ $\frac{4309531839494932764007791.pH.ratio\_prop\_ac}{390625000000000000000000000}+\frac{1694597974957530246170 61.pH^2}{48828125000000000000000000}+\frac{3423899266425075033675603.ratio\_prop\_ac^2}{390625000000000000000000000}$ $+\frac{1029072123173243949615 09.pH}{122070312500000000000000000}+\frac{5239792378738543016463633.ratio\_prop\_ac}{390625000000000000000000000}+\frac{2489079151745342807251 59}{488281250000000000000000000}$	g COD/g N	Biomass growth per nitrate consumed	
$y_{no3\_gly\_gao}^{w}$	$\frac{\left(\frac{95004009.ratio\_prop\_ac}{39062500000}+\frac{200564019.pH}{1367187500000}+\frac{202909797}{136718750000}\right)\left(\frac{4612972437.pH}{19531250000000}+\frac{59757521661.ratio\_prop\_ac}{15625000000000}+\frac{5194725381}{1953125000000}\right)}{\frac{606211757741656107.pH.ratio\_prop\_ac}{24414062500000000000000000}+\frac{49165020321306219.pH^2}{61035156250000000000000000}+\frac{465885305885276181.ratio\_prop\_ac^2}{24414062500000000000000000}+}$ $+\frac{66729557086812747.pH}{30517578125000000000000000}+\frac{830382459816088341.ratio\_prop\_ac}{24414062500000000000000000}+\frac{87755276065822911}{61035156250000000000000000}$	g COD/g N	Glycogen produced per nitrate consumed	
$y_{no2\_x\_gao}^{x}$	$\left(\frac{4612972437.pH}{78125000000}+\frac{59757521661.ratio\_prop\_ac}{62500000000}+\frac{5194725381}{7812500000}\right)\left(\frac{1704727306827.pH}{1093750000000000}+\frac{2777463315117.ratio\_prop\_ac}{109375000000000}+\frac{1869243755301}{109375000000000}\right)$ $\frac{4309531839494932764007791.pH.ratio\_prop\_ac}{390625000000000000000000000}+\frac{1694597974957530246170 61.pH^2}{48828125000000000000000000}+\frac{3423899266425075033675603.ratio\_prop\_ac^2}{390625000000000000000000000}$ $+\frac{1029072123173243949615 09.pH}{122070312500000000000000000}+\frac{5239792378738543016463633.ratio\_prop\_ac}{390625000000000000000000000}+\frac{2489079151745342807251 59}{488281250000000000000000000}$	g COD/g N	Biomass growth per nitrite consumed	

Table IV.1: (cont.)

Parameter	Value	Units	Description	Source
yno2_gly_gao	$\left(\frac{285012027.ratio\_prop\_ac}{78125000000}+\frac{601692057.pH}{2734375000000}+\frac{608729391}{273437500000}\right)\left(\frac{4612972437.pH}{19531250000000}+\frac{59757521661.ratio\_prop\_ac}{15625000000000}+\frac{5194725381}{1953125000000}\right)$ $\frac{606211757741656107.pH.ratio\_prop\_ac}{24414062500000000000000000}+\frac{49165020321306219.pH^2}{610351562500000000000000000}+\frac{465885305885276181.ratio\_prop\_ac^2}{2441406250000000000000000}+\frac{66729557086812747.pH}{3051757812500000000000000}+\frac{830382459816088341.ratio\_prop\_ac}{244140625000000000000000}+\frac{87755276065822911}{6103515625000000000000000}$	g COD/g N	Glycogen produced per nitrite consumed	
Composite variable stoichiometry:				
pH	7.00	-	-	-
fpaoI	0.50	-	PAO I fraction	-
fdgb	0.50	-	DGB fraction	-
fddef	0.50	-	DDEF fraction	-
Organic fractions:				
ratio_prop_ac	25/75	-	Propionate to acetate ratios	(Lopez-Vazquez et al., 2009)
icv	1.48	g COD/g VSS	XCOD/VSS	GPS-X
fbod	0.66	g BOD/g BOD	BOD5/BODultimate ratio	GPS-X
Nutrient fractions:				
insi	0.01	g N/g COD	N content of Si	(Henze et al., 1999)
insf	0.03	g N/g COD	N content of Sf	
inxi	0.02	g N/g COD	N content of Xi	
inxs	0.04	g N/g COD	N content of Xs	
inbm	0.07	g N/g COD	N content of active biomass	
ipsi	0.00	g P/g COD	P content of Si	
ipsf	0.01	g P/g COD	P content of Sf	
ipxi	0.01	g P/g COD	P content of Xi	
ipxs	0.01	g P/g COD	P content of Xs	
ipbm	0.02	g P/g COD	P content of active biomass	

Determination of the percentage of acetyl-CoA* (λ) and propionyl-CoA* (β) in the PHA polymer for PAOs and GAOs:

$$\lambda_{PAOs}\left(\frac{C-mol}{C-mol}\right)=\frac{\frac{4}{3}}{\frac{4}{3}+1.23.ratio\_prop\_ac}+\frac{2}{5}\cdot\left(\frac{0.56}{\frac{4}{3.ratio\_prop\_ac}+1.23}\right)=\frac{\frac{369.ratio\_prop\_ac}{400}+\frac{615}{112}}{\frac{45387.ratio\_prop\_ac}{8960}+\frac{615}{112}}$$

$$\beta_{PAOs}\left(\frac{C-mol}{C-mol}\right)=\frac{0.67}{\frac{4}{3.ratio\_prop\_ac}+1.23}+\frac{3}{5}\cdot\left(\frac{0.56}{\frac{4}{3.ratio\_prop\_ac}+1.23}\right)=\frac{ratio\_prop\_ac}{\frac{615.ratio\_prop\_ac}{503}+\frac{2000}{1509}}$$

$$\lambda_{GAOs}\left(\frac{C-mol}{C-mol}\right)=\frac{\left(\frac{\left(\frac{19.pH}{500}+\frac{191}{150}\right)^2}{\frac{19.pH}{250}+\frac{91}{75}}\right)+(0.05.ratio\_prop\_ac)}{\left(\frac{19.pH}{200}+\frac{71}{60}\right)+(1.5.ratio\_prop\_ac)}+\left(\frac{2}{5}\cdot\left(\frac{\left(\frac{\left(\frac{19.pH}{200}-\frac{3}{20}\right)\left(\frac{19.pH}{500}+\frac{191}{150}\right)}{\frac{19.pH}{250}+\frac{91}{75}}\right)+(0.7.ratio\_prop\_ac)}{\left(\frac{19.pH}{200}+\frac{71}{60}\right)+(1.5.ratio\_prop\_ac)}\right)\right)$$

$$=\frac{\frac{35739.pH.ratio\_prop\_ac}{12500000}+\frac{20577.pH^2}{62500000}+\frac{50901.pH}{3125000}+\frac{57057.ratio\_prop\_ac}{1250000}+\frac{330239}{1875000}}{\frac{3249.pH.ratio\_prop\_ac}{250000}+\frac{20577.pH^2}{25000000}+\frac{5187.ratio\_prop\_ac}{25000}+\frac{29241.pH}{1250000}+\frac{122759}{750000}}$$

$$\beta_{GAOs}\left(\frac{C-mol}{C-mol}\right)=\frac{\left(\frac{\left(\frac{19.pH}{500}-\frac{3}{50}\right)^2}{\frac{19.pH}{375}+\frac{182}{225}}\right)+(0.75.ratio\_prop\_ac)}{\left(\frac{19.pH}{200}+\frac{71}{60}\right)+(1.5.ratio\_prop\_ac)}+\left(\frac{3}{5}\cdot\left(\frac{\left(\frac{\left(\frac{19.pH}{200}-\frac{3}{20}\right)\left(\frac{19.pH}{500}+\frac{191}{150}\right)}{\frac{19.pH}{250}+\frac{91}{75}}\right)+(0.7.ratio\_prop\_ac)}{\left(\frac{19.pH}{200}+\frac{71}{60}\right)+(1.5.ratio\_prop\_ac)}\right)\right)$$

$$=\frac{\frac{42237.pH\ .ratio\_prop\_ac}{6250000}+\frac{20577.pH^2}{62500000}+\frac{14801.pH}{3125000}+\frac{67431.ratio\_prop\_ac}{625000}-\frac{5187}{625000}}{\frac{1083.pH\ .ratio\_prop\_ac}{125000}+\frac{6859.pH^2}{12500000}+\frac{1729.ratio\_prop\_ac}{12500}+\frac{9747.pH}{625000}+\frac{122759}{1125000}}$$

Polyphosphate accumulating organisms parameters:

A

$$\text{ypha\_x\_pao}\left(\frac{C-mol\ biomass}{C-mol\ PHA}\right)=\frac{250\,(106\,\lambda+127\,\beta)\,(6\,\lambda+27\,\lambda\,\delta+8\,\beta+30\,\beta\,\delta)}{201930\,\lambda+318000\,K_1\,\lambda+678771\,\lambda\,\delta+813435\,\beta\,\delta+269240\,\beta+381000\,K_2\,\beta}=$$

$$=\frac{\left(\frac{17340965703\,ratio\_prop\_ac}{2861868800}+\frac{84646755}{14309344}\right)\left(\frac{85955035275\,ratio\_prop\_ac}{2073051902656}+\frac{2505740625}{64782871958}\right)}{\left(\frac{5582601\,ratio\_prop\_ac}{114474752}+\frac{378225}{7154672}\right)\left(\frac{1253263706243883\,ratio\_prop\_ac}{207305190265600}+\frac{3023162031915}{518262975664}\right)}$$

$$\text{ypha\_x\_pao}\left(\frac{g\ COD\ biomass}{g\ COD\ PHA}\right)=\text{ypha\_x\_pao}\left(\frac{C-mol\ biomass}{C-mol\ PHA}\right).\left(\frac{34.4\ g\ COD\ biomass}{C-mol\ biomass}\right)=$$

$$=\frac{\left(\frac{\mathbf{17340965703}.\boldsymbol{ratio\_prop\_ac}}{\mathbf{2861868800}}+\frac{\mathbf{84646755}}{\mathbf{14309344}}\right)\left(\frac{\mathbf{90923236313895}.\boldsymbol{ratio\_prop\_ac}}{\mathbf{4790822947038016}}+\frac{\mathbf{2650572433125}}{\mathbf{149713217094938}}\right)}{\left(\frac{\mathbf{5582601}.\boldsymbol{ratio\_prop\_ac}}{\mathbf{114474752}}+\frac{\mathbf{378225}}{\mathbf{7154672}}\right)\left(\frac{\mathbf{1253263706243883}.\boldsymbol{ratio\_prop\_ac}}{\mathbf{207305190265600}}+\frac{\mathbf{3023162031915}}{\mathbf{518262975664}}\right)}$$

B

$$\text{ypha\_pp\_pao}\left(\frac{\text{P}-\text{mol}}{C-mol\ PHA}\right)=\frac{\varepsilon\,(6\,\lambda+27\,\lambda\cdot\beta+8\,\beta+30\,\beta\cdot\delta)}{12\,(\varepsilon+\delta)}=\frac{\frac{17340965703\,ratio\_prop\_ac}{2861868800}+\frac{84646755}{14309344}}{\frac{2964361131\,ratio\_prop\_ac}{2003308160}+\frac{40167495}{25041352}}$$

$$\text{ypha\_pp\_pao}\left(\frac{\text{g P}}{g\ COD\ PHA}\right)=\text{ypha\_pp\_pao}\left(\frac{\text{P}-\text{mol}}{C-mol\ PHA}\right).\frac{\frac{30.97\ \text{g P}}{P-mol}}{\frac{9244}{123}\frac{g\ COD\ PHA}{C-mol\ PHA}}=\frac{\frac{\mathbf{6605711406209493}.\boldsymbol{ratio\_prop\_ac}}{\mathbf{2645511518720000}}+\frac{\mathbf{6448914605781}}{\mathbf{2645511518720}}}{\frac{\mathbf{2964361131}.\boldsymbol{ratio\_prop\_ac}}{\mathbf{2003308160}}+\frac{\mathbf{40167495}}{\mathbf{25041352}}}$$

C

$$\text{ypha\_gly\_pao}\left(\frac{\text{C}-\text{mol gly}}{C-mol\ PHA}\right)=\frac{(3\,\lambda+4\,\beta)\,(6\,\lambda+27\,\lambda\cdot\delta+8\,\beta+30\,\beta\cdot\delta)}{24\,(2\,\lambda+3\,\lambda\cdot\delta+2\,\beta+4\,\beta\cdot\delta)}$$

$$=\frac{\left(\frac{1127851821\ ratio\_prop\_ac}{677834752}+\frac{240172875}{169458688}\right)\left(\frac{17340965703\ ratio\_prop\_ac}{2861868800}+\frac{84646755}{14309344}\right)}{\left(\frac{5582601\ ratio\_prop\_ac}{3605504}+\frac{378225}{225344}\right)\left(\frac{1264890303\ ratio\_prop\_ac}{211823360}+\frac{57111975}{10591168}\right)}$$

$$\text{ypha\_gly\_pao}\left(\frac{g\ COD\ \text{gly}}{g\ COD\ PHA}\right)=\text{ypha\_gly\_pao}\left(\frac{\text{C}-\text{mol gly}}{C-mol\ PHA}\right).\frac{\frac{32\ g\ COD\ \text{gly}}{\text{C}-\text{mol gly}}}{\frac{9244}{123}\frac{g\ COD\ PHA}{C-mol\ PHA}}$$

$$=\frac{\left(\mathbf{\frac{17340965703.ratio\_prop\_ac}{2861868800}+\frac{84646755}{14309344}}\right)\left(\mathbf{\frac{138725773983.ratio\_prop\_ac}{195809513984}+\frac{29541263625}{48952378496}}\right)}{\left(\mathbf{\frac{5582601.ratio\_prop\_ac}{3605504}+\frac{378225}{225344}}\right)\left(\mathbf{\frac{1264890303.ratio\_prop\_ac}{211823360}+\frac{57111975}{10591168}}\right)}$$

D

$$\text{yo2\_x\_pao}\left(\frac{\text{C}-\text{mol biomass}}{O_2\ mol}\right)=\left(\frac{RedoxPHA}{4}.\frac{1}{\text{ypha\_x\_pao}}-\frac{RedoxBM}{4}\right)^{-1}=$$

$$=\frac{\left(\frac{17340965703\ ratio\_prop\_ac}{2861868800}+\frac{84646755}{14309344}\right)\left(\frac{85955035275\ ratio\_prop\_ac}{2073051902656}+\frac{2505740625}{64782871958}\right)}{\frac{84396361654744704675513\ ratio\_prop\_ac^2}{9492484097586949652480000}+\frac{178116561581996667897\ ratio\_prop\_ac}{949248409758694965248}+\frac{729556340882223375}{7416003201239804416}}$$

$$\text{yo2\_x\_pao}\left(\frac{\text{g COD biomass}}{g\ O_2}\right)=\text{yo2\_x\_pao}\left(\frac{\text{C}-\text{mol biomass}}{O_2\ mol}\right).\frac{\frac{34.4\ g\ COD\ biomass}{C-mol\ biomass}}{\frac{32\ g\ O_2}{O_2\ mol}}$$

$$=\frac{\left(\mathbf{\frac{17340965703.ratio\_prop\_ac}{2861868800}+\frac{84646755}{14309344}}\right)\left(\mathbf{\frac{739213303365.ratio\_prop\_ac}{16584415221248}+\frac{21549369375}{518262975664}}\right)}{\mathbf{\frac{84396361654744704675513\,.ratio\_prop\_ac^2}{9492484097586949652480000}+\frac{178116561581996667897.ratio\_prop\_ac}{949248409758694965248}+\frac{729556340882223375}{7416003201239804416}}}$$

E

$$\text{yo2\_pp\_pao}\left(\frac{\text{P}-\text{mol}}{O_2\ mol}\right)=\left(\frac{RedoxPHA}{4}.\frac{1}{\text{ypha\_pp\_pao}}\right)^{-1}=\frac{\frac{17340965703.ratio\_prop\_ac}{2861868800}+\frac{84646755}{14309344}}{\frac{72759400443.ratio\_prop\_ac}{40066163200}+\frac{361507455}{200330816}}$$

$$\text{yo2\_pp\_pao}\left(\frac{\text{g P}}{g\ O_2}\right)=\text{yo2\_pp\_pao}\left(\frac{\text{P}-\text{mol}}{O_2\ mol}\right).\frac{\frac{30.97\ g\ P}{\text{P}-\text{mol}}}{\frac{32\ g\ O_2}{O_2\ mol}}=\frac{\mathbf{\frac{53704970782191.ratio\_prop\_ac}{9157980160000}+\frac{52430200047}{9157980160}}}{\mathbf{\frac{72759400443.ratio\_prop\_ac}{40066163200}+\frac{361507455}{200330816}}}$$

F

$$\text{yo2\_gly\_pao}\left(\frac{\text{C}-\text{mol gly}}{O_2\ mol}\right)=\left(\frac{RedoxPHA}{4}.\frac{1}{\text{ypha\_gly\_pao}}-1\right)^{-1}=\frac{\left(\frac{1127851821.ratio\_prop\_ac}{677834752}+\frac{240172875}{169458688}\right)\left(\frac{17340965703.ratio\_prop\_ac}{2861868800}+\frac{84646755}{14309344}\right)}{\frac{275988536191467.ratio\_prop\_ac^2}{218208563363840}+\frac{118054007261775.ratio\_prop\_ac}{38186498588672}+\frac{2145812259375}{1193328080896}}$$

$$\text{yo2\_gly\_pao}\left(\frac{\text{g COD gly}}{g\ O_2}\right)=\text{yo2\_gly\_pao}\left(\frac{\text{C}-\text{mol gly}}{O_2\ mol}\right).\frac{\frac{32\text{ g COD gly}}{\text{C}-\text{mol gly}}}{\frac{32\ g\ O_2}{O_2\ mol}}$$

$$=\frac{\mathbf{\left(\frac{1127851821.ratio\_prop\_ac}{677834752}+\frac{240172875}{169458688}\right)\left(\frac{17340965703.ratio\_prop\_ac}{2861868800}+\frac{84646755}{14309344}\right)}}{\mathbf{\frac{275988536191467.ratio\_prop\_ac^2}{218208563363840}+\frac{118054007261775.ratio\_prop\_ac}{38186498588672}+\frac{2145812259375}{1193328080896}}}$$

G

$$\text{yno\_pha\_x\_pao}\left(\frac{C-mol\ biomass}{C-mol\ PHA}\right)=\frac{250\ (106\ \lambda+127\ \beta)\ (6\ \lambda+27\ \lambda\ \delta_N+8\ \beta+30\ \beta\ \delta_N)}{201930\ \lambda+318000\ K_1\ \lambda+678771\ \lambda\ \delta_N+813435\ \beta\ \delta_N+269240\ \beta+381000\ K_2\ \beta}=$$

$$=\frac{\left(\frac{680759613.ratio\_prop\_ac}{112672000}+\frac{4584087}{788704}\right)\left(\frac{429775176375.ratio\_prop\_ac}{12486836445632}+\frac{12528703125}{390213638926}\right)}{\left(\frac{5582601.ratio\_prop\_ac}{114474752}+\frac{378225}{7154672}\right)\left(\frac{417433571157231.ratio\_prop\_ac}{68825082771200}+\frac{1023797509155}{172062706928}\right)}$$

$$\text{yno\_pha\_x\_pao}\left(\frac{g\ COD\ biomass}{g\ COD\ PHA}\right) = \text{yno\_pha\_x\_pao}\left(\frac{C-mol\ biomass}{C-mol\ PHA}\right).\left(\frac{\frac{34.4\ g\ COD\ biomass}{C-mol\ biomass}}{\frac{9244}{123}\frac{g\ COD\ PHA}{C-mol\ PHA}}\right) =$$

$$= \frac{\left(\frac{\mathbf{680759613.ratio\_prop\_ac}}{\mathbf{112672000}} + \frac{\mathbf{4584087}}{\mathbf{788704}}\right)\left(\frac{\mathbf{454616181569475.ratio\_prop\_ac}}{\mathbf{28857079025855552}} + \frac{\mathbf{13252862165625}}{\mathbf{901783719557986}}\right)}{\left(\frac{\mathbf{5582601.ratio\_prop\_ac}}{\mathbf{114474752}} + \frac{\mathbf{378225}}{\mathbf{7154672}}\right)\left(\frac{\mathbf{417433571157231.ratio\_prop\_ac}}{\mathbf{68825082771200}} + \frac{\mathbf{1023797509155}}{\mathbf{172062706928}}\right)}$$

H

$$\text{yno\_pha\_pp\_pao}\left(\frac{\text{P}-\text{mol}}{C-mol\ PHA}\right) = \frac{\varepsilon_N\ (6\ \lambda + 27\ \lambda\cdot\beta + 8\ \beta + 30\ \beta\cdot\delta_N)}{12\ (\varepsilon_N + \delta_N)} = \frac{\frac{680759613\ .ratio\_prop\_ac}{112672000} + \frac{4584087}{788704}}{\frac{2964361131\ .ratio\_prop\_ac}{1104185600} + \frac{8033499}{2760464}}$$

$$\text{yno\_pha\_pp\_pao}\left(\frac{\text{g P}}{g\ COD\ PHA}\right) = \text{yno\_pha\_pp\_pao}\left(\frac{\text{P}-\text{mol}}{C-mol\ PHA}\right).\frac{\frac{30.97\ \text{g P}}{P-mol}}{\frac{9244}{123}\frac{g\ COD\ PHA}{C-mol\ PHA}} = \frac{\mathbf{259322440139703.ratio\_prop\_ac}}{\mathbf{104153996800000}} + \frac{\mathbf{1746220844997}}{\mathbf{729077977600}}}{\mathbf{\frac{2964361131.ratio\_prop\_ac}{1104185600}} + \frac{\mathbf{8033499}}{\mathbf{2760464}}}$$

I

$$\text{yno\_pha\_gly\_pao}\left(\frac{\text{C}-\text{mol gly}}{C-mol\ PHA}\right) = \frac{(3\ \lambda + 4\ \beta)\ (6\ \lambda + 27\ \lambda\cdot\delta_N + 8\ \beta + 30\ \beta\cdot\delta_N)}{24\ (2\ \lambda + 3\ \lambda\cdot\delta_N + 2\ \beta + 4\ \beta\cdot\delta_N)}$$

$$= \frac{\left(\frac{44403615.ratio\_prop\_ac}{28844032} + \frac{9455625}{7211008}\right)\left(\frac{680759613.ratio\_prop\_ac}{112672000} + \frac{4584087}{788704}\right)}{\left(\frac{5582601.ratio\_prop\_ac}{3605504} + \frac{378225}{225344}\right)\left(\frac{27096039.ratio\_prop\_ac}{4506880} + \frac{17776575}{3154816}\right)}$$

$$\text{yno\_pha\_gly\_pao}\left(\frac{g\ COD\ \text{gly}}{g\ COD\ PHA}\right) = \text{yno\_pha\_gly\_pao}\left(\frac{\text{C}-\text{mol gly}}{C-mol\ PHA}\right).\frac{\frac{32\ g\ COD\ \text{gly}}{\text{C}-\text{mol gly}}}{\frac{9244}{123}\frac{g\ COD\ PHA}{C-mol\ PHA}}$$

$$= \frac{\left(\frac{\mathbf{680759613.ratio\_prop\_ac}}{\mathbf{112672000}} + \frac{\mathbf{4584087}}{\mathbf{788704}}\right)\left(\frac{\mathbf{5461644645.ratio\_prop\_ac}}{\mathbf{8332319744}} + \frac{\mathbf{1163041875}}{\mathbf{2083079936}}\right)}{\left(\frac{\mathbf{5582601.ratio\_prop\_ac}}{\mathbf{3605504}} + \frac{\mathbf{378225}}{\mathbf{225344}}\right)\left(\frac{\mathbf{27096039.ratio\_prop\_ac}}{\mathbf{4506880}} + \frac{\mathbf{17776575}}{\mathbf{3154816}}\right)}$$

J

$$\text{yno3\_x\_pao}\left(\frac{\text{C}-\text{mol biomass}}{N\ mol}\right)=\frac{2}{4}\left(\frac{RedoxPHA}{4}.\frac{1}{\text{yno\_pha\_x\_pao}}-\frac{RedoxBM}{4}\right)^{-1}=$$

$$=\frac{\left(\frac{680759613\ .ratio\_prop\_ac}{112672000}+\frac{4584087}{788704}\right)\left(\frac{429775176375\ .ratio\_prop\_ac}{24973672891264}+\frac{12528703125}{780427277852}\right)}{\frac{43207290995686453554741\ .ratio\_prop\_ac^2}{3151493712645037096960000}+\frac{91012957246249044129\ .ratio\_prop\_ac}{315149371264503709696}+\frac{372168219113663625}{2462104463003935232}}$$

$$\text{yno3\_x\_pao}\left(\frac{\text{g COD biomass}}{g\ N}\right)=\text{yno3\_x\_pao}\left(\frac{\text{C}-\text{mol biomass}}{N\ mol}\right).\frac{\frac{34.4\ g\ COD\ biomass}{C-mol\ biomass}}{\frac{14\ g\ N}{N\ mol}}$$

$$=\frac{\left(\mathbf{\frac{680759613.ratio\_prop\_ac}{112672000}+\frac{4584087}{788704}}\right)\left(\mathbf{\frac{3696066516825.ratio\_prop\_ac}{87407855119424}+\frac{107746846875}{2731495472482}}\right)}{\mathbf{\frac{43207290995686453554741\ .ratio\_prop\_ac^2}{3151493712645037096960000}+\frac{91012957246249044129.ratio\_prop\_ac}{315149371264503709696}+\frac{372168219113663625}{2462104463003935232}}}$$

K

$$\text{yno3\_pp\_pao}\left(\frac{\text{P}-\text{mol}}{N\ mol}\right)=\frac{2}{4}\left(\frac{RedoxPHA}{4}.\frac{1}{\text{yno\_pha\_pp\_pao}}\right)^{-1}=\frac{\frac{680759613.ratio\_prop\_ac}{225344000}+\frac{4584087}{1577408}}{\frac{72759400443.ratio\_prop\_ac}{22083712000}+\frac{72301491}{22083712}}$$

$$\text{yno3\_pp\_pao}\left(\frac{\text{g P}}{g\ N}\right)=\text{yno3\_pp\_pao}\left(\frac{\text{P}-\text{mol}}{N\ mol}\right).\frac{\frac{30.97\ g\ P}{\text{P}-\text{mol}}}{\frac{14\ g\ N}{N\ mol}}=\frac{\mathbf{\frac{2108312521461.ratio\_prop\_ac}{315481600000}+\frac{14196917439}{2208371200}}}{\mathbf{\frac{72759400443.ratio\_prop\_ac}{22083712000}+\frac{72301491}{22083712}}}$$

L

$$\text{yno3\_gly\_pao}\left(\frac{\text{C}-\text{mol gly}}{N\ mol}\right)=\frac{2}{4}\left(\frac{RedoxPHA}{4}.\frac{1}{\text{yno\_pha\_gly\_pao}}-1\right)^{-1}$$

$$=\frac{\left(\frac{44403615.ratio\_prop\_ac}{57688064}+\frac{9455625}{14422016}\right)\left(\frac{680759613.ratio\_prop\_ac}{112672000}+\frac{4584087}{788704}\right)}{\frac{275988536191467\ .ratio\_prop\_ac^2}{129996590940160}+\frac{118054007261775\ .ratio\_prop\_ac}{22749403414528}+\frac{2145812259375}{710918856704}}$$

$$\text{yno3\_gly\_pao}\left(\frac{\text{g COD gly}}{g\ N}\right) = \text{yno3\_gly\_pao}\left(\frac{\text{C} - \text{mol gly}}{N\ mol}\right).\frac{\frac{32\ \text{g COD gly}}{\text{C} - \text{mol gly}}}{\frac{14\ g\ N}{N\ mol}}$$

$$= \frac{\left(\frac{\mathbf{44403615}.\boldsymbol{ratio\_prop\_ac}}{\mathbf{25238528}} + \frac{\mathbf{9455625}}{\mathbf{6309632}}\right)\left(\frac{\mathbf{680759613}.\boldsymbol{ratio\_prop\_ac}}{\mathbf{112672000}} + \frac{\mathbf{4584087}}{\mathbf{788704}}\right)}{\frac{\mathbf{275988536191467}.\boldsymbol{ratio\_prop\_ac^2}}{\mathbf{129996590940160}} + \frac{\mathbf{118054007261775}.\boldsymbol{ratio\_prop\_ac}}{\mathbf{22749403414528}} + \frac{\mathbf{2145812259375}}{\mathbf{710918856704}}}$$

M

$$\text{yno2\_x\_pao}\left(\frac{\text{C} - \text{mol biomass}}{N\ mol}\right) = \frac{3}{4}\left(\frac{RedoxPHA}{4}.\frac{1}{\text{yno\_pha\_x\_pao}} - \frac{RedoxBM}{4}\right)^{-1} =$$

$$= \frac{\left(\frac{680759613\ .ratio\_prop\_ac}{112672000} + \frac{4584087}{788704}\right)\left(\frac{1289325529125\ .ratio\_prop\_ac}{49947345782528} + \frac{37586109375}{1560854555704}\right)}{\frac{43207290995686453554741\ .ratio\_prop\_ac^2}{315149371264503709696000} + \frac{91012957246249044129.ratio\_prop\_ac}{3151493712645037096} + \frac{372168219113663625}{2462104463003935232}}$$

$$\text{yno2\_x\_pao}\left(\frac{\text{g COD biomass}}{g\ N}\right) = \text{yno2\_x\_pao}\left(\frac{\text{C} - \text{mol biomass}}{N\ mol}\right).\frac{\frac{34.4\ g\ COD\ biomass}{C - mol\ biomass}}{\frac{14\ g\ N}{N\ mol}}$$

$$= \frac{\left(\frac{\mathbf{680759613}.\boldsymbol{ratio\_prop\_ac}}{\mathbf{112672000}} + \frac{\mathbf{4584087}}{\mathbf{788704}}\right)\left(\frac{\mathbf{11088199550475}.\boldsymbol{ratio\_prop\_ac}}{\mathbf{174815710238848}} + \frac{\mathbf{323240540625}}{\mathbf{5462990944964}}\right)}{\frac{\mathbf{43207290995686453554741}.\boldsymbol{ratio\_prop\_ac^2}}{\mathbf{315149371264503709696000}} + \frac{\mathbf{91012957246249044129}.\boldsymbol{ratio\_prop\_ac}}{\mathbf{3151493712645037096}} + \frac{\mathbf{372168219113663625}}{\mathbf{2462104463003935232}}}$$

N

$$\text{yno2\_pp\_pao}\left(\frac{\text{P} - \text{mol}}{N\ mol}\right) = \frac{3}{4}\left(\frac{RedoxPHA}{4}.\frac{1}{\text{yno\_pha\_pp\_pao}}\right)^{-1} = \frac{\frac{2042278839.ratio\_prop\_ac}{450688000} + \frac{13752261}{3154816}}{\frac{72759400443.ratio\_prop\_ac}{22083712000} + \frac{72301491}{22083712}}$$

$$\text{yno2\_pp\_pao}\left(\frac{\text{g P}}{g\ N}\right) = \text{yno2\_pp\_pao}\left(\frac{\text{P} - \text{mol}}{N\ mol}\right).\frac{\frac{30.97\ g\ P}{\text{P} - \text{mol}}}{\frac{14\ g\ N}{N\ mol}} = \frac{\frac{\mathbf{6324937564383}.\boldsymbol{ratio\_prop\_ac}}{\mathbf{630963200000}} + \frac{\mathbf{42590752317}}{\mathbf{4416742400}}}{\frac{\mathbf{72759400443}.\boldsymbol{ratio\_prop\_ac}}{\mathbf{22083712000}} + \frac{\mathbf{72301491}}{\mathbf{22083712}}}$$

O

$$\text{yno2\_gly\_pao}\left(\frac{\text{C}-\text{mol gly}}{N\ mol}\right)=\frac{3}{4}\left(\frac{RedoxPHA}{4}.\frac{1}{\text{yno\_pha\_gly\_pao}}-1\right)^{-1}$$

$$=\frac{\left(\frac{133210845.ratio\_prop\_ac}{115376128}+\frac{28366875}{28844032}\right)\left(\frac{680759613.ratio\_prop\_ac}{112672000}+\frac{4584087}{788704}\right)}{\frac{275988536191467\ .ratio\_prop\_ac^2}{129996590940160}+\frac{118054007261775.ratio\_prop\_ac}{22749403414528}+\frac{2145812259375}{710918856704}}$$

$$\text{yno2\_gly\_pa}\left(\frac{\text{g COD gly}}{g\ N}\right)=\text{yno2\_gly\_pao}\left(\frac{\text{C}-\text{mol gly}}{N\ mol}\right).\frac{\frac{32\ \text{g COD gly}}{\text{C}-\text{mol gly}}}{\frac{14\ g\ N}{N\ mol}}$$

$$=\frac{\left(\mathbf{\frac{133210845.ratio\_prop\_ac}{50477056}}+\mathbf{\frac{28366875}{12619264}}\right)\left(\mathbf{\frac{680759613.ratio\_prop\_ac}{112672000}}+\mathbf{\frac{4584087}{788704}}\right)}{\mathbf{\frac{275988536191467.ratio\_prop\_ac^2}{129996590940160}}+\mathbf{\frac{118054007261775.ratio\_prop\_ac}{22749403414528}}+\mathbf{\frac{2145812259375}{710918856704}}}$$

Glycogen accumulating organisms parameters:

P

$$\text{ypha\_x\_gao}\left(\frac{C-mol\ biomass}{C-mol\ PHA}\right)=\frac{250\ (106\ \lambda+127\ \beta)\ (6\ \lambda+27\ \lambda\ \delta+8\ \beta+30\ \beta\ \delta)}{201930\ \lambda+318000\ K_1\ \lambda+678771\ \lambda\ \delta+813435\ \beta\ \delta+269240\ \beta+381000\ K_2\ \beta}=$$

$$=\frac{\left(\frac{4211844399.pH}{39062500000}+\frac{217590848613.ratio\_prop\_ac}{125000000000}+\frac{9607133799}{7812500000}\right)\left(\frac{13214940363.pH}{15625000000000}+\frac{21530723373.ratio\_prop\_ac}{1562500000000}+\frac{14490261669}{1562500000000}\right)}{\left(\frac{3518667.ratio\_prop\_ac}{31250000000}+\frac{22284891.pH}{3125000000000}+\frac{27758373}{312500000000}\right)\left(\frac{3929504275305117.ratio\_prop\_ac}{15625000000000}+\frac{4856384485036449.pH}{312500000000000}+\frac{5483156828651487}{31250000000000}\right)}$$

$$\text{ypha\_x\_gao}\left(\frac{g\ COD\ biomass}{g\ COD\ PHA}\right)=\text{ypha\_x\_gao}\left(\frac{C-mol\ biomass}{C-mol\ PHA}\right).\left(\frac{\frac{34.4\ g\ COD\ biomass}{C-mol\ biomass}}{\left(\frac{\frac{57.pH}{500}+\frac{33}{25}}{\frac{19.pH}{6400}+\frac{71}{1920}}+\frac{8792}{225}\right)\frac{g\ COD\ PHA}{C-mol\ PHA}}\right)=$$

$$= \frac{\left(\frac{\mathbf{19.pH}}{\mathbf{6400}} + \frac{\mathbf{71}}{\mathbf{1920}}\right)\left(\frac{\mathbf{4211844399.pH}}{\mathbf{39062500000}} + \frac{\mathbf{217590848613.ratio\_prop\_ac}}{\mathbf{125000000000}} + \frac{\mathbf{9607133799}}{\mathbf{7812500000}}\right)\left(\frac{\mathbf{568242435609.pH}}{\mathbf{19531250000000}} + \frac{\mathbf{925821105039.ratio\_prop\_ac}}{\mathbf{1953125000000}} + \frac{\mathbf{623081251767}}{\mathbf{1953125000000}}\right)}{\left(\frac{\mathbf{41401.pH}}{\mathbf{180000}} + \frac{\mathbf{149309}}{\mathbf{54000}}\right)\left(\frac{\mathbf{3518667.ratio\_prop\_ac}}{\mathbf{31250000000}} + \frac{\mathbf{22284891.pH}}{\mathbf{3125000000000}} + \frac{\mathbf{27758373}}{\mathbf{312500000000}}\right)\left(\frac{\mathbf{3929504275305117.ratio\_prop\_ac}}{\mathbf{15625000000000}} + \frac{\mathbf{4856384485036449.pH}}{\mathbf{312500000000000}} + \frac{\mathbf{5483156828651487}}{\mathbf{31250000000000}}\right)}$$

Q

$$\text{ypha\_gly\_gao}\left(\frac{\text{C} - \text{mol gly}}{C - mol\ PHA}\right) = \frac{(3\,\lambda + 4\,\beta)\,(6\,\lambda + 27\,\lambda \cdot \delta + 8\,\beta + 30\,\beta \cdot \delta)}{24\,(2\,\lambda + 3\,\lambda \cdot \delta + 2\,\beta + 4\,\beta \cdot \delta)} =$$

$$= \frac{\left(\frac{1270238787.pH}{156250000000000} + \frac{4211844399.ratio\_prop\_ac}{31250000000000} + \frac{1285095381}{15625000000000}\right)\left(\frac{26675014527.pH}{976562500000000} + \frac{1378075374549.ratio\_prop\_ac}{3125000000000000} + \frac{60845180727}{195312500000000}\right)}{\left(\frac{22284891.ratio\_prop\_ac}{3125000000000} + \frac{141137643.pH}{312500000000000} + \frac{175803029}{31250000000000}\right)\left(\frac{183337798257.pH}{390625000000000} + \frac{601224074289.ratio\_prop\_ac}{78125000000000} + \frac{195386495991}{39062500000000}\right)}$$

$$= \text{ypha\_gly\_gao}\left(\frac{g\ COD\ \text{gly}}{g\ COD\ PHA}\right) = \text{ypha\_gly\_gao}\left(\frac{\text{C} - \text{mol gly}}{C - mol\ PHA}\right).\frac{\frac{32\ g\ COD\ \text{gly}}{\text{C} - \text{mol gly}}}{\left(\frac{\frac{57.pH}{500} + \frac{33}{25}}{\frac{19.pH}{6400} + \frac{71}{1920}} + \frac{8792}{225}\right)\frac{g\ COD\ PHA}{C - mol\ PHA}} =$$

$$= \frac{\left(\frac{\mathbf{19.pH}}{\mathbf{6400}} + \frac{\mathbf{71}}{\mathbf{1920}}\right)\left(\frac{\mathbf{1270238787.pH}}{\mathbf{4882812500000}} + \frac{\mathbf{4211844399.ratio\_prop\_ac}}{\mathbf{976562500000}} + \frac{\mathbf{1285095381}}{\mathbf{488281250000}}\right)\left(\frac{\mathbf{26675014527.pH}}{\mathbf{976562500000000}} + \frac{\mathbf{1378075374549.ratio\_prop\_ac}}{\mathbf{3125000000000000}} + \frac{\mathbf{60845180727}}{\mathbf{195312500000000}}\right)}{\left(\frac{\mathbf{41401.pH}}{\mathbf{180000}} + \frac{\mathbf{149309}}{\mathbf{54000}}\right)\left(\frac{\mathbf{22284891.ratio\_prop\_ac}}{\mathbf{3125000000000}} + \frac{\mathbf{141137643.pH}}{\mathbf{312500000000000}} + \frac{\mathbf{175803029}}{\mathbf{31250000000000}}\right)\left(\frac{\mathbf{183337798257.pH}}{\mathbf{390625000000000}} + \frac{\mathbf{601224074289.ratio\_prop\_ac}}{\mathbf{78125000000000}} + \frac{\mathbf{195386495991}}{\mathbf{39062500000000}}\right)}$$

R

$$\text{yo2\_x\_gao}\left(\frac{\text{C} - \text{mol biomass}}{O_2\ mol}\right) = \left(\frac{RedoxPHA}{4}.\frac{1}{\text{ypha\_x\_gao}} - \frac{RedoxBM}{4}\right)^{-1} =$$

$$= \frac{\left(\frac{4211844399.pH}{39062500000} + \frac{217590848613.ratio\_prop\_ac}{125000000000} + \frac{9607133799}{7812500000}\right)\left(\frac{13214940363.pH}{15625000000000} + \frac{21530723373.ratio\_prop\_ac}{1562500000000} + \frac{14490261669}{1562500000000}\right)}{\frac{842268825870275371308663.pH.ratio\_prop\_ac}{781250000000000000000000000} + \frac{207081143688001961548 53.pH^2}{610351562500000000000000000} + \frac{668902292330018979882537 9.ratio\_prop\_ac^2}{781250000000000000000000000} + \frac{403033076982025604464599.pH}{488281250000000000000000000} + \frac{1025715386231011997201016 9.ratio\_prop\_ac}{781250000000000000000000000} + \frac{244042791451183639987281}{488281250000000000000000000}}$$

$$\text{yo2\_x\_gao}\left(\frac{\text{g COD biomass}}{g\ O_2}\right) = \text{yo2\_x\_gao}\left(\frac{\text{C} - \text{mol biomass}}{O_2\ mol}\right).\frac{\frac{34.4\ g\ COD\ biomass}{C - mol\ biomass}}{\frac{32\ g\ O_2}{O_2\ mol}} =$$

$$= \frac{\left(\frac{\mathbf{4211844399.pH}}{\mathbf{39062500000}} + \frac{\mathbf{217590848613.ratio\_prop\_ac}}{\mathbf{125000000000}} + \frac{\mathbf{9607133799}}{\mathbf{7812500000}}\right)\left(\frac{\mathbf{568242435609.pH}}{\mathbf{625000000000000}} + \frac{\mathbf{925821105039.ratio\_prop\_ac}}{\mathbf{62500000000000}} + \frac{\mathbf{623081251767}}{\mathbf{62500000000000}}\right)}{\frac{\mathbf{842268825870275371308 6663.pH.ratio\_prop\_ac}}{\mathbf{781250000000000000000000000}} + \frac{\mathbf{207081143688001961548 53.pH^2}}{\mathbf{610351562500000000000000000}} + \frac{\mathbf{668902292330018979882 5379.ratio\_prop\_ac^2}}{\mathbf{781250000000000000000000000}} + \frac{\mathbf{403033076982025604464599.pH}}{\mathbf{488281250000000000000000000}} + \frac{\mathbf{102571538623101199720101 69.ratio\_prop\_ac}}{\mathbf{781250000000000000000000000}} + \frac{\mathbf{244042791451183639987281}}{\mathbf{488281250000000000000000000}}}$$

s

$$\text{yo2\_gly\_gao}\left(\frac{\text{C} - \text{mol gly}}{O_2\ mol}\right) = \left(\frac{RedoxPHA}{4}.\frac{1}{\text{ypha\_gly\_gao}} - 1\right)^{-1} =$$

$$= \frac{\left(\frac{1270238787.pH}{156250000000000} + \frac{4211844399.ratio\_prop\_ac}{31250000000000} + \frac{1285095381}{15625000000000}\right)\left(\frac{26675014527.pH}{976562500000000} + \frac{1378075374549.ratio\_prop\_ac}{3125000000000000} + \frac{60845180727}{195312500000000}\right)}{\frac{2431582717163753 9403.pH.ratio\_prop\_ac}{244140625000000000000000000} + \frac{197206359288794 9451.pH^2}{610351562500000000000000000} + \frac{186817726939830 0149.ratio\_prop\_ac^2}{244140625000000000000000000} + \frac{267659667870437 7963.pH}{305175781250000000000000000} + \frac{333075631104008 76789.ratio\_prop\_ac}{244140625000000000000000000} + \frac{351996162886245 2319}{610351562500000000000000000}}$$

$$\text{yo2\_gly\_gao}\left(\frac{\text{g COD gly}}{g\ O_2}\right) = \text{yo2\_gly\_gao}\left(\frac{\text{C} - \text{mol gly}}{O_2\ mol}\right).\frac{\frac{32\text{ g COD gly}}{\text{C} - \text{mol gly}}}{\frac{32\ g\ O_2}{O_2\ mol}} =$$

$$= \frac{\left(\frac{\mathbf{1270238787.pH}}{\mathbf{156250000000000}} + \frac{\mathbf{4211844399.ratio\_prop\_ac}}{\mathbf{31250000000000}} + \frac{\mathbf{1285095381}}{\mathbf{15625000000000}}\right)\left(\frac{\mathbf{26675014527.pH}}{\mathbf{976562500000000}} + \frac{\mathbf{1378075374549.ratio\_prop\_ac}}{\mathbf{3125000000000000}} + \frac{\mathbf{60845180727}}{\mathbf{195312500000000}}\right)}{\frac{\mathbf{2431582717163753 9403.pH.ratio\_prop\_ac}}{\mathbf{244140625000000000000000000}} + \frac{\mathbf{197206359288794 9451.pH^2}}{\mathbf{610351562500000000000000000}} + \frac{\mathbf{186817726939830 0149.ratio\_prop\_ac^2}}{\mathbf{244140625000000000000000000}} + \frac{\mathbf{267659667870437 7963.pH}}{\mathbf{305175781250000000000000000}} + \frac{\mathbf{333075631104008 76789.ratio\_prop\_ac}}{\mathbf{244140625000000000000000000}} + \frac{\mathbf{351996162886245 2319}}{\mathbf{610351562500000000000000000}}}$$

τ

$$\text{yno\_pha\_x\_gao}\left(\frac{C-mol\ biomass}{C-mol\ PHA}\right)=\frac{250\,(106\,\lambda+127\,\beta)\,(6\,\lambda+27\,\lambda\,\delta_N+8\,\beta+30\,\beta\,\delta_N)}{201930\,\lambda+318000\,K_1\,\lambda+678771\,\lambda\,\delta_N+813435\,\beta\,\delta_N+269240\,\beta+381000\,K_2\,\beta}=$$

$$=\frac{\left(\frac{4612972437.pH}{78125000000}+\frac{59757521661.ratio\_prop\_ac}{62500000000}+\frac{5194725381}{7812500000}\right)\left(\frac{13214940363.pH}{15625000000000}+\frac{21530723373.ratio\_prop\_ac}{1562500000000}+\frac{14490261669}{1562500000000}\right)}{\left(\frac{3518667.ratio\_prop\_ac}{31250000000}+\frac{22284891.pH}{3125000000000}+\frac{27758373}{312500000000}\right)\left(\frac{1309736024639019.ratio\_prop\_ac}{7812500000000}+\frac{1624163481436293.pH}{156250000000000}+\frac{1860107807372859}{15625000000000}\right)}$$

$$\text{yno\_pha\_x\_gao}\left(\frac{g\ COD\ biomass}{g\ COD\ PHA}\right)=\text{yno\_pha\_x\_gao}\left(\frac{C-mol\ biomass}{C-mol\ PHA}\right).\left(\frac{\frac{34.4\ g\ COD\ biomass}{C-mol\ biomass}}{\left(\frac{\frac{57.pH}{500}+\frac{33}{25}}{\frac{19.pH}{6400}+\frac{71}{1920}}+\frac{8792}{225}\right)\frac{g\ COD\ PHA}{C-mol\ PHA}}\right)=$$

$$=\frac{\left(\frac{\mathbf{19.pH}}{\mathbf{6400}}+\frac{\mathbf{71}}{\mathbf{1920}}\right)\left(\frac{\mathbf{4612972437.pH}}{\mathbf{78125000000}}+\frac{\mathbf{59757521661.ratio\_prop\_ac}}{\mathbf{62500000000}}+\frac{\mathbf{5194725381}}{\mathbf{7812500000}}\right)}{\left(\frac{\mathbf{568242435609.pH}}{\mathbf{19531250000000}}+\frac{\mathbf{925821105039.ratio\_prop\_ac}}{\mathbf{1953125000000}}+\frac{\mathbf{623081251767}}{\mathbf{1953125000000}}\right)}$$
$$\left(\frac{\mathbf{41401.pH}}{\mathbf{180000}}+\frac{\mathbf{149309}}{\mathbf{54000}}\right)\left(\frac{\mathbf{3518667.ratio\_prop\_ac}}{\mathbf{31250000000}}+\frac{\mathbf{22284891.pH}}{\mathbf{3125000000000}}+\frac{\mathbf{27758373}}{\mathbf{312500000000}}\right)$$
$$\left(\frac{\mathbf{1309736024639019.ratio\_prop\_ac}}{\mathbf{7812500000000}}+\frac{\mathbf{1624163481436293.pH}}{\mathbf{156250000000000}}+\frac{\mathbf{1860107807372859}}{\mathbf{15625000000000}}\right)$$

υ

$$\text{yno\_pha\_gly\_gao}\left(\frac{\text{C}-\text{mol gly}}{C-mol\ PHA}\right)=\frac{(3\,\lambda+4\,\beta)\,(6\,\lambda+27\,\lambda\cdot\delta_N+8\,\beta+30\,\beta\cdot\delta_N)}{24\,(2\,\lambda+3\,\lambda\cdot\delta_N+2\,\beta+4\,\beta\cdot\delta_N)}=$$

$$=\frac{\left(\frac{200564019.pH}{1562500000000}+\frac{665028063.ratio\_prop\_ac}{312500000000}+\frac{202909797}{156250000000}\right)\left(\frac{4612972437.pH}{19531250000000}+\frac{59757521661.ratio\_prop\_ac}{15625000000000}+\frac{5194725381}{1953125000000}\right)}{\left(\frac{3518667.ratio\_prop\_ac}{31250000000}+\frac{22284891.pH}{3125000000000}+\frac{27758373}{312500000000}\right)\left(\frac{8757962163.pH}{1953125000000}+\frac{28511758701.ratio\_prop\_ac}{390625000000}+\frac{9642320469}{195312500000}\right)}$$

$$\text{yno\_pha\_gly\_gao}\left(\frac{g\ COD\ \text{gly}}{g\ COD\ PHA}\right) = \text{yno\_pha\_gly\_gao}\left(\frac{\text{C}-\text{mol gly}}{C-mol\ PHA}\right).\frac{\frac{32\ g\ COD\ \text{gly}}{\text{C}-\text{mol gly}}}{\left(\frac{\frac{57.pH}{500}+\frac{33}{25}}{\frac{19.pH}{6400}+\frac{71}{1920}}+\frac{8792}{225}\right)\frac{g\ COD\ PHA}{C-mol\ PHA}} =$$

$$= \frac{\left(\frac{\mathbf{19}.\boldsymbol{pH}}{\mathbf{6400}}+\frac{\mathbf{71}}{\mathbf{1920}}\right)\left(\frac{\mathbf{200564019}.\boldsymbol{pH}}{\mathbf{48828125000}}+\frac{\mathbf{665028063}.\boldsymbol{ratio\_prop\_ac}}{\mathbf{9765625000}}+\frac{\mathbf{202909797}}{\mathbf{4882812500}}\right)}{\left(\frac{\mathbf{4612972437}.\boldsymbol{pH}}{\mathbf{19531250000000}}+\frac{\mathbf{59757521661}.\boldsymbol{ratio\_prop\_ac}}{\mathbf{15625000000000}}+\frac{\mathbf{5194725381}}{\mathbf{1953125000000}}\right)}$$
$$\left(\frac{\mathbf{41401}.\boldsymbol{pH}}{\mathbf{180000}}+\frac{\mathbf{149309}}{\mathbf{54000}}\right)\left(\frac{\mathbf{3518667}.\boldsymbol{ratio\_prop\_ac}}{\mathbf{31250000000}}+\frac{\mathbf{22284891}.\boldsymbol{pH}}{\mathbf{3125000000000}}+\frac{\mathbf{27758373}}{\mathbf{312500000000}}\right)$$
$$\left(\frac{\mathbf{8757962163}.\boldsymbol{pH}}{\mathbf{1953125000000}}+\frac{\mathbf{28511758701}.\boldsymbol{ratio\_prop\_ac}}{\mathbf{390625000000}}+\frac{\mathbf{9642320469}}{\mathbf{195312500000}}\right)$$

v

$$\text{yno3\_x\_gao}\left(\frac{\text{C}-\text{mol biomass}}{N\ mol}\right) = \frac{2}{4}\left(\frac{RedoxPHA}{4}.\frac{1}{\text{yno\_pha\_x\_gao}}-\frac{RedoxBM}{4}\right)^{-1} =$$

$$= \frac{\left(\frac{4612972437.pH}{78125000000}+\frac{59757521661.ratio\_prop\_ac}{62500000000}+\frac{5194725381}{7812500000}\right)\left(\frac{13214940363.pH}{31250000000000}+\frac{21530723373.ratio\_prop\_ac}{3125000000000}+\frac{14490261669}{3125000000000}\right)}{\frac{43095318394949327640077 91.pH.ratio\_prop\_ac}{3906250000000000000000000000}+\frac{16945979749575302461706 1.pH^2}{4882812500000000000000000000}+\frac{34238992664250750336756 03.ratio\_prop\_ac^2}{3906250000000000000000000000}+}$$
$$\frac{10290721231732439496150 9.pH}{1220703125000000000000000000}+\frac{52397923787385430164636 33.ratio\_prop\_ac}{3906250000000000000000000000}+\frac{24890791517453428072515 9}{4882812500000000000000000000}$$

$$\text{yno3\_x\_gao}\left(\frac{\text{g COD biomass}}{g\ N}\right) = \text{yno3\_x\_gao}\left(\frac{\text{C}-\text{mol biomass}}{N\ mol}\right).\frac{\frac{34.4\ g\ COD\ biomass}{C-mol\ biomass}}{\frac{14\ g\ N}{N\ mol}} =$$

$$= \frac{\left(\frac{\mathbf{4612972437}.\boldsymbol{pH}}{\mathbf{78125000000}}+\frac{\mathbf{59757521661}.\boldsymbol{ratio\_prop\_ac}}{\mathbf{62500000000}}+\frac{\mathbf{5194725381}}{\mathbf{7812500000}}\right)\left(\frac{\mathbf{568242435609}.\boldsymbol{pH}}{\mathbf{546875000000000}}+\frac{\mathbf{925821105039}.\boldsymbol{ratio\_prop\_ac}}{\mathbf{54687500000000}}+\frac{\mathbf{623081251767}}{\mathbf{54687500000000}}\right)}{\frac{\mathbf{43095318394949327640077 91}.\boldsymbol{pH}.\boldsymbol{ratio\_prop\_ac}}{\mathbf{3906250000000000000000000000}}+\frac{\mathbf{16945979749575302461706 1}.\boldsymbol{pH^2}}{\mathbf{4882812500000000000000000000}}+\frac{\mathbf{34238992664250750336756 03}.\boldsymbol{ratio\_prop\_ac^2}}{\mathbf{3906250000000000000000000000}}}$$
$$+\frac{\mathbf{10290721231732439496150 9}.\boldsymbol{pH}}{\mathbf{1220703125000000000000000000}}+\frac{\mathbf{52397923787385430164636 33}.\boldsymbol{ratio\_prop\_ac}}{\mathbf{3906250000000000000000000000}}+\frac{\mathbf{24890791517453428072515 9}}{\mathbf{4882812500000000000000000000}}$$

w

$$\text{yno3\_gly\_gao}\left(\frac{\text{C}-\text{mol gly}}{N\ mol}\right)=\frac{2}{4}\left(\frac{RedoxPHA}{4}.\frac{1}{\text{yno\_pha\_gly\_gao}}-1\right)^{-1}=$$

$$=\frac{\left(\frac{200564019.pH}{3125000000000}+\frac{665028063\ y}{625000000000}+\frac{202909797}{312500000000}\right)\left(\frac{4612972437.pH}{19531250000000}+\frac{59757521661\ y}{15625000000000}+\frac{5194725381}{1953125000000}\right)}{\frac{606211757741656107.pH\ y}{24414062500000000000000000}+\frac{49165020321306219.pH^2}{61035156250000000000000000}+\frac{465885305885276181\ y^2}{2441406250000000000000000}+\frac{66729557086812747.pH}{3051757812500000000000000}+\frac{830382459816088341\ y}{2441406250000000000000000}+\frac{87755276065822911}{6103515625000000000000000}}$$

$$\text{yno3\_gly\_gao}\left(\frac{\text{g COD gly}}{g\ N}\right)=\text{yno3\_gly\_gao}\left(\frac{\text{C}-\text{mol gly}}{N\ mol}\right).\frac{\frac{32\ \text{g COD gly}}{\text{C}-\text{mol gly}}}{\frac{14\ g\ N}{N\ mol}}=$$

$$=\frac{\left(\frac{\mathbf{95004009.ratio\_prop\_ac}}{\mathbf{39062500000}}+\frac{\mathbf{200564019.pH}}{\mathbf{1367187500000}}+\frac{\mathbf{202909797}}{\mathbf{136718750000}}\right)\left(\frac{\mathbf{4612972437.pH}}{\mathbf{19531250000000}}+\frac{\mathbf{59757521661.ratio\_prop\_ac}}{\mathbf{15625000000000}}+\frac{\mathbf{5194725381}}{\mathbf{1953125000000}}\right)}{\frac{\mathbf{606211757741656107.pH.ratio\_prop\_ac}}{\mathbf{24414062500000000000000000}}+\frac{\mathbf{49165020321306219.pH^2}}{\mathbf{61035156250000000000000000}}+\frac{\mathbf{465885305885276181\ .ratio\_prop\_ac^2}}{\mathbf{2441406250000000000000000}}+\frac{\mathbf{66729557086812747.pH}}{\mathbf{3051757812500000000000000}}+\frac{\mathbf{830382459816088341.ratio\_prop\_ac}}{\mathbf{2441406250000000000000000}}+\frac{\mathbf{87755276065822911}}{\mathbf{6103515625000000000000000}}}$$

x

$$\text{yno2\_x\_gao}\left(\frac{\text{C}-\text{mol biomass}}{N\ mol}\right)=\frac{3}{4}\left(\frac{RedoxPHA}{4}.\frac{1}{\text{yno\_pha\_x\_gao}}-\frac{RedoxBM}{4}\right)^{-1}=$$

$$=\frac{\left(\frac{4612972437.pH}{78125000000}+\frac{59757521661.ratio\_prop\_ac}{62500000000}+\frac{5194725381}{7812500000}\right)\left(\frac{39644821089.pH}{62500000000000}+\frac{64592170119.ratio\_prop\_ac}{6250000000000}+\frac{43470785007}{6250000000000}\right)}{\frac{430953183949493276400779 1.pH.ratio\_prop\_ac}{390625000000000000000000000}+\frac{16945979749575302461706 1.pH^2}{48828125000000000000000000000}+\frac{34238992664250750336756 03.ratio\_prop\_ac^2}{390625000000000000000000000}+\frac{10290721231732439496150 9.pH}{12207031250000000000000000}+\frac{52397923787385430164636 33.ratio\_prop\_ac}{390625000000000000000000000}+\frac{24890791517453428072515 9}{48828125000000000000000000}}$$

$$\text{yno2\_x\_gao}\left(\frac{\text{g COD biomass}}{g\ N}\right)=\text{yno2\_x\_gao}\left(\frac{\text{C}-\text{mol biomass}}{N\ mol}\right).\frac{\frac{34.4\ g\ COD\ biomass}{C-mol\ biomass}}{\frac{14\ g\ N}{N\ mol}}=$$

$$= \frac{\left(\frac{\mathbf{4612972437}.\boldsymbol{pH}}{\mathbf{78125000000}} + \frac{\mathbf{59757521661}.\boldsymbol{ratio\_prop\_ac}}{\mathbf{62500000000}} + \frac{\mathbf{5194725381}}{\mathbf{7812500000}}\right)\left(\frac{\mathbf{1704727306827}.\boldsymbol{pH}}{\mathbf{1093750000000000}} + \frac{\mathbf{2777463315117}.\boldsymbol{ratio\_prop\_ac}}{\mathbf{109375000000000}} + \frac{\mathbf{1869243755301}}{\mathbf{109375000000000}}\right)}{\frac{\mathbf{43095318394949327640007791}.\boldsymbol{pH}.\boldsymbol{ratio\_prop\_ac}}{\mathbf{390625000000000000000000000}} + \frac{\mathbf{16945979749575302461706 1}.\boldsymbol{pH^2}}{\mathbf{488281250000000000000000000}} + \frac{\mathbf{34238992664250750336756 03}.\boldsymbol{ratio\_prop\_ac^2}}{\mathbf{390625000000000000000000000}} + \frac{\mathbf{10290721231732439496150 9}.\boldsymbol{pH}}{\mathbf{122070312500000000000000000}} + \frac{\mathbf{52397923787385430164636 33}.\boldsymbol{ratio\_prop\_ac}}{\mathbf{390625000000000000000000000}} + \frac{\mathbf{24890791517453428072515 9}}{\mathbf{488281250000000000000000000}}}$$

Y

$$\text{yno2\_gly\_gao}\left(\frac{\text{C} - \text{mol gly}}{N\ mol}\right) = \frac{3}{4}\left(\frac{RedoxPHA}{4}.\frac{1}{\text{yno\_pha\_gly\_gao}} - 1\right)^{-1} =$$

$$= \frac{\left(\frac{601692057.\ pH}{6250000000000} + \frac{1995084189.\ ratio\_prop\_ac}{1250000000000} + \frac{608729391}{625000000000}\right)\left(\frac{4612972437.\ pH}{19531250000000} + \frac{59757521661.\ ratio\_prop\_ac}{15625000000000} + \frac{5194725381}{1953125000000}\right)}{\frac{606211757741656107.\ pH.\ ratio\_prop\_ac}{24414062500000000000000000} + \frac{49165020321306219.\ pH^2}{61035156250000000000000000} + \frac{465885305885276181.\ ratio\_prop\_ac^2}{2441406250000000000000000} + \frac{66729557086812747.\ pH}{3051757812500000000000000} + \frac{830382459816088341.\ ratio\_prop\_ac}{2441406250000000000000000} + \frac{87755276065822911}{6103515625000000000000000}}$$

$$\text{yno2\_gly\_gao}\left(\frac{\text{g COD gly}}{g\ N}\right) = \text{yno2\_gly\_gao}\left(\frac{\text{C} - \text{mol gly}}{N\ mol}\right).\frac{\frac{32\ \text{g COD gly}}{\text{C} - \text{mol gly}}}{\frac{14\ g\ N}{N\ mol}} =$$

$$= \frac{\left(\frac{\mathbf{285012027}.\boldsymbol{ratio\_prop\_ac}}{\mathbf{78125000000}} + \frac{\mathbf{601692057}.\boldsymbol{pH}}{\mathbf{2734375000000}} + \frac{\mathbf{608729391}}{\mathbf{273437500000}}\right)\left(\frac{\mathbf{4612972437}.\boldsymbol{pH}}{\mathbf{19531250000000}} + \frac{\mathbf{59757521661}.\boldsymbol{ratio\_prop\_ac}}{\mathbf{15625000000000}} + \frac{\mathbf{5194725381}}{\mathbf{1953125000000}}\right)}{\frac{\mathbf{606211757741656107}.\boldsymbol{pH}.\boldsymbol{ratio\_prop\_ac}}{\mathbf{24414062500000000000000000}} + \frac{\mathbf{49165020321306219}.\boldsymbol{pH^2}}{\mathbf{61035156250000000000000000}} + \frac{\mathbf{465885305885276181}.\boldsymbol{ratio\_prop\_ac^2}}{\mathbf{24414062500000000000000000}} + \frac{\mathbf{66729557086812747}.\boldsymbol{pH}}{\mathbf{30517578125000000000000000}} + \frac{\mathbf{830382459816088341}.\boldsymbol{ratio\_prop\_ac}}{\mathbf{24414062500000000000000000}} + \frac{\mathbf{87755276065822911}}{\mathbf{61035156250000000000000000}}}$$

Table IV. 2: Kinetic parameters.

Parameter	Description	Value	Units	Source
Heterotrophic organisms				
kf	Fermentable substrate half saturation coefficient for heterotrophic growth	4.00	gCOD/m^3	(Henze et al., 1999)
kacHET	Acetate half saturation coefficient	0.03	gCOD/m^3	(Oehmen et al., 2010c)
kpropHET	Propionate half saturation coefficient	0.04	gCOD/m^3	(Oehmen et al., 2010c)
kalk	Alkalinity half saturation coefficient	0.10	mole/m^3	(Henze et al., 1999)
muh	Heterotrophic maximum specific growth rate	6.00	1/d	(Henze et al., 1999)
nno3HET	Reduction factor for NO_3 denitrification	0.80	-	(Sin et al., 2006)
nno2HET	Reduction factor for NO_2 denitrification	0.80	-	(Sin et al., 2006)
bh	Lysis and decay rate constant	0.40	1/d	(Henze et al., 1999)
Polyphosphate accumulating organisms				
qacphaPAO	Maximum anaerobic acetate uptake rate	4.47	gCOD/(gCOD*d)	(Lopez-Vazquez et al., 2009)
kacPAO	Acetate half-saturation coefficient	0.03	gCOD/m^3	(Oehmen et al., 2010c)
qpropphaPAO	Maximum anaerobic propionate uptake rate	5.21	gCOD/(gCOD*d)	(Lopez-Vazquez et al., 2009)
kpropPAO	Propionate half-saturation coefficient	0.04	gCOD/m^3	(Oehmen et al., 2010c)
kpp	Polyphosphate half-saturation coefficient	0.31	gP/m^3	(Oehmen et al., 2010c)
kalkPAO	Alkalinity half saturation coefficient	0.10	mole HCO_3^-/m^3	(Henze et al., 1999)
manPAO	Anaerobic maintenance rate	0.05	gP/(gCOD*D)	(Smolders et al., 1994a, Brdjanovic et al., 1998)
kphaoxacPAO	Aerobic PHA degradation rate on acetate	41.95	gCOD/(gCOD*d)	(Lopez-Vazquez et al., 2009)
kglyoxacPAO	Aerobic glycogen production rate on acetate	0.33	gCOD/(gCOD*d)	(Lopez-Vazquez et al., 2009)
kppoxacPAO	Aerobic poly-P formation rate on acetate	0.43	gP/(gCOD*D)	(Lopez-Vazquez et al., 2009)

Table IV. 2: (cont.)

Parameter	Description	Value	Units	Source
mphaoxPAO [A]	Aerobic maintenance rate	$\frac{\frac{954624771.ratio\_prop\_ac}{1788668000}+\frac{2587059}{4471670}}{\frac{17340965703.ratio\_prop\_ac}{2861868800}+\frac{84646755}{14309344}}$	gCOD/(gCOD*d)	(Smolders et al., 1994b, Kuba et al., 1996, Zeng et al., 2003a)
kphaaxacPAO	Anoxic PHA degradation rate on acetate	41.95	gCOD/(gCOD*d)	-
kglyaxacPAO	Anoxic glycogen production rate on acetate	0.33	gCOD/(gCOD*d)	-
kppaxacPAO	Anoxic poly-P formation rate on acetate	0.43	gP/(gCOD*D)	-
mphaaxPAO [B]	Anoxic maintenance rate	$\frac{\frac{50243409.ratio\_prop\_ac}{98588000}+\frac{136161}{246470}}{\frac{680759613.ratio\_prop\_ac}{112672000}+\frac{4584087}{788704}}$	gCOD/(gCOD*d)	-
kfphaPAO	Half-saturation coefficient for the fraction of PHA in biomass	0.02	gCOD/gCOD	(Oehmen et al., 2010c)
kphaPAO	PHA half saturation coefficient	0.75	$gCOD/m^3$	(Oehmen et al., 2010c)
kpo4PAO	Orthophosphate half saturation coefficient	0.31	gP/m^3	(Oehmen et al., 2010c)
fppmaxPAO	Maximum poly-P content per PAO biomass concentration	0.27	gP/gCOD	(Oehmen et al., 2010c)
fphamaxPAO	Maximum PHA content per PAO biomass concentration	2.18	gCOD/gCOD	(Oehmen et al., 2010c)
fglymaxPAO	Maximum glycogen content per PAO biomass concentration	0.25	gCOD/gCOD	(Smolders et al., 1995)
Glycogen accumulating organisms				
qacphaGBa	Anaerobic acetate uptake rate of *Competibacter* (when T is equal to T1)	4.91	gCOD/(gCOD*d)	(Lopez-Vazquez et al., 2009)
qacphaGBb	Anaerobic acetate uptake rate of *Competibacter* (when T is equal to T2)	5.36	gCOD/(gCOD*d)	(Lopez-Vazquez et al., 2009)
kacGAO	Acetate half-saturation coefficient	0.03	$gCOD/m^3$	(Oehmen et al., 2010c)
qpropphaGB	Anaerobic propionate uptake rate of *Competibacter*	0.26	gCOD/(gCOD*d)	(Lopez-Vazquez et al., 2009)
kalkGAO	Alkalinity half saturation coefficient	0.10	mole HCO_3^-/m^3	(Oehmen et al., 2010c)

Table IV. 2: (cont.)

Parameter	Description	Value	Units	Source
kpropGAO	Propionate half-saturation coefficient	0.04	gCOD/m3	(Oehmen et al., 2010c)
manGB	Anaerobic maintenance rate of *Competibacter*	0.10	gCOD/(gCOD*d)	(Zeng et al., 2003a, Lopez-Vazquez et al., 2007)
qphaoxGB	Aerobic PHA degradation rate of *Competibacter*	$\frac{\frac{1881.\mathrm{pH}}{26875}+\frac{4356}{5375}}{\frac{19.\mathrm{pH}}{6400}+\frac{71}{1920}}+\frac{386848}{16125}$	gCOD/(gCOD*d)	(Lopez-Vazquez et al., 2009)
qglyoxGB	Aerobic glycogen production rate of *Competibacter*	6.70	gCOD/(gCOD*d)	(Lopez-Vazquez et al., 2009)
mphaoxGB [C]	Aerobic maintenance rate of *Competibacter*	$\frac{\frac{66854673.ratio\_prop\_ac}{390625000000}+\frac{423412929.pH}{39062500000000}+\frac{527409087}{3906250000000}}{\frac{467982711.pH}{3906250000000}+\frac{24176760957.ratio\_prop\_ac}{12500000000000}+\frac{1067459311}{781250000000}}$	gCOD/(gCOD*d)	(Smolders et al., 1994b, Kuba et al., 1996, Zeng et al., 2003a)
qphaaxGB	Anoxic PHA degradation rate of *Competibacter*	$\frac{\frac{1881.\mathrm{pH}}{26875}+\frac{4356}{5375}}{\frac{19.\mathrm{pH}}{6400}+\frac{71}{1920}}+\frac{386848}{16125}$	gCOD/(gCOD*d)	-
qglyaxGB	Anoxic glycogen production rate of *Competibacter*	6.70	gCOD/(gCOD*d)	-
mphaaxGB [D]	Anoxic maintenance rate of *Competibacter*	$\frac{\frac{66854673.ratio\_prop\_ac}{390625000000}+\frac{423412929.pH}{39062500000000}+\frac{527409087}{3906250000000}}{\frac{9738497367.pH}{78125000000000}+\frac{126154767951.ratio\_prop\_ac}{62500000000000}+\frac{10966642471}{7812500000000}}$	gCOD/(gCOD*d)	-
kphaGAO	Half-saturation coefficient for PHA	$\frac{57*\frac{pH}{50000}+\frac{33}{2500}}{19*\frac{pH}{6400}+\frac{71}{1920}}+\frac{2198}{5625}$	gCOD/m^3	(Oehmen et al., 2010c)
kfphaGAO	Half-saturation coefficient for the fraction of PHA in biomass	$\frac{\frac{57.pH}{1720000}+\frac{33}{86000}}{\frac{19.pH}{6400}+\frac{71}{1920}}+\frac{1099}{96750}$	gCOD/gCOD	(Oehmen et al., 2010c)
fphamaxGAO	Maximum PHA content per GAO biomass concentration	$\frac{\left(\frac{57.pH}{17200}+\frac{33}{860}\right)}{\frac{19.pH}{6400}+\frac{71}{1920}}+\frac{2198}{1935}$	gCOD/gCOD	(Oehmen et al., 2010c)

Table IV. 2: (cont.)

Parameter	Description	Value	Units	Source
fglymaxGAO	Maximum glycogen content per GAO biomass concentration	0.33	gCOD/gCOD	(Lopez-Vazquez et al., 2008)
qacphaDEFa	Anaerobic acetate uptake rate of *Defluviicocus* (when T is equal to T1)	2.46	gCOD/(gCOD*d)	(Lopez-Vazquez et al., 2009)
qacphaDEFb	Anaerobic acetate uptake rate of *Defluviicocus* (when T is equal to T2)	2.90	gCOD/(gCOD*d)	(Lopez-Vazquez et al., 2009)
qpropphaDEFa	Anaerobic propionate uptake rate of *Defluviicocus* (when T is equal to T1)	5.73	gCOD/(gCOD*d)	(Lopez-Vazquez et al., 2009)
qpropphaDEFb	Anaerobic propionate uptake rate of *Defluviicocus* (when T is equal to T2)	6.25	gCOD/(gCOD*d)	(Lopez-Vazquez et al., 2009)
manDEF	ATP necessary for anaerobic maintenance purposes of *Defluviicocus*	0.10	gCOD/(gCOD*d)	(Zeng et al., 2003a, Lopez-Vazquez et al., 2007)
qphaoxDEF	Aerobic PHA degradation rate of *Defluviicocus*	$\frac{\left(\frac{171.\mathrm{pH}}{5375}+\frac{396}{1075}\right)}{\frac{19.\mathrm{pH}}{6400}+\frac{71}{1920}}+\frac{35168}{3225}$	gCOD/(gCOD*d)	(Lopez-Vazquez et al., 2009)
qglyoxDEF	Aerobic glycogen production rate of *Defluviicocus*	1.34	gCOD/(gCOD*d)	(Lopez-Vazquez et al., 2009)
mphaoxDEF [C]	Aerobic maintenance of *Defluviicocus*	$\frac{66854673.ratio\_prop\_ac}{390625000000}+\frac{423412929.pH}{39062500000000}+\frac{527409087}{3906250000000}$ / $\frac{467982711.pH}{3906250000000}+\frac{24176760957.ratio\_prop\_ac}{12500000000000}+\frac{1067459311}{781250000000}$	gCOD/(gCOD*d)	(Smolders et al., 1994b, Kuba et al., 1996, Zeng et al., 2003a)
qphaaxDEF	Anoxic PHA degradation rate of *Defluviicocus*	$\frac{\left(\frac{171.\mathrm{pH}}{5375}+\frac{396}{1075}\right)}{\frac{19.\mathrm{pH}}{6400}+\frac{71}{1920}}+\frac{35168}{3225}$	gCOD/(gCOD*d)	-
qglyaxDEF	Anoxic glycogen production rate of *Defluviicocus*	1.34	gCOD/(gCOD*d)	-
mphaaxDEF [D]	Anoxic maintenance rate of *Defluviicocus*	$\frac{66854673.ratio\_prop\_ac}{390625000000}+\frac{423412929.pH}{39062500000000}+\frac{527409087}{3906250000000}$ / $\frac{9738497367.pH}{78125000000000}+\frac{126154767951.ratio\_prop\_ac}{62500000000000}+\frac{10966642471}{7812500000000}$	gCOD/(gCOD*d)	-

Table IV. 2: (cont.)

Parameter	Description	Value	Units	Source
General half-saturation coefficients				
ko	Oxygen half saturation coefficient	0.32	gO^{2}/m^{3}	(Oehmen et al., 2010c)
kno3	Nitrate half saturation coefficient	0.01	gN/m^{3}	(Oehmen et al., 2010c)
kno2	Nitrite half saturation coefficient	0.01	gN/m^{3}	(Oehmen et al., 2010c)
knh	Ammonium (as nutrient) half saturation coefficient	0.05	gN/m^{3}	(Henze et al., 1999)
kpo4	Phosphate (as nutrient) half saturation coefficient	0.01	gP/m^{3}	(Oehmen et al., 2010c)
kgly	Glycogen half-saturation coefficient	0.32	$gCOD/m^{3}$	(Oehmen et al., 2010c)
Autotrophic ammonia oxidisers				
koanh	Oxygen half saturation coefficient for autotrophic ammonia oxidisers growth	0.30	gO^{2}/m^{3}	GPS-X (model twostepmantis)
knha	Ammonium (as substrate) half saturation coefficient for autotrophic ammonia oxidisers growth	1.00	gN/m^{3}	GPS-X (model twostepmantis)
kalknha	Alkalinity half saturation coefficient for autotrophic ammonia oxidisers growth	0.50	mole HCO_3^-/m^3	(Henze et al., 1999)
muautnh	Maximum specific growth rate of autotrophic ammonia oxidisers	0.26	1/d	GPS-X (model twostepmantis)
bautnh	Decay rate of autotrophic ammonia oxidisers	0.04	1/d	GPS-X (model twostepmantis)
Autotrophic nitrite oxidisers				
koano2	Oxygen half saturation coefficient for autotrophic nitrite oxidisers growth	0.72	gO^{2}/m^{3}	GPS-X (model twostepmantis)
kno2a	Nitrite half saturation coefficient for autotrophic nitrite oxidisers growth	0.69	gN/m^{3}	GPS-X (model twostepmantis)
kalkno2a	Alkalinity half saturation coefficient for autotrophic nitrite oxidisers growth	0.50	mole HCO_3^-/m^3	(Henze et al., 1999)

Table IV. 2: (cont.)

Parameter	Description	Value	Units	Source
muautno2	Maximum specific growth rate of autotrophic nitrite oxidisers	0.30	1/d	GPS-X (model twostepmantis)
bautno2	Decay rate of autotrophic nitrite oxidisers	0.04	1/d	GPS-X (model twostepmantis)
Hydrolysis				
kx	Slowly biodegradable substrate half saturation coefficient for hydrolysis	0.10	-	(Henze et al., 1999)
kh	Hydrolysis rate	3.00	1/d	(Henze et al., 1999)
nno3hydrol	Anoxic hydrolysis reduction factor (on NO3)	0.60	-	(Henze et al., 1999)
nno2hydrol	Anoxic hydrolysis reduction factor (on NO2)	0.60	-	(Henze et al., 1999)
nfe	Anaerobic hydrolysis reduction factor	0.40	-	(Henze et al., 1999)
Fermentation				
kfe	Fermentable substrate half saturation coefficient	4.00	$gCOD/m^3$	(Henze et al., 1999)
qh_ac	Fermentation maximum rate on acetate	3.00	1/d	(Henze et al., 1999)
qh_prop	Fermentation maximum rate on propionate	3.00.ratioprop_ac	1/d	This thesis
Phosphorus precipitation				
kalkpre	Alkalinity half saturation coefficient for phosphates redissolution	0.50	mole HCO_3^-/m^3	(Henze et al., 1999)
kpre	Phosphorus precipitation with metal hydroxides rate constant	1.00	$m^3/g/d$	(Henze et al., 1999)
kred	Redissolution of phosphates rate constant	0.60	1/d	(Henze et al., 1999)
High concentration inhibition				
kXh	High concentration inhibition for heterotrophs	30000	$gCOD/m^3$	GPS-X (asm2d model)
kXnh	High concentration inhibition for autotrophic ammonia oxidisers	5000	$gCOD/m^3$	GPS-X (asm2d model)
kXno2	High concentration inhibition for autotrophic nitrite oxidisers	5000	$gCOD/m^3$	GPS-X (asm2d model)

A

$$\text{mphaox\_pao}\left(\frac{\text{C}-\text{mol biomass}}{C-mol\ biomass.\text{h}}\right)=\frac{12\cdot m_{ATP,ox}}{6\,\lambda+27\,\lambda\cdot\delta+8\,\beta+30\,\beta\cdot\delta}=\frac{\frac{318208257.ratio\_prop\_ac}{14309344000}+\frac{862353}{35773360}}{\frac{17340965703.ratio\_prop\_ac}{2861868800}+\frac{84646755}{14309344}}$$

$$\text{mphaox\_PAO}\left(\frac{g\ COD\ biomass}{g\ COD\ biomass.D}\right)=\text{mphaox\_PAO}\left(\frac{\text{C}-\text{mol biomass}}{C-mol\ biomass.\text{h}}\right).\frac{\frac{34.4\ g\ COD\ biomass}{C-mol\ biomass}}{\frac{34.4\ g\ COD\ biomass}{C-mol\ biomass}.\frac{D}{24\ h}}=\frac{\mathbf{\frac{954624771.ratio\_prop\_ac}{1788668000}+\frac{2587059}{4471670}}}{\mathbf{\frac{17340965703.ratio\_prop\_ac}{2861868800}+\frac{84646755}{14309344}}}$$

B

$$\text{mphaax\_PAO}\left(\frac{\text{C}-\text{mol biomass}}{C-mol\ biomass.\text{h}}\right)=\frac{12\cdot m_{ATP,ax}}{6\,\lambda+27\,\lambda\cdot\delta_N+8\,\beta+30\,\beta\cdot\delta_N}=\frac{\frac{16747803.ratio\_prop\_ac}{788704000}+\frac{45387}{1971760}}{\frac{680759613.ratio\_prop\_ac}{112672000}+\frac{4584087}{788704}}$$

$$\text{mphaax\_PAO}\left(\frac{g\ COD\ biomass}{g\ COD\ biomass.D}\right)=\text{mphaax\_PAO}\left(\frac{\text{C}-\text{mol biomass}}{C-mol\ biomass.\text{h}}\right).\frac{\frac{34.4\ g\ COD\ biomass}{C-mol\ biomass}}{\frac{34.4\ g\ COD\ biomass}{C-mol\ biomass}.\frac{D}{24\ h}}=\frac{\mathbf{\frac{50243409.ratio\_prop\_ac}{98588000}+\frac{136161}{246470}}}{\mathbf{\frac{680759613.ratio\_prop\_ac}{112672000}+\frac{4584087}{788704}}}$$

C

$$\text{mphaox\_GB or mphaox\_DEF}\left(\frac{\text{C}-\text{mol biomass}}{C-mol\ biomass.\text{h}}\right)=\frac{12\cdot m_{ATP,ox}}{6\,\lambda+27\,\lambda\cdot\delta+8\,\beta+30\,\beta\cdot\delta}=\frac{\frac{22284891.ratio\_prop\_ac}{3125000000000}+\frac{141137643.pH}{312500000000000}+\frac{175803029}{31250000000000}}{\frac{467982711.pH}{3906250000000}+\frac{24176760957.ratio\_prop\_ac}{12500000000000}+\frac{1067459311}{781250000000}}$$

$$\text{mphaox\_GB or mphaox\_DEF}\left(\frac{g\ COD\ biomass}{g\ COD\ biomass.D}\right)=\text{mphaox\_GB or mphaox\_DEF}\left(\frac{\text{C}-\text{mol biomass}}{C-mol\ biomass.\text{h}}\right).\frac{\frac{34.4\ g\ COD\ biomass}{C-mol\ biomass}}{\frac{34.4\ g\ COD\ biomass}{C-mol\ biomass}.\frac{D}{24\ h}}=$$

$$=\frac{\mathbf{\frac{66854673.ratio\_prop\_ac}{390625000000}+\frac{423412929.pH}{39062500000000}+\frac{527409087}{3906250000000}}}{\mathbf{\frac{467982711.pH}{3906250000000}+\frac{24176760957.ratio\_prop\_ac}{12500000000000}+\frac{1067459311}{781250000000}}}$$

D

$$\text{mphaax\_GB or mphaax\_DEF}\left(\frac{\text{C}-\text{mol biomass}}{C-mol\ biomass.\text{h}}\right)=\frac{12\cdot m_{ATP,ax}}{6\,\lambda+27\,\lambda\cdot\delta_N+8\,\beta+30\,\beta\cdot\delta_N}=\frac{\frac{22284891.ratio\_prop\_ac}{3125000000000}+\frac{141137643.pH}{312500000000000}+\frac{175803029}{31250000000000}}{\frac{9738497367.pH}{78125000000000}+\frac{126154767951.ratio\_prop\_ac}{62500000000000}+\frac{10966642471}{7812500000000}}$$

$$\text{mphaax\_GB or mphaax\_DEF}\left(\frac{g\ COD\ biomass}{g\ COD\ biomass.D}\right)=\text{mphaax\_GB or mphaax\_DEF}\left(\frac{\text{C}-\text{mol biomass}}{C-mol\ biomass.\text{h}}\right).\frac{\frac{34.4\ g\ COD\ biomass}{C-mol\ biomass}}{\frac{34.4\ g\ COD\ biomass}{C-mol\ biomass}.\frac{D}{24\ h}}=$$

$$=\frac{\mathbf{\frac{66854673.ratio\_prop\_ac}{390625000000}+\frac{423412929.pH}{39062500000000}+\frac{527409087}{3906250000000}}}{\mathbf{\frac{9738497367.pH}{78125000000000}+\frac{126154767951.ratio\_prop\_ac}{62500000000000}+\frac{10966642471}{7812500000000}}}$$

APPENDIX V – COMPOSITE VARIABLES

GPS-X Cryptic Name	Variable Name	Corresponding Model Stoichiometry
insi	N content of soluble inert organic material	insi
inss	N content of readily biodegradable substrate	Zero
insf	N content of fermentable readily biodegradable substrate	insf
inxi	N content of particulate inert organic material	inxi
inxs	N content of slowly biodegradable substrate	inxs
inxu	N content of unbiodegradable particulates from cell decay	Zero
ipsi	P content of soluble inert organic material	ipsi
ipss	P content of readily biodegradable substrate	Zero
ipsf	P content of fermentable readily biodegradable substrate	ipsf
ipxi	P content of particulate inert organic material	ipxi
ipxs	P content of slowly biodegradable substrate	ipxs
ipxu	P content of unbiodegradable particulates from cell decay	Zero
inxh	N content of active heterotrophic biomass	inbm
inxnh	N content of active autotrophic ammonia oxidisers biomass	inbm
inxno2	N content of active autotrophic nitrite oxidisers biomass	inbm
inxpao	N content of active poly-P accumulating biomass	inbm
inxgb	N content of active Competibacter biomass	inbm
inxdef	N content of active Defluviicoccus biomass	inbm
ipxh	P content of active heterotrophic biomass	ipbm
ipxnh	P content of active autotrophic ammonia oxidisers biomass	ipbm
ipxno2	P content of active autotrophic nitrite oxidisers biomass	ipbm
ipxpao	P content of active poly-P accumulating biomass	ipbm
ipxgb	P content of active Competibacter biomass	ipbm
ipxdef	P content of active Defluviicoccus biomass	ipbm